

# The role of ceramide synthase 2 in sphingosine-1-phosphate-mediated thymic egress

- Dissertation -

zur

Erlangung des Doktorgrades (Dr. rer. nat.)

der

Mathematisch-Naturwissenschaftlichen Fakultät

der

Rheinischen Friedrich-Wilhelms-Universität Bonn

vorgelegt von

**Michael Rieck**

aus Bonn

Bonn, Juni 2017

Angefertigt mit Genehmigung der Mathematisch-Naturwissenschaftlichen Fakultät der  
Rheinischen Friedrich-Wilhelms-Universität Bonn

1. Gutachter: Prof. Dr. Waldemar Kolanus

2. Gutachter: Prof. Dr. Irmgard Förster

Tag der Promotion: 08.11.2017

Erscheinungsjahr: 2017

---

## Contents

<b>Preliminary remarks</b>	<b>vi</b>
<b>Abbreviations</b>	<b>vii</b>
<b>1 Introduction</b>	<b>1</b>
1.1 T cell-mediated immunity . . . . .	1
1.2 Thymic T cell development . . . . .	2
1.2.1 Thymus anatomy . . . . .	3
1.2.2 The stages of T cell development . . . . .	3
1.3 S1P and the regulation of thymic egress . . . . .	7
1.3.1 S1P metabolism . . . . .	7
1.3.2 S1P-mediated thymic emigration of mature SP thymocytes . . . . .	8
1.3.3 Excursus: S1P-dependent lymph node egress of circulating lymphocytes . . . . .	9
1.4 Ceramide synthases and their role in sphingolipid metabolism . . . . .	11
1.4.1 Sphingolipid metabolism . . . . .	12
1.4.2 Ceramide synthases as central enzymes in sphingolipid metabolism . . . . .	14
<b>2 Aim of the study</b>	<b>17</b>
<b>3 Materials and methods</b>	<b>19</b>
3.1 Materials . . . . .	19
3.1.1 Devices . . . . .	19
3.1.2 Consumables . . . . .	21
3.1.3 (Bio-)chemicals . . . . .	22
3.1.4 Kits and enzymes . . . . .	24
3.1.5 DNA and protein standards . . . . .	24
3.1.6 Buffer and sera . . . . .	25
3.1.7 Antibodies . . . . .	25
3.1.8 Primer for genotyping . . . . .	27
3.1.9 Primer for RT-PCR . . . . .	28

3.1.10	Mice . . . . .	29
3.2	Methods . . . . .	30
3.2.1	Animal experimental methods . . . . .	30
3.2.2	Molecular biology . . . . .	33
3.2.3	Biochemistry . . . . .	35
3.2.4	Cell biology . . . . .	39
<b>4</b>	<b>Results</b>	<b>45</b>
4.1	CERS2 facilitates S1P-mediated thymic egress of mature SP thymocytes into the circulation . . . . .	45
4.1.1	Introductory remarks concerning the use of CERS2-deficient mice for the analysis of S1P-dependent thymic egress . . . . .	45
4.1.2	CERS2-deficiency impairs thymic egress . . . . .	48
4.1.3	CERS2-deficiency distorts the S1P gradient between thymus and blood . . . . .	54
4.1.4	Summary . . . . .	56
4.2	S1P-mediated thymic egress is not regulated by CERS2 in thymic stromal or hematopoietic cells . . . . .	57
4.2.1	CERS2 in hematopoietic cells is dispensable for S1P-mediated thymic egress . . . . .	59
4.2.2	CERS2 in thymic stromal cells is dispensable for S1P-mediated thymic egress . . . . .	63
4.2.3	Summary . . . . .	65
4.3	S1P-mediated thymic egress is independent of CERS4 . . . . .	66
4.4	Excursus: Early T cell development in female mice depends on CERS2 . . . . .	68
<b>5</b>	<b>Discussion</b>	<b>72</b>
5.1	CERS2 in vascular endothelial cells maintains the thymic S1P gradient and facilitates efficient thymic egress by limiting the levels of S1P in the blood . . . . .	72
5.2	CERS2 regulates S1P-mediated egress of circulating lymphocytes from lymph nodes into efferent lymphatics . . . . .	75
5.3	CERS2 is a multifunctional enzyme in basal sphingolipid metabolism . . . . .	77
5.4	The regulation of S1P-mediated thymic egress is a specific function of CERS2 . . . . .	79
5.5	CERS2 as putative pharmacological target . . . . .	80
5.6	Concluding remarks on the role of CERS2 in early T cell development in female mice . . . . .	81

<b>6 Summary</b>	<b>83</b>
<b>References</b>	<b>84</b>
<b>Acknowledgements</b>	<b>109</b>

## Formal remarks

In accordance with the common practice in English scientific writing, the present manuscript is partially written in the first-person plural narrative.

Official murine gene and protein symbols in this manuscript were formatted according to the guidelines of "The Journal of Clinical Investigation":

- Genes, mRNA and genotypes: italicized, first letter capitalized (e. g. *Cers2<sup>gt/gt</sup>* mice)
- Proteins: non-italicized, capitalized (e. g. CERS2)

Some of the results that are shown in the present manuscript have already been published in a peer-reviewed journal with me as lead author [1]. The respective parts are highlighted in the figure legends.

The mass spectrometric measurements that are shown in this manuscript (Figure 4.9, 4.12, 4.13 and 4.16) were performed by Prof. Dr. Markus Gräler on a collaborative basis (Department of Anesthesiology and Intensive Care Medicine, Center for Sepsis Control and Care (CSCC), and the Center for Molecular Biomedicine (CMB), Jena University Hospital, Jena, Germany).

The generation of bone marrow chimeras, as well as the transplantation of thymic lobes under the kidney capsule of recipient mice (see 4.2.1 and 4.2.2) were performed in collaboration with the laboratory of Prof. Dr. Christian Kurts (Institute for Experimental Immunology, University Hospital Bonn, Germany). The analyses of chimeric mice and thymic grafts were completely conducted by myself.

Mice of the *Cers2<sup>gt</sup>* and the *Cers4<sup>Δneo</sup>* lines (see 3.1.10) were a kind gift from the lab of Prof. Dr. Klaus Willecke (Molecular Genetics & Cell Biology, Life and Medical Sciences Institute, University of Bonn, Bonn, Germany). Husbandry of *Cers2<sup>gt</sup>* mice was organized by myself. Breeding of *Cers4<sup>Δneo</sup>* mice remained under the control of the group of Prof. Willecke.

## Abbreviations

<b>3-KR</b>	3-ketosphinganine reductase
<b>ABC transporters</b>	ATP-binding cassette transporter
<b>aCDase (Ac)</b>	acid ceramidase
<b>AIRE</b>	autoimmune regulator
<b>alkCDase (Acer)</b>	alkaline ceramidase
<b>APC</b>	antigen-presenting cell
<b>APC</b>	allophycocyanine
<b>APS</b>	ammonium persulfate
<b>ASC</b>	antibody-secreting cell
<b>aSMase</b>	acid sphingomyelinase
<b>BCA</b>	bicinchoninic acid
<b>BCR</b>	B cell receptor
<b>BSA</b>	bovine serum albumin
<b>CERS</b>	ceramide synthase
<b>CERT</b>	ceramide transporter
<b>CD</b>	cluster of differentiation
<b>CD40L</b>	CD40 ligand
<b>CD4SP thymocytes</b>	CD4 single positive thymocytes
<b>CD8SP thymocytes</b>	CD8 single positive thymocytes
<b>CDase</b>	ceramidase
<b>cDNA</b>	complementary DNA
<b>CGT</b>	ceramide glucosyl transferase
<b>CMJ</b>	corticomedullary junction
<b>CoA</b>	coenzyme A
<b>cTEC</b>	cortical thymic epithelial cell
<b>CTL</b>	cytotoxic T lymphocyte
<b>CTLA4</b>	cytotoxic T lymphocyte associated protein 4
<b>DC</b>	dendritic cell
<b>DES</b>	desaturase
<b>DLL4</b>	delta-like 4
<b>DMSO</b>	dimethyl sulfoxide
<b>DNA</b>	desoxyribonucleic acid
<b>DN thymocytes</b>	double negative thymocytes
<b>DP thymocytes</b>	double positive thymocytes
<b>dsRNA</b>	double-stranded ribonucleic acid
<b>DTT</b>	dithiothreitol
<b>EAE</b>	experimental autoimmune encephalomyelitis
<b>ECL</b>	enhanced chemoluminescence
<b>EDTA</b>	ethylenediaminetetraacetic acid

<b>EGF</b>	epidermal growth factor
<b>ER</b>	endoplasmic reticulum
<b>ETP</b>	early thymic progenitor
<b>FC</b>	flow cytometry
<b>FCS</b>	fetal calf serum
<b>Foxp3</b>	forkhead box P3
<b>GalNAcT</b>	N-acetylgalactosamine transferase
<b>GCS</b>	glycosphingolipid synthase
<b>GPCR</b>	G protein-coupled receptor
<b>GSL</b>	glycosphingolipid
<b>HDL</b>	high-density lipoprotein
<b>HEV</b>	high endothelial venule
<b>HRP</b>	horseradish peroxidase
<b>ICOS</b>	inducible T cell co-stimulator
<b>IEL</b>	intraepithelial lymphocytes
<b>IFN-<math>\gamma</math></b>	interferon gamma
<b>IgG</b>	immunoglobulin G
<b>IL</b>	interleukin
<b>IL7R</b>	interleukin 7 receptor
<b>IRBP</b>	interphotoreceptor retinoid-binding protein
<b>KLF2</b>	kruppel-like factor 2
<b>LC (technique)</b>	liquid chromatography
<b>LC (fatty acid)</b>	long-chain
<b>LCS</b>	lactosyl ceramide synthase
<b>LPP</b>	phospholipid phosphatase
<b>LPS</b>	lipopolysaccharide
<b>MCF-7</b>	Michigan cancer foundation 7
<b>MHC</b>	major histocompatibility complex
<b>MS</b>	mass spectrometry
<b>mTEC</b>	medullary thymic epithelial cell
<b>nCDase (NC)</b>	neutral ceramidase
<b>NK-<math>\kappa</math>B</b>	nuclear factor kappa B
<b>NK cell</b>	natural killer cell
<b>nSMase</b>	neutral sphingomyelinase
<b>ORMDL</b>	ORM-like
<b>PAMP</b>	pathogen-associated molecular pattern
<b>PBMC</b>	peripheral blood mononuclear cell
<b>PBS</b>	phosphate-buffered saline
<b>PCR</b>	polymerase chain reaction
<b>PD1</b>	programmed cell death 1
<b>PKC</b>	protein kinase C

<b>PMSF</b>	phenylmethane sulfonyl fluoride
<b>PP2A</b>	protein phosphatase 2A
<b>PRR</b>	pattern recognition receptor
<b>qPCR</b>	quantitative PCR
<b>RNA</b>	ribonucleic acid
<b>RRMS</b>	relapsing-remitting multiple sclerosis
<b>RT-PCRs</b>	real time PCR
<b>S1P</b>	sphingosine-1-phosphate
<b>S1PR</b>	S1P receptor
<b>SCZ</b>	subcapsular zone
<b>SDS</b>	sodium dodecyl sulfate
<b>siRNA</b>	small interfering RNA
<b>SM</b>	sphingomyelin
<b>SMase</b>	sphingomyelinase
<b>SMS</b>	sphingomyelin synthase
<b>SP thymocytes</b>	single positive thymocytes
<b>Sph</b>	sphingosine
<b>SPHK</b>	sphingosine kinase
<b>SPNS2</b>	spinster homolog 2
<b>SPP</b>	S1P phosphatase
<b>SPT</b>	serine palmitoyltransferase
<b>sSMase</b>	soluble sphingomyelinase
<b>TBST</b>	Tris-buffered saline plus Tween-20
<b>TCR</b>	T cell receptor
<b>TEMED</b>	tetramethylethylenediamine
<b>T<sub>FH</sub></b>	follicular helper T cell
<b>TGF-<math>\beta</math></b>	transforming growth factor beta
<b>T<sub>H</sub>cell</b>	T helper cell
<b>TLC domain</b>	TRAM/LAG1/CLN8 domain
<b>TNF-<math>\alpha</math></b>	tumor necrosis factor alpha
<b>TRAF2</b>	TNF receptor associated factor 2
<b>T<sub>Reg</sub></b>	regulatory T cell
<b>TRIS</b>	tris(hydroxymethyl)aminomethane
<b>TSP</b>	thymic seeding progenitor
<b>ULC (fatty acid)</b>	ultra long-chain
<b>VLC (fatty acid)</b>	very long-chain
<b>WB</b>	western blot

# 1 Introduction

## 1.1 T cell-mediated immunity

In the course of evolution, metazoan organisms developed complex strategies and mechanisms, collectively called immune system, to protect themselves from infections with pathogens. In mammals and most other vertebrates, the immune system can be subdivided into the innate immune system and the adaptive immune system [2, 3, 4]. Whereas the innate immune system is based on the detection of evolutionary broadly conserved structures of microbial or viral origin, collectively termed PAMPs (pathogen-associated molecular patterns), such as LPS (lipopolysaccharide) from Gram-negative bacteria or dsRNA (double-stranded DNA) from certain viruses, the adaptive immune system induces immune responses that are highly specific for individual pathogens [3, 5]. Adaptive immune responses are mediated by lymphocytes, which can be subdivided into B and T cells. Specific somatic recombination mechanisms, which randomly rearrange a certain set of gene segments during lymphocyte development, lead to the expression of a unique and highly specific antigen receptor on each B and T cell (BCR = B cell receptor and TCR = T cell receptor) [6, 7]. Therefore, only few cells of the whole lymphocyte pool are able to detect the presence of a given pathogen. However, those cells that are stimulated by a cognate interaction between their antigen receptor and an invading pathogen undergo massive clonal expansion and differentiate into effector cells to induce a highly specific immune response [3].

Effector B cells (plasma cells or ASCs (antibody-secreting cells)) secrete large amounts of antibodies, which represent the soluble form of their BCR, recognizing the same antigen by which the original B cell was activated [8]. Antibodies bind and cross-link their target structures, causing their inactivation, e.g. in the case of a soluble toxin, and/or their endocytosis by professional phagocytes of the innate immune system, e.g. in the case of a pathogenic bacterium [3].

T cells can be subdivided into  $CD8^+$  T cells that differentiate into effector cytotoxic T lymphocytes (CTLs) and  $CD4^+$  T cells that differentiate into effector T helper ( $T_H$ ) cells upon activation [3, 9]. CTLs propagate local inflammatory responses by releasing type 1 cytokines, such as TNF- $\alpha$  or IFN- $\gamma$ , and eliminate intracellularly infected host cells by the directed release of cytotoxic granules, containing granzyme B or perforin [3, 10, 11, 12, 13]. In contrast to  $CD8^+$  T cells,  $CD4^+$  T cells can differentiate into several distinct effector subtypes ( $T_H1$ ,  $T_H2$ ,  $T_H9$ ,  $T_H17$ ,  $T_{FH}$  or  $T_{Reg}$ ), which contribute to immune responses by different mechanisms, such as licensing the activation of innate immune cells or supporting antibody production by B cells. The polarization into the respective subtypes is mainly driven by the cytokine environment and partially by the strength of TCR stimulation. As infections with different pathogens induce specific cytokine profiles, fate determination of naive  $CD4^+$  T cells into the specific effector subsets is a direct and specific response to particular pathogens. Thus, the organism promotes production of those  $T_H$  subsets that

are capable of supporting an appropriate and customized immune response to the invading pathogen [14].

Under homeostatic, non-infected conditions, resting (non-activated)  $CD4^+$  and  $CD8^+$  T cells patrol constantly through blood, lymph nodes, lymphatics and spleen in a process termed lymphocyte circulation. With regard to the small number of lymphocytes whose receptor is specific for a given antigen, their continuous recirculation drastically increases the chance of detecting cognate antigens on antigen-presenting cells (APCs), such as DCs (dendritic cells), which transport pathogenic material from all peripheral tissues into the lymph nodes [3, 15, 16]. After 8 - 12 hours without cognate interaction, T cells leave the lymph nodes via the efferent lymphatics and re-enter the blood through the thoracic duct [15]. Upon a cognate interaction, however, T cells stay in the lymph nodes until their differentiation into effector cells is completed and they have performed several rounds of cell division. As fully differentiated effector T cells, they leave the lymph node and travel to the site of infection, where they participate in the (local) battle against the infectious agents [3, 17]. After successful clearance of invading pathogens, most effector T cells die by apoptosis, except for a small group that differentiates into memory T cells and thus provides long-term protection. In case of a second infection with an already encountered pathogen, cognate memory cells can induce an adaptive immune response, which is faster and more efficient than the mechanisms upon the first encounter [18].

## 1.2 Thymic T cell development

At a given time, the peripheral T cell pool of a human, which contains approximately  $10^{11}$  naive T cells, comprises at least  $10^8$  unique TCR specificities, enabling the induction of adaptive immune responses against a broad spectrum of different pathogens [19]. This enormous diversity is the result of special genomic recombination mechanisms, which randomly rearrange the coding sequences of the TCRs during T cell development. Each TCR is a heterodimer, composed of an  $\alpha$  and a  $\beta$  chain. Both chains contain an invariant and a variable domain. While the invariant domains anchor the TCR in the plasma membrane and interact with cytosolic and other membrane-bound effectors, the variable domains extend into the extracellular space and form the antigen binding site. The variable domains of  $\alpha$  and  $\beta$  chains are genetically encoded by special gene segments, termed V (variable), D (diversity) and J (joining) segments. In germline configuration, the locus of an  $\alpha$  chain contains 70 V and 61 J segments, whereas the locus of a  $\beta$  chain contains 52 V, 2 D and 13 J segments. During T cell development, however, these segments are randomly rearranged in a regulated process called V(D)J recombination. As each segment has a unique sequence and both chains are independently recombined, a large number of TCRs with different antigen specificities is generated. This diversity is even more increased by the addition or removal of single nucleotides at the junctions between the segments. Taken together, the theoretical number of different TCRs is larger than  $10^{18}$  [3, 6, 20, 21]. However, the generation of TCRs by stochastic means is a two-edged sword, as it accidentally produces TCRs

that are either non-functional or reactive to self antigens. To prevent immunosuppression on the one side and severe autoimmune reactions on the other side, those inoperative and autoreactive TCRs must be rapidly eliminated from the TCR pool. Consequently, T cell development comprises not only the steps that regulate antigen receptor diversification, but also various mechanisms which ensure that only the cells with functional and self-tolerant TCRs complete their differentiation and become part of the peripheral T cell pool [22]. T cell development is located in the thymus, which provides a unique microenvironment for efficient TCR recombination and the subsequent selection procedures [3, 23].

### 1.2.1 Thymus anatomy

The thymus is a two-lobed primary lymphoid organ, which is located within the thoracic cavity. Both lobes are of comparable size and have identical functions. The thymus is surrounded by a collagenous capsule, which occasionally extends into the organ, forming trabeculae, which subdivide the lobes into several smaller lobules. Each lobule consists of an outer cortex and an inner medulla, which have contact at the corticomedullary junction (CMJ). The cortex, especially the zone close to the capsule (subcapsular zone (SCZ)), is the area of early T cell differentiation, TCR rearrangement and positive selection of functional TCRs. Besides a high number of developing T cells, the cortex is characterized by the presence cTECs (cortical thymic epithelial cells), which mediate positive selection. The medulla is the area of negative selection of TCRs that recognize self-antigens. Harboring fewer developing T cells than the cortex, the medulla can be identified by the presence of mTECs, which mediate negative selection. The corticomedullary junction contains blood vessels, through which hematopoietic progenitors enter the thymus and terminally differentiated T cells emigrate into the circulation [3, 24, 25, 26]. Worthy of note is that the thymus size is dependent on the age of the organism. After reaching its maximal size at adolescence, the thymus involutes constantly by reducing the cortical and medullary mass, as well as by incorporating fat tissue. Thymus involution is accompanied by a reduced T cell output [27, 28].

### 1.2.2 The stages of T cell development

The development of hematopoietic precursors into T cells can be subdivided into several stages (Figure 1.1). As the developmental processes in each stage require a distinct microenvironment, involving e.g. intercellular contacts to specific stromal cells, developing T cells travel sequentially through the discrete areas of the thymus in the course of their differentiation. Starting at the CMJ, developing T cells migrate through the cortex into the SCZ, from which they head to the medulla, before they travel back to the CMJ, where they eventually emigrate into the periphery. The stages of development can be identified by the expression of specific marker molecules (e.g. CD4, CD8, CD25, CD44, CD117, etc. ...) on the surface of the developing T cells. Whereas the late stages can be characterized

by the differential expression of CD4 and CD8 (DP = double positive, CD4SP and CD8SP = CD4 and CD8 single positive), the early stage is marked by the absence of CD4 and CD8 (DN = double negative). However, the DN stage can be further subdivided into four large fractions (DN1 – DN4) on the basis of different expression patterns of CD25 and CD44 (DN1 = CD25<sup>-</sup>/CD44<sup>+</sup>, DN2 = CD25<sup>+</sup>/CD44<sup>+</sup>, DN3 = CD25<sup>+</sup>/CD44<sup>-</sup> and DN4 = CD25<sup>-</sup>/CD44<sup>-</sup>) [24, 29].

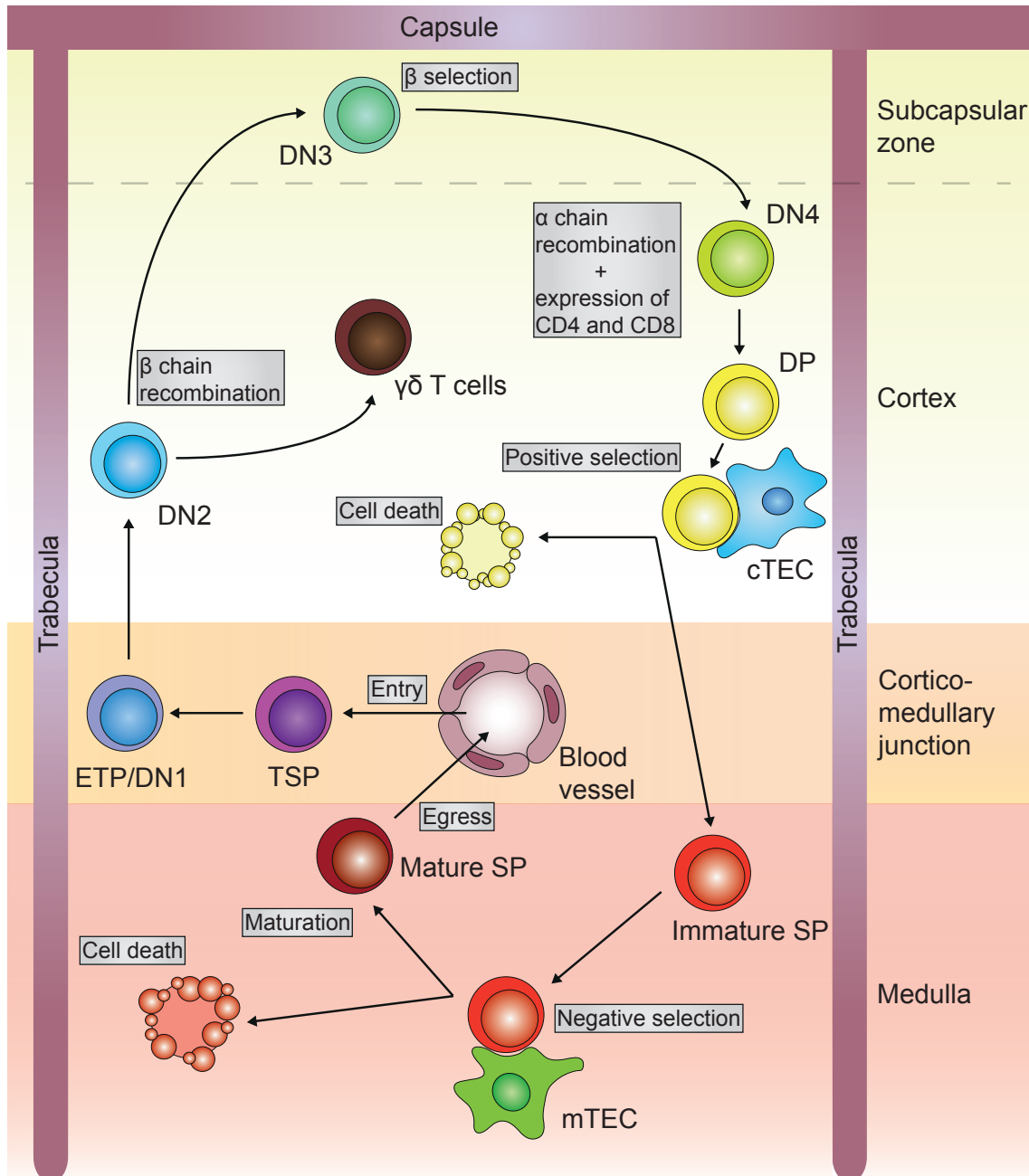


**Figure 1.1:** Overview of T cell development in the thymus. The layout of this figure is based on the graphics of [24, 25].

T cell development begins at the CMJ, where bone marrow-derived TSPs (thymic seeding progenitors) enter the thymus, differentiate into ETPs (early thymic progenitors) upon the contact with thymic stroma cells and become thus part of the DN1 subset ( $CD4^-/CD8^-/CD25^-/CD44^+$ ), which represents the earliest stage of T cell development [30]. The cells of the DN1 subset proliferate extensively and become more committed to the T cell line via Notch1-DLL4 signaling. After approximately 10 days of proliferation, DN1 cells leave the CMJ and migrate into the cortex, while progressing into the DN2 stage ( $CD4^-/CD8^-/CD25^+/CD44^+$ ) [31, 32, 33, 34]. Besides further commitment to the T cell lineage, most DN2 thymocytes begin to diversify their TCR by rearranging the VDJ segments of the  $\beta$  chain locus [35, 36]. Worthy of note is that a small DN2 thymocyte population, which is characterized by a high expression of IL7R, recombines the alternative  $\gamma$  and  $\delta$  TCR chains, instead of the  $\beta$  chain. Those cells give rise to the non-canonical  $\gamma\delta$  T cells, a divergent tissue-associated T cell subset with special functions, which, for instance, forms a large fraction of the IELs (intraepithelial lymphocytes) in the gut [37, 38, 39]. The transition from the DN2 to the DN3 ( $CD4^-/CD8^-/CD25^+/CD44^-$ ) stage occurs in the SCZ. In the DN3 stage, the success of the  $\beta$  chain recombination is monitored in a process termed  $\beta$ -selection. While the developing T cells intensively rearrange their  $\beta$  chain, they begin to express an invariant surrogate  $\alpha$  chain, in addition to several other TCR proximal signaling components like CD3. The invariant  $\alpha$  chain dimerizes with the randomly recombined  $\beta$  chains, forming a pre-TCR. As soon as functional  $\beta$  chains are produced, the pre-TCR induces a signaling cascade that immediately stops further  $\beta$  chain recombination [30, 40, 41]. After a massive proliferation at the late DN3 stage, the developing T cells progress into the DN4 stage ( $CD4^-/CD8^-/CD25^-/CD44^-$ ), which is characterized by their reentry into the cortex, the downregulation of the pre-TCR, the recombination of the  $\alpha$  chain locus and the co-induction of CD4 and CD8. In the course of these processes, the DN4 cells transit into the DP stage ( $\alpha\beta TCR^+$ ,  $CD4^+/CD8^+/CD25^-/CD44^-$ ), as they co-express CD4 and CD8 in addition to a TCR with completely recombined  $\alpha$  and  $\beta$  chains [42, 43, 44, 45, 46, 47].

As a consequence of the stochastic rearrangement of  $\alpha$  and  $\beta$  chains, some DP thymocytes express TCRs that are not able to recognize peptide-MHC complexes. In a process called positive selection, those cells are efficiently eliminated from the DP thymocyte pool, ensuring that only cells with functional TCRs continue the differentiation into mature T cells [48, 49]. Positive selection is mainly mediated by cTECs, which present autoantigens on MHC class I and class II molecules to the DP thymocytes. Only upon low affinity/avidity interactions between TCRs and peptide:MHC complexes, the corresponding DP thymocytes receive survival signals by the cTECs and can progress into the next stage. If the TCRs of DP thymocytes cannot recognize peptide:MHC complexes, they fail to receive survival signals and “die by neglect”. However, if the interactions between the TCRs and the peptide:MHC complexes are too strong, the cTEC induces apoptosis in the corresponding DP thymocytes, as their highly autoreactive TCR might elicit severe autoimmune reactions in the periphery [50]. In general, only 3-5 % of all DP thymocytes are positively

selected for further differentiation [24].

The transition into the next stage is accompanied by an important lineage decision. In response to the cognate low-affinity interaction with MHC class I or class II molecules, the DP thymocytes down-regulate one co-receptor (CD4 or CD8) and differentiate into CD4SP or CD8SP thymocytes, the precursors of CD4<sup>+</sup> T cells (T<sub>H</sub> cells) and CD8<sup>+</sup> T cells (CTLs)[34]. Simultaneously, the positively selected thymocytes migrate into the medulla, where they are subjected to another selection procedure, which is mediated by mTECs [50, 51].

In contrast to cTECs, mTECs are capable of expressing and presenting autoantigens, which are normally restricted to specific peripheral tissues. Thus, the TCRs of the SP thymocytes are tested for their reactivity against autoantigens, which are normally not present in the thymus. The expression of tissue-restricted antigens by mTECs depends partially on AIRE (autoimmune regulator), a transcription factor, which promotes the ectopic expression of genes such as insulin, IRBP (interphotoreceptor retinoid-binding protein) or myelin protein zero [52, 53]. Additionally, mTECs can also transfer these ectopic antigens to DCs for presentation [54]. After having entered the medulla, the SP thymocytes intensively interact with the mTECs and the DCs [34, 50]. Only SP thymocytes that do not recognize self-peptide:MHC complexes on the APCs are allowed to complete the differentiation into conventional naive CD4<sup>+</sup> or CD8<sup>+</sup> T cells. If cognate interactions between TCRs and autoantigen:MHC complexes can be established, the corresponding SP thymocyte either receives a death signal and is eliminated via apoptosis or differentiates into a regulatory T cell (T<sub>reg</sub>). Most likely, the decision between the induction of apoptosis and the differentiation into T<sub>reg</sub>s depends on the strength of the interaction between the SP thymocyte and the mTEC. Whereas strong interactions are thought to promote apoptosis, intermediate interactions might support the deviation into T<sub>reg</sub>s. These thymus-derived T<sub>reg</sub>s can enter the periphery and suppress autoimmune-reactions in an antigen-dependent manner [54, 55]. The mTEC-mediated negative selection of SP thymocytes, which are non-reactive to tissue-specific self-antigens, as well as the elimination and clonal deviation of autoreactive SP thymocytes are important immunological mechanisms, which minimize the risk of T cell-driven autoimmunity. The condition that results from these thymus-intrinsic processes is called central tolerance [22, 49, 50].

In the course of negative selection in the medulla, the SP thymocytes develop from an immature/semi-mature into a mature state, which can be monitored by the differential surface expression of CD62L and CD69 (immature = CD62L<sup>-</sup>/CD69<sup>+</sup> and mature = CD62L<sup>+</sup>/CD69<sup>intermediate</sup>). During this maturation process, the SP thymocytes obtain full immunological functionality and resistance to various apoptotic stimuli (e.g. dexamethasone). As mature SP thymocytes, the cells have completed their development and emigrate at the CMJ through the perivascular space into the blood to become a part of the peripheral T cell pool [24, 26, 34].

### 1.3 S1P and the regulation of thymic egress

To become a part of the peripheral T cell pool that provides immunity to a broad range of pathogens, SP thymocytes need to emigrate from the thymus into the blood after having completed their maturation. The process of thymic egress is mainly mediated via the sphingolipid mediator sphingosine-1-phosphate (S1P) [24, 26, 34].

#### 1.3.1 S1P metabolism

Sphingosine-1-phosphate is a pleiotropic bioactive sphingolipid, which is involved in the regulation of diverse physiological processes besides lymphocyte trafficking, such as cell growth, differentiation or the control of vascular permeability [56, 57, 58, 59]. S1P is formed intracellularly via the phosphorylation of sphingosine, the molecular backbone of most sphingolipids, by two specific kinases, sphingosine kinase 1 or 2 (SPHK1 or -2). Although both kinases are ubiquitously expressed, they differ in their subcellular localization, their spectrum of agonists and partially in their involvement in different cellular functions [60, 61]. Whereas SPHK1 is a cytosolic protein, which is activated and translocated to the plasma membrane in response to a variety of different stimuli, such as growth factors, hormones or cytokines, SPHK2 is localized in the nucleus, the mitochondria or other intracellular compartments [62, 63, 64, 65, 66, 67]. Whereas SPHK1 can be activated by EGF (epidermal growth factor), phorbol esters or hypoxia in a context- and cell type-dependent manner, SPHK2 agonism is insufficiently understood [68, 69, 70, 71]. However, due to the ubiquitous expression of SPHK1 and SPHK2, S1P is present in almost every cell type [72]. Although intracellular functions of S1P, like the regulation of histone acetylation or the role as co-factor for TRAF2 (TNF receptor associated factor 2) in the NF- $\kappa$ B (nuclear factor kappa B) pathway, have been described, a considerable amount of S1P is exported into the extracellular space, where it acts as auto- and paracrine signaling molecule [59, 69, 73]. Even though several *in vitro* studies suggested that the release of S1P from the cytosol is mediated by the family of ABC transporters (ATP binding cassette), only SPNS2 (spinster homolog 2), a member of the major facilitator superfamily of transmembrane proteins, was found to be involved in the release of S1P from selected cell types *in vivo* [74, 75, 76, 77, 78].

While S1P is bound to albumin or HDL (high-density lipoprotein) in the plasma, no carriers are known which bind extracellular S1P in the interstitial fluids of tissues [26, 79]. Extracellular S1P signals via the interaction with five non-redundant G-protein-coupled cell surface receptors (GPCRs), S1P receptor 1 – 5 (S1PR1 - 5) [80]. Whereas S1PR1-3 are broadly expressed in most tissues, the expression of S1PR4 is restricted to lymphoid tissues and the lung, and S1PR5 to the brain, the skin and the spleen. In addition to the differential expression, each S1P receptor is coupled to a different set of G proteins, which induce specific down-stream signaling pathways upon engagement. Thus, S1P signaling is involved in a broad spectrum of different physiological processes, which are sum-

marized in [81]. In contrast to the production of S1P, which is catalyzed by only two kinases, six different enzymes are able to degrade S1P [79]. In general, these enzymes can be subdivided into the S1P lyase, which irreversibly degrades S1P into hexadecanal and phosphoethanolamine, and 5 different phosphatases (SPP1-2 (S1P phosphatase), LPP1-3 (phospholipid phosphatase)), which dephosphorylate S1P back to sphingosine [79]. S1P lyase is broadly expressed and localized to the ER (endoplasmic reticulum) [82, 83]. On the one hand, the terminal degradation of S1P by S1P lyase is necessary to limit the intracellular levels of S1P and thus the amount that is available for intracellular functions or for the export into the interstitium [59, 79]. On the other hand, the conversion of S1P into hexadecanal and phosphoethanolamine by S1P lyase represents a biochemical one-way road between sphingolipid and glycerolipid metabolism, as hexadecanal can be used for palmitoyl-CoA (Coenzyme A) synthesis and phosphoethanolamine for the synthesis of phosphatidylethanolamine [84, 85]. The S1P dephosphorylating enzymes can be subgrouped by their substrate specificities and their subcellular localization. Whereas SPP1 and -2 are ER-resident proteins with considerable specificity for S1P, LPP1-3 are cell surface proteins with broad specificity for phosphorylated lipids. As the active sites of LPP1-3 are directed into the extracellular space, these enzymes can dephosphorylate interstitial S1P. Consequently, SPP1-2 regulate intracellular levels of S1P, while LPP1-3 regulate extracellular levels of S1P and thus signaling via S1P receptors [86, 87, 88, 89, 90]. Additionally, the dephosphorylation by phosphatases is considered as a sphingolipid recycling mechanism, as the generated sphingosine can be reused for the production of complex sphingolipids, such as sphingomyelins [85].

### 1.3.2 S1P-mediated thymic emigration of mature SP thymocytes

Within the thymus, the interstitial S1P levels are inhomogeneously distributed (Figure 1.2) [26, 79]. On the one hand, the activity of S1P degrading enzymes, such as LPP3 on TECs and S1P lyase in DCs (and thymocytes), results in low S1P levels in the whole parenchyma [89, 91]. On the other hand, the robust SPHK-dependent production of S1P by neural crest-derived pericytes and presumably also vascular endothelial cells leads to elevated S1P levels at the thymic exit sites to the blood stream (the perivascular space at the CMJ) [78, 92]. The resulting S1P gradient between the parenchyma and the perivascular space provides directional information, where cells can leave the thymus into the circulation [79]. As long as they are immature (not sufficiently negatively selected), SP thymocytes are insensitive to the S1P gradient [26]. This condition is maintained by CD69, which represses the (surface) expression of S1PR1 [92]. Upon maturation (negative selection is completed), however, SP thymocytes become gradually sensitive to the S1P gradient via up-regulation of the transcription factor KLF-2 (krueppel-like factor 2), which strongly promotes the expression of S1PR1. In a feedback loop, initial signaling via the S1P-S1PR1 axis causes down-regulation of CD69, which in turn supports further expression of S1PR1 [93, 94, 95, 96]. At the end of this maturation process, the SP thymocytes are

“egress-competent”, as they can process the directional information of the S1P gradient via robust expression of S1PR. Presumably, the mature SP thymocytes are recruited along the S1P gradient into the perivascular space, where they form contacts with the vascular endothelium [26, 79, 92]. In response to the high S1P levels in the blood, which are even higher than those in the perivascular space, the mature SP thymocytes subsequently transmigrate across the vessel wall and enter the blood stream as T cells [26, 59, 97]. Although it is known that the high levels of S1P in the blood, which are collectively maintained by vascular endothelial cells, hepatocytes, erythrocytes and platelets, are indispensable for efficient thymic egress, the underlying mechanisms, by which circulatory S1P affects the mature SP thymocytes on the abluminal side of the blood vessels, are still insufficiently understood [78, 79, 98, 99]. Likewise, the exact intrathymic architecture of the S1P gradient, especially in the perivascular space, remains unclear [79].

Generally, S1PR1 is rapidly internalized from the cell surface upon ligation of S1P. Therefore, almost all S1PR1s are engaged and subsequently internalized after the mature SP thymocytes have entered the blood stream as naive T cells. In this desensitized condition, the cells are unresponsive to further stimulation with S1P, are thus no longer attracted by the (high levels of) S1P in the blood and can leave the vasculature somewhere else in the organism [100, 101]. Canonically, naive T cells transmigrate via HEVs into lymph nodes, where they form contacts with APCs to screen for cognate antigens [15].

### 1.3.3 Excursus: S1P-dependent lymph node egress of circulating lymphocytes

Worthy of note is that S1P gradients are not only important to mediate egress of mature SP thymocytes into the blood, but also to facilitate emigration of circulating T and B cells from lymph nodes into efferent lymphatics and back into the blood. Similar to the thymus, S1P levels are relatively low in the lymph node parenchyma, but high at the exit sites close to the cortical sinuses, resulting in a gradient that provides directional information, where the lymph node can be left into the efferent lymphatics [26, 102, 103]. After entering the lymph nodes from the blood as desensitized cells, T and B cells migrate into the T cell zones or the B cell follicles on their search for antigens [104]. In response to the low S1P levels in the parenchyma, both cell types gradually re-express S1PR1. Thus, the lymphocytes become competent to sense the S1P-gradient, migrate to the exit sites and leave the lymph nodes S1P-dependently into the efferent lymphatics [17, 26]. However, if T and B cells are activated by cognate antigens, they need to stay in the lymph node to proliferate and differentiate into effector cells. In this case, both cell types immediately upregulate CD69, which suppresses S1PR1 surface expression and thus their sensitivity for the S1P gradient. After complete differentiation, effector cells down-regulate CD69, re-express S1PR1 and exit via the S1P gradient into the circulation [17, 105].

The increasing knowledge about S1P-mediated lymphocyte egress is of medical benefit, as

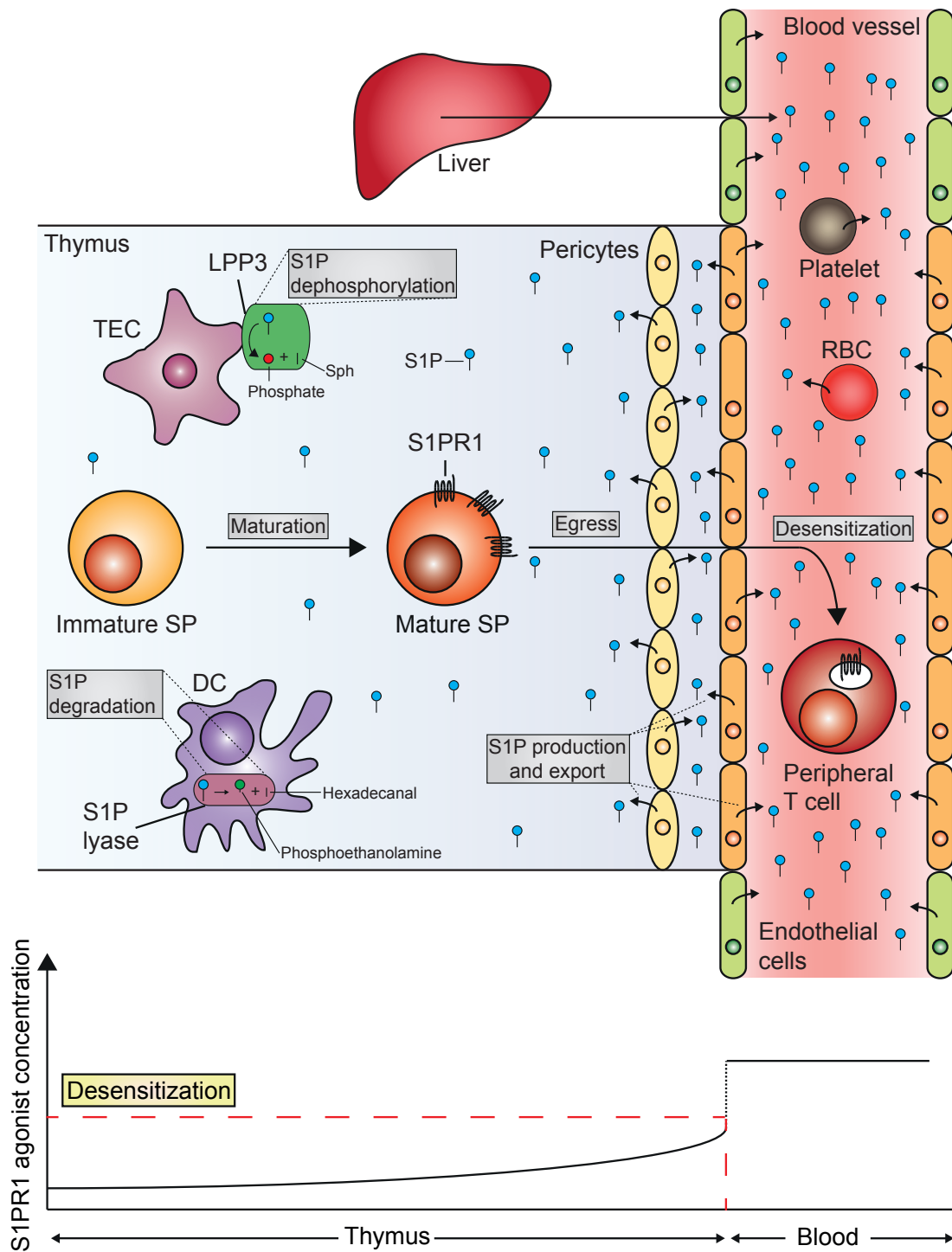


**Figure 1.2:** Thymic egress of mature SP thymocytes along the S1P gradient. The layout of this figure is based on the graphics of [59, 79].

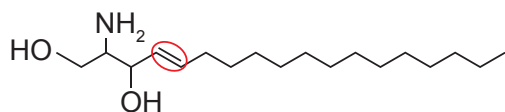
it led to the development of novel therapeutic strategies for the treatment of people with autoimmune disorders. The most prominent example is the development of the drug FTY720, which is used to treat patients with relapsing-remitting multiple sclerosis (RRMS), a severe autoimmune disease of the central nervous system, driven by autoreactive T cells [106, 107].

FTY720 is a synthetic analogue to sphingosine, which is phosphorylated by sphingosine kinase 2. As phospho-FTY720, it binds to S1PR1, S1PR3, S1PR4 and S1PR5 and induces their internalization from the cell surface [107, 108, 109]. Thus, although FTY720 acts agonistically, long-term treatment establishes a functional antagonism as cells down-modulate their S1P receptors and become desensitized. Thereby, lymphocytes become unresponsive to S1P gradients and subsequently sequestered in secondary lymphoid organs. Consequently, FTY720 treatment extenuates neuro-inflammation, as many autoreactive lymphocytes are hindered to reach the central nervous system [107, 110, 111].

#### 1.4 Ceramide synthases and their role in sphingolipid metabolism

By regulating emigration of lymphocytes from thymus and lymph nodes, S1P is of fundamental importance for the adaptive immune system [99]. From a biochemical point of view, S1P belongs to the class of sphingolipids, a large and diverse group (close to 600 different species [112]) of bioactive lipids, which all share a sphingoid base backbone (e.g. sphingosine or dihydrosphingosine) as common feature (Figure 1.3). Due to their hydrophobic character, most sphingolipids are integral constituents of membranes. Sphingolipids have crucial physiological and pathophysiological functions, as they are involved in various cellular processes, such as growth, survival, inflammation or the development of cancer [85, 113, 114]. Although the underlying mechanisms are often not exactly understood, it is generally accepted that sphingolipids function either directly by acting as signaling molecules, or indirectly by influencing the biophysical properties of membranes, which can affect e.g. transport, localization and function of transmembrane proteins [84]. The biochemical network of sphingolipid metabolism consists of various interconnected and mostly bidirectional pathways that are regulated by a large number of different enzymes. However, the only way to enter sphingolipid metabolism is the *de novo* synthesis pathway, in which sphingoid bases are synthesized from non-sphingoid substrates by SPT (serine palmitoyltransferase). Likewise, sphingolipids can exclusively be converted into non-sphingolipid molecules by S1P lyase, which catalyzes the breakdown of S1P into hexadecanal and phosphoethanolamine. Thus, despite its complexity, sphingolipid metabolism is an almost self-contained system [85, 114].

Sphingosine



Dihydrosphingosine

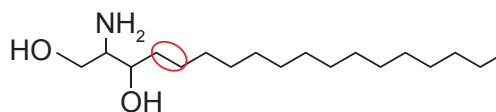


**Figure 1.3:** Chemical structures of sphingosine and dihydrosphingosine (sphinganine). Red circles indicate the position, where the two molecules differ from each other. This figure was taken from [115] and modified.

### 1.4.1 Sphingolipid metabolism

The generation of new sphingolipids via the *de novo* synthesis pathway starts at the ER with the condensation of serine and palmitate to 3-ketodihydrosphingosine (Figure 1.4). This rate-limiting step is catalyzed by the serine palmitoyltransferase (SPT), whose activity is regulated by ORMDL proteins (Orm-like) [116, 117]. Next, 3-ketodihydrosphingosine is reduced by 3-ketosphinganine reductase (3-KR) to dihydrosphingosine, which is subsequently converted into dihydroceramide via N-acylation with fatty acids by enzymes of the ceramide synthase family (CERS1-6) [118]. This step marks the beginning of sphingolipid diversification, as fatty acids of different chain lengths (mostly C14 – C26) can be used for dihydroceramide synthesis [85, 119]. Nonetheless, all dihydroceramides are enzymatically transformed into ceramides by desaturase (DES) [120].

Ceramides are the central molecules within sphingolipid metabolism, as they serve as substrates for all major anabolic pathways [113]. Additionally, several studies indicate that ceramide species themselves are important bioactive molecules, which are involved in the induction of apoptosis, the inhibition of cell growth and the control of autophagy [121, 122, 123, 124, 125]. In general, it is assumed that ceramides mediate these processes via the formation of special lipid microdomains in mitochondrial membranes or in the plasma membrane that putatively control membrane-proximal signaling events [114, 115]. Furthermore, ceramides can directly and indirectly regulate the activity of proteins such as PP2A (protein phosphatase 2A), PKC $\zeta$  (protein kinase C $\zeta$ ) or p38 and thus influence cellular survival [126, 127, 128].

By vesicular trafficking or by CERT (ceramide transporter), a special ceramide transporter, ceramides are transferred from the ER to the Golgi apparatus [130, 131]. In the golgi network, ceramides can be converted into various subclasses of complex sphingolipids, such as sphingomyelins (SMs), via the addition of phosphocholine head groups by SMS enzymes (sphingomyelin synthase), or glycosphingolipids (GSLs), like cerebroside or ganglioside, via the addition of mono- or oligosaccharides by several different enzymes (glycosphingolipid synthases (GCS)), such as CGT (ceramide glucosyl transferase), LCS (lactosyl ceramide synthase) or GlcNAcT (N-acetylgalactosamine transferase) [85, 132, 133]. Eventually, most of these complex sphingolipids are shuttled to the plasma membrane, where they influence the biophysical properties of the lipid bilayer, organize lipid microdomains and contribute to intercellular recognition processes [84, 134].

The breakdown of complex sphingolipids occurs either at the plasma membrane or via the endocytic pathway and is mediated by a large number of different enzymes. In general, sphingomyelins are degraded by sphingomyelinases (SMases), a group of five different enzymes, via the conversion into ceramide and phosphocholine. Although all sphingomyelinases catalyze the same biochemical reaction, they differ in their expression pattern, their subcellular localization and their evolutionary origin. Whereas the alkaline sphingomyelinase is exclusively expressed in intestine and liver, processing sphingomyelins from food, the other

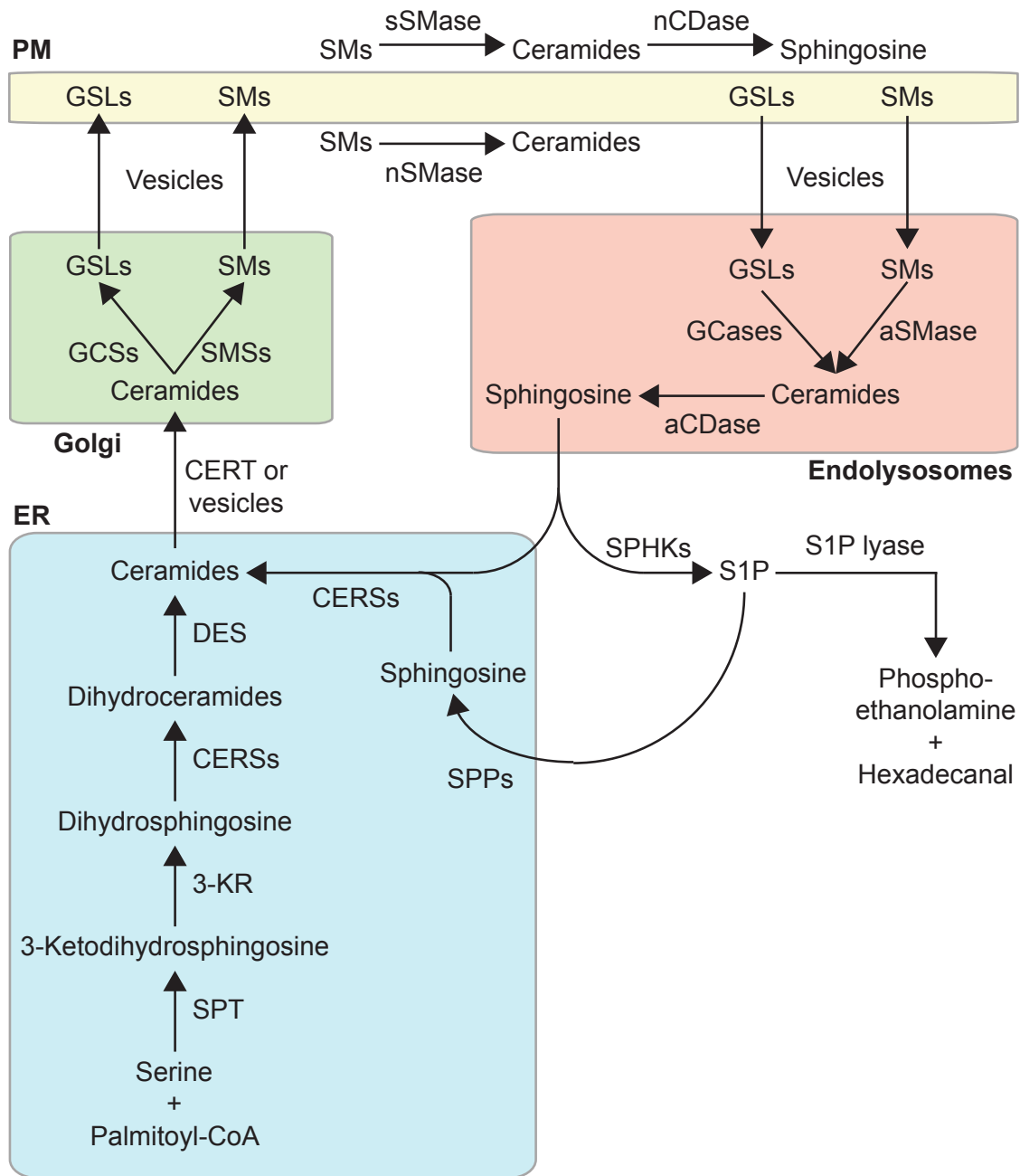


**Figure 1.4:** Overview of sphingolipid metabolism. The layout of this figure is based on the graphics of [129]

four sphingomyelinases, acid sphingomyelinase (aSMase) and neutral sphingomyelinase 1-3 (nSMase), are ubiquitously expressed [85, 135, 136]. Although, aSMase is predominantly localized to lysosomes, degrading sphingomyelins that were internalized by endocytosis, it can also be secreted into the extracellular space (sSMase), where it might degrade sphingomyelins in the plasma membrane or blood plasma [137, 138]. nSMases are associated with the plasma membrane, the Golgi apparatus or the ER, degrading sphingomyelins on the cytosolic leaflet of the lipid bilayer. Worthy of note is that recent studies indicated

that nSMase1 functions rather as lysophospholipase for lyso-PAF (platelet-activating factor) than as SMase for sphingomyelins [139, 140, 141]. In contrast, the breakdown of glycosphingolipids occurs exclusively via the endolysosomal pathway by a plethora of hydrolytic enzymes that successively remove the carbohydrate moieties from the ceramide backbone (GCases (glycosidases)) [85, 133]. Ceramides that are produced by the breakdown of sphingomyelins and glycosphingolipids can be further degraded by ceramidases (CDases), a group of five different enzymes, acid ceramidase (aCDase or AC), neutral ceramidase (nCDase or NC) and alkaline ceramidase1-3 (alkCDase or ACER1-3). Although all ceramidases degrade ceramides via conversion into sphingosine by deacylation, their subcellular localization and biochemical properties differ from each other [142]. The acid ceramidase is a lysosomal protein, which degrades ceramides that originate from the breakdown of endocytosed sphingomyelins and glycosphingolipids [142, 143]. The neutral ceramidase is a type II transmembrane protein, which can be cleaved at the N-terminus to produce a soluble form, which associates with the extracellular leaflet of the plasma membrane. Thus, NC is involved in the degradation of ceramides at the cell surface and in the interstitium [142, 144, 145]. The alkaline ceramidases share a high degree of homology and localize mainly to the ER and the Golgi apparatus, where they presumably degrade ceramides from various origins [85, 142].

The degradation of ceramides by ceramidases is the only way to produce sphingosine, which is sufficiently amphipatic to freely diffuse from one membrane to another [85]. Sphingosine is either reacylated to ceramides by ceramide synthases or phosphorylated to S1P by sphingosine kinases (SPHKs). The processes of recycling back into ceramides and thus into sphingolipid anabolism is termed salvage pathway and accounts for more than 50% of the produced sphingosine [114, 115]. Despite its pleiotropic physiological functions, S1P is likewise the final product of sphingolipid catabolism. Via the activity of S1P lyase, S1P is irreversibly converted into the non-sphingoid molecules hexadecanal and phosphoethanolamine. As this process is the only way to break down sphingoid bases, it represents the exit from sphingolipid metabolism. Nonetheless, S1P can also be dephosphorylated to sphingosine by different phosphatases (SPPs). Thus, even S1P can be redirected into the salvage pathway [85].

#### 1.4.2 Ceramide synthases as central enzymes in sphingolipid metabolism

Ceramides represent the most central sphingolipid species, as they are the substrate for the synthesis of all complex sphingolipids [113]. Therefore, ceramide synthases, which catalyze the formation of (dihydro-)ceramides by N-acylation of (dihydro-)sphingosine with fatty acids, are regarded as the central enzymes in the network of sphingolipid metabolism [129]. The family of ceramide synthases comprises six members in mammals (CERS1-6). All CERSs are transmembrane proteins with 5 – 8 transmembrane domains (depending on the algorithm for prediction) [146]. Although some studies demonstrate that ceramide synthases can be present in mitochondria and the Golgi apparatus, they mainly localize to the

ER and the nuclear membranes [147, 148, 149, 150]. Besides a TLC (TRAM/LAG1/CLN8) domain, which harbors the enzymatic activity within the Lag1p motif, all ceramide synthases, except for CERS1, contain a Hox-like domain of controversially discussed function [151, 152, 153, 154]. Although all members of the CERS family catalyze the same biochemical reaction, each CERS is restricted to an individual spectrum of fatty acid chain lengths that can be used for N-acylation. Whereas, CERS2 and CERS3 mainly use fatty acid chain lengths of C20 to C26, CERS5 and CERS6 are restricted to C14 and C16 fatty acids, while CERS1 and CERS4 cover the intermediate spectrum. Thus, ceramide synthases are functionally non-redundant, as each enzyme is responsible for the production of (dihydro-)ceramides and the subsequent complex sphingolipids with specific acyl chain lengths [129, 146]. In addition to diverging substrate specificities, ceramide synthases are differentially expressed in various tissues [155].

**1.4.2.1 CERS1** CERS1 has substrate specificity for C18 fatty acids and is almost exclusively expressed in brain and skeletal muscle [147, 149, 155, 156, 157]. *In vitro* experiments and analyses of CERS1-deficient mice demonstrated that CERS1 and/or C18 sphingolipids are crucially involved in the regulation of cerebellar development and neuronal turnover, as well as in the suppression of head and neck cancer [158, 159]. Additional studies indicated that CERS1 and/or C18 sphingolipids increase the sensitivity to chemotherapeutic drugs, such as cisplatin, carboplatin, vincristin and doxorubicin. However, the underlying mechanisms of action are insufficiently understood [150].

**1.4.2.2 CERS2** CERS2 has substrate specificity for C22 and C24 fatty acids and is not only almost ubiquitously expressed, but also by far the most abundant CERS family member, with highest expression levels in liver and kidney [155]. Due to these characteristics, CERS2 has been intensively studied in various *in vitro* and *in vivo* studies. Especially analyses of CERS2-deficient mice revealed that CERS2 is involved in various important physiological processes, such as brain myelination, cellular homeostasis in the liver, insulin sensitivity and neutrophil migration [160, 161, 162, 163]. As CERS2-deficient mice lack C22 and C24, but accumulate C16 sphingolipids and sphingoid bases, which are both supposed to have a cytotoxic potential [164, 165], it is generally assumed that CERS2 regulates these processes by maintaining a balance between sphingolipids with different acyl chain lengths [160, 162, 166, 167, 168, 169, 170, 171, 172].

**1.4.2.3 CERS3** CERS3 is exclusively expressed in testes and in the skin. In contrast to the other CERS family members, CERS3 has a broad substrate specificity, using not only long chain fatty acids (LCFA, C16-C20) and very long chain fatty acids (VLCFA, C22-C26), but also ultra-long chain fatty acids (ULCFA, >C26) for the production of ceramides [156]. Studies with CERS3-deficient mice demonstrated that the CERS3-dependent sphingolipids, especially those with ULCFAs, are important for cytokinesis

during male meiosis and for the maintenance of the skin barrier [173, 174, 175].

**1.4.2.4 CERS4** CERS4 has substrate specificity for C18 and C20 fatty acids and is broadly expressed in several tissues, with highest expression levels in skin, heart and liver [155]. Via analyses of CERS4-deficient mice, it was shown that CERS4 and CERS4-dependent sphingolipids are crucially involved in maintaining skin functions, as they control stem cell homeostasis, hair follicle cycling and sebum composition [176, 177].

**1.4.2.5 CERS5** CERS5 has substrate specificity for C16 fatty acids and is mainly expressed in white adipose tissue, testes, lung, spleen and thymus [178]. Due to its capacity to generate C16 sphingolipids, which are suspected pro-apoptotic mediators, CERS5 has been extensively studied *in vitro*, revealing its putative involvement in stress-induced p38 signaling and cell death, as well as in the sensitivity regulation to chemotherapeutic agents, such as doxorubicin and vincristine [150, 179, 180]. Additionally, recent analyses of CERS5-deficient mice demonstrated that CERS5 promotes diet-induced obesity and the concomitant complications, like insulin resistance [178].

**1.4.2.6 CERS6** Like CERS5, CERS6 has substrate specificity for C16 fatty acids. Additionally, CERS6 is able to use C14 fatty acids for ceramide generation [156]. CERS6 is widely expressed with highest expression levels in the kidney and the intestine [155, 181]. The physiological role of CERS6 has been extensively analyzed by the use of CERS6-deficient mice. The corresponding studies demonstrated that CERS6 regulates behavior and promotes diet-induced obesity, but suppresses the development of EAE (experimental autoimmune encephalomyelitis) [167, 182]. Moreover, recent investigations indicate a pro-metastatic role of CERS6 in lung cancer cells [183].

## 2 Aim of the study

In order to finish their developmental program and become a part of the peripheral T cell pool, SP thymocytes undergo a maturation process after having completed negative selection. This maturation enables them to emigrate from the thymus into the circulation along a gradient of the chemoattractive lipid mediator sphingosine-1-phosphate (S1P) [24, 26, 34]. As this egress is needed to constantly replace defective or senescent T cells and supply the periphery with TCRs of new specificities, the thymic S1P gradient is of fundamental importance for the adaptive immune system to provide effective protection against a broad range of pathogens [19, 26, 184]. Although a considerable number of different components (enzymes, cell types, the blood) were identified to be involved in the regulation of S1P-dependent thymic egress, the exact architecture of the thymic S1P gradient, as well as the underlying mechanisms that maintain functional differences in the concentration of S1P remain poorly understood. A deeper insight into the processes that generate the S1P gradient would be of medical interest, as S1P-mediated lymphocyte egress represents a promising therapeutic target for the treatment of autoimmune diseases and other disorders of the adaptive immune system [79].

It is known that the production of S1P, which can be regulated via the amount of sphingosine (substrate for S1P synthesis) or via the activity of the SPHKs (mediate S1P synthesis by phosphorylation of sphingosine), is of fundamental importance for S1P-dependent thymic egress [92, 97, 103, 185, 186, 187]. Prominent regulators of free sphingosine are ceramide synthases (CERS). These enzymes efficiently limit the amount of free sphingosine by using it as substrate for the production of ceramides within the sphingolipid salvage pathway [129, 146]. Different studies demonstrated that especially the enzymatic activity of CERS2, the most abundant member of the ceramide synthase family, is crucial to keep the levels of free sphingosine within physiological boundaries, e.g. in the liver [166, 188]. Moreover, recent investigations indicate that the CERS2-dependent regulation of sphingosine levels might indeed affect the production of S1P in aged gastric smooth muscle cells or the brain [189, 190].

With regard to these findings, the aim of the present study was to investigate the role of CERS2 for the maintenance of the chemoattractive S1P gradient in the thymus and for efficient emigration of newly formed T cells into the periphery (Figure 2.1). For this purpose, S1P-dependent thymic egress was analyzed in wild type and CERS2-deficient mice. Furthermore, via transfer experiments between wild type and CERS2-deficient mice (bone marrow chimeras and thymus transplantation), the relative contribution of CERS2 in hematopoietic and thymic stromal cells to the regulation of S1P-mediated thymic egress was determined. Additionally, analyses of CERS4-deficient mice gave insight into the question if S1P gradients are exclusively regulated by CERS2 or also by other ceramide synthases.

Is CERS2-dependent sphingosine consumption essential for S1P-mediated thymic egress?

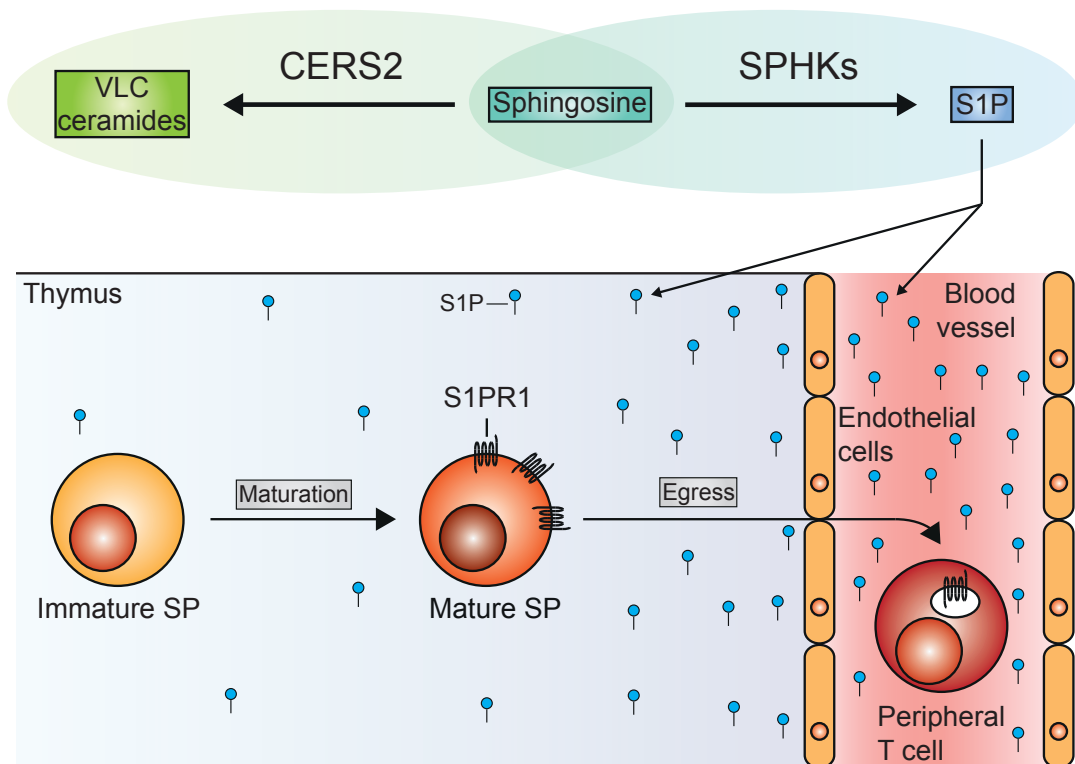


**Figure 2.1:** Aim of the study. The layout of this figure is based on the graphics of [59, 79].

### 3 Materials and methods

#### 3.1 Materials

##### 3.1.1 Devices

Device	Model, company (office)
Autoclave	135T, H + P Medizintechnik (Oberschleißheim, Germany)
Balance	JB2002-G/FACT and AG285, Mettler Toledo (Greifensee, Switzerland)
Binocular	Wild Heerbrugg (Bad Dürkheim, Germany)
Blotting equipment	Mini Trans-Blot Cell, Bio-Rad (Munich, Germany)
Centrifuges	5810R, 5424 and 5415R, Eppendorf (Hamburg, Germany) Avanti J-20XP, Beckman Coulter (Munich, Germany) Multifuge 4KR, Heraeus Instruments GmbH (München, Germany)
CO <sub>2</sub> incubator	CB, Binder (Tuttlingen, Germany)
Developing machine	SRX-101A, Konica Minolta (Langenhagen, Germany)
Dissecting set	FST Dumont Biology (Heidelberg, Germany)
Electrophoresis chamber (agarose gels)	Polymehr (Paderborn, Germany)
Electrophoresis chamber (SDS-PAGE)	Mini Trans-Blot Cell, Bio-Rad (Munich, Germany)
Flow cytometer	Canto II and LSR, BD Bioscience (Heidelberg, Germany)
Gel documentation	Gel Max, Intas (Göttingen, Germany)
Heat block	Thermomixer compact, Eppendorf (Hamburg, Germany)
Laminar flow hood	BioFlow, BDK (Sonnenbühl-Genkingen, Germany)

Magnetic stirrer	Combimac RCT, IKA (Staufen, Germany)
Microplate reader	Infinite M200, Tecan (Männedorf, Switzerland) Synergy HT, Biotek (Bad Friedrichshall, Germany)
Microscope	Axiovert 100, Zeiss (Jena, Germany)
Neubauer chamber	Marienfeld (Lauda-Königshofen, Germany)
PCR cycler	MyCycler, Bio-Rad (Munich, Germany) Vapoprotect, Eppendorf (Hamburg, Germany)
PH meter	MP220, Mettler Toledo (Greifensee, Switzerland)
Pipettes	Gilson (Middleton, USA) ErgoLine, StarLab (Helsinki, Finland)
Pipette controller	Pipetus-Akku, Hirschmann Laborgeräte (Eberstadt, Germany) Accu-jet pro, Brand (Wertheim, Germany)
Power supply	EV-243, Consort (Turnhout, Belgium) Elite300Plus, Schütt Labortechnik (Göttingen, Germany)
Tissue homogenizer	Precellys, Bertin (Rockville, USA)
Real-time PCR cycler	iCycler iQ5 and CFX96, Bio-Rad (Munich, Germany)
Rocker	WS-10, Edmund Bühler (Hechingen, Germany)
Roller mixer	RS-TR05, Phoenix Instrument (Garbsen, Germany)
Scanner	Scan Maker 8700, Mikrotek (Hsinchu, Taiwan)
Spectrophotometer	NanoDrop2000, Thermo Scientific (Waltham, USA)
Suction pump	AC, HLC BioTech (Bovenden, Germany)
Ultrasonic homogenizer	Sonoplus, Bandelin Electronic (Berlin, Germany)
Vortex mixer	UNIMAG ZX3, VELP scientifica (Milan, Italy)
Waterbath	WNE, Memmert (Schwabach, Germany)

## 3.1.2 Consumables

Consumable	Model, company (office)
Capillary tips	Roth (Karlsruhe, Germany)
Cell culture plates and multiwell plates	Greiner Bio-one (Frickenhausen, Germany)
Cover slips	Marienfeld GmbH (Lauda-Königshofen, Germany)
Falcon tubes	Greiner Bio-one (Frickenhausen, Germany)
Filter paper	Whatman No.4, Schleicher and Schuell (Dassel, Germany)
Filter tips	10, 200 and 1000 $\mu$ l, Sarstedt (Nümbrecht, Germany)
Flow cytometry tubes	Sarstedt (Nümbrecht, Germany)
Glass beads (acid-washed)	Sigma-Aldrich (St. Louis, USA)
Hollow needles	Braun (Melsungen, Germany)
2 ml micro tubes	Sarstedt (Nümbrecht, Germany)
Blood collection tubes	Microvette® CB 300 $\mu$ l, Lithium-Heparin, Sarstedt (Nümbrecht, Germany)
Nitrocellulose membrane	Protran, Schleicher and Schuell (Dassel, Germany)
Nylon cell strainer	40 and 70 $\mu$ m pore size, BD Biosciences, (Heidelberg, Germany)
Pasteur pipettes	Roth (Karlsruhe, Germany)
Pipette tips	Roth (Karlsruhe, Germany)
Polypropylene reaction tubes	Starlab (Helsinki, Finland)
Radiographic film	Hyperfilm MP, Amersham Biosciences (Buckinghamshire, UK)
Sterile filters	0.2 and 0.45 $\mu$ m, Schleicher and Schuell (Dassel, Germany)
Syringes	Braun (Melsungen, Germany)

PCR reaction tubes	200 µl thin wall tubes, Axygen (Tewksbury, USA)
Serological pipettes	5, 10, 25 ml, Greiner Bio-one (Frickenhausen, Germany)
RT-PCR plates	Bio-Rad (Munich, Germany)
RT-PCR seals	Bio-Rad (Munich, Germany)

### 3.1.3 (Bio-)chemicals

Reagent	Company (office)
2-Mercaptoethanol	Roth (Karlsruhe, Germany)
2-Propanol	Merck (Darmstadt, Germany)
Acrylamide/Bisacrylamide solution (30%)	Roth (Karlsruhe, Germany)
Agarose	Life Technologies (Carlsbad, USA)
Ammonium chloride (NH <sub>4</sub> Cl)	Sigma-Aldrich (St. Louis, USA)
Ammonium persulfate (APS)	Roth (Karlsruhe, Germany)
Antipain	Sigma-Aldrich (St. Louis, USA)
Aprotinin	Sigma-Aldrich (St. Louis, USA)
Benzamidin	Roth (Karlsruhe, Germany)
Bovine serum albumin (BSA)	Roth (Karlsruhe, Germany)
Bromphenolblue	Roth (Karlsruhe, Germany)
Chloroform	Roth (Karlsruhe, Germany)
Dimethyl sulfoxide (DMSO)	Roth (Karlsruhe, Germany)
Dithiothreitol (DTT)	Applichem (Gatersleben, Germany)
DNA loading dye (6x)	Thermo Scientific (Waltham, USA)
dNTPs	Thermo Scientific (Waltham, USA)
Ethanol	VWR (Darmstadt, Germany)

Ethidiumbromide (EtBr)	Roth (Karlsruhe, Germany)
Ethylenediaminetetraacetic acid (EDTA)	Sigma-Aldrich (St. Louis, USA)
Fixable viability dye eFluor450	eBioscience (San Diego, USA)
Glycerol	Grüssing (Filsum, Germany)
Glycerolphosphate	Sigma-Aldrich (St. Louis, USA)
Glycin	Roth (Karlsruhe, Germany)
Hydrochloric acid (HCl)	Roth (Karlsruhe, Germany)
Leupeptin	Sigma-Aldrich (St. Louis, USA)
Methanol	Roth (Karlsruhe, Germany)
Milk powder	Roth (Karlsruhe, Germany)
Phenylmethane sulfonyl fluoride (PMSF)	Sigma-Aldrich (St. Louis, USA)
Ponceau S	Roth (Karlsruhe, Germany)
Potassium bicarbonate ( $\text{KHCO}_3$ )	Sigma-Aldrich (St. Louis, USA)
Sodium azide ( $\text{NaN}_3$ )	Roth (Karlsruhe, Germany)
Sodium chloride (NaCl)	Roth (Karlsruhe, Germany)
Sodium deoxycholate	Sigma-Aldrich (St. Louis, USA)
Sodium dodecyl sulfate (SDS)	Roth (Karlsruhe, Germany)
Sodium fluoride (NaF)	Roth (Karlsruhe, Germany)
Sodium orthovanadate	Sigma-Aldrich (St. Louis, USA)
Sodium pyrophosphate	Sigma-Aldrich (St. Louis, USA)
Tetramethylethylenediamine (TEMED)	Sigma-Aldrich (St. Louis, USA)
Tris(hydroxymethyl)aminomethane (TRIS)	Roth (Karlsruhe, Germany)
Triton X-100	Roth (Karlsruhe, Germany)
TRIzol Reagent	Thermo Scientific (Waltham, USA)

Trypanblue solution Sigma-Aldrich (St. Louis, USA)

### 3.1.4 Kits and enzymes

<b>Product</b>	<b>Company (office)</b>
Annexin V Apoptosis Detection Kit APC	eBioscience (San Diego, USA)
Anti-Biotin Microbeads	Miltenyi (Bergisch Gladbach, Germany)
Anti-CD45 Microbeads	Miltenyi (Bergisch Gladbach, Germany)
BCA Protein Assay Reagent	Thermo Scientific (Waltham, USA)
DNase I (RNase-free)	Thermo Scientific (Waltham, USA)
Dreamtaq DNA Polymerase	Thermo Scientific (Waltham, USA)
ECL PlusWestern-Blotting Substrate	Thermo Scientific (Waltham, USA)
Foxp3/Transcription Factor Staining Buffer Set	eBioscience (San Diego, USA)
High-Capacity cDNA Reverse Transcription Kit	Thermo Scientific (Waltham, USA)
iTaq Universal SYBR Green Supermix	Bio-Rad (Munich, Germany)
Kapa Sybr Fast qPCR Mastermix for Bio-Rad iCycler	Peqlab (Erlangen, Germany)
Liberase TM	Roche (Mannheim, Germany)
Proteinase K	Peqlab (Erlangen, Germany)

### 3.1.5 DNA and protein standards

<b>Product</b>	<b>Company (office)</b>
GeneRuler™ 100 bp DNA ladder	Thermo Scientific (Waltham, USA)
Protein-Marker IV ('Prestained')	Peqlab (Erlangen, Germany)
Precision Plus Protein™ All Blue Prestained Protein Standards	Bio-Rad (Munich, Germany)

### 3.1.6 Buffer and sera

Product	Company (office)
Phosphate-buffered saline (PBS)	Sigma-Aldrich (St. Louis, USA)
Lymphoprep	Stem cell technologies (Vancouver, Canada)
Fetal calf serum (FCS)	Sigma-Aldrich (St. Louis, USA)

### 3.1.7 Antibodies

Target	Clone	Conjugate	Host	Use	Dilution	Company (office)
<b>CD4</b>	GK1.5 or RM4	Fluorochrome	Rat	FC	According to manufac- turer's instructions	Biolegend /San Diego, USA)
<b>CD8a</b>	53-6.7	Fluorochrome	Rat	FC	According to manufac- turer's instructions	Biolegend /San Diego, USA) or BD Biosciences, (Heidelberg, Germany)
<b>CD11c</b>	N418	Fluorochrome	Armenian hamster	FC	According to manufac- turer's instructions	Biolegend /San Diego, USA)
<b>CD25</b>	7D4 or PC61	Fluorochrome	Rat	FC	According to manufac- turer's instructions	BD Biosciences, (Heidelberg, Germany)
<b>CD31</b>	390	Fluorochrome	Rat	FC	According to manufac- turer's instructions	Biolegend /San Diego, USA)

<b>CD44</b>	IM7	Fluorochrome	Rat	FC	According to manufacturer's instructions	Biolegend /San Diego, USA) or BD Biosciences, (Heidelberg, Germany)
<b>CD45</b>	30-F11	Fluorochrome	Rat	FC	According to manufacturer's instructions	Biolegend /San Diego, USA)
<b>CD45.1</b>	A20	Fluorochrome	Mouse	FC	According to manufacturer's instructions	Biolegend /San Diego, USA)
<b>CD45.2</b>	104	Fluorochrome or Biotin	Mouse	FC	According to manufacturer's instructions	Biolegend /San Diego, USA)
<b>CD62L</b>	MEL14	Fluorochrome	Rat	FC	According to manufacturer's instructions	Biolegend /San Diego, USA)
<b>CD69</b>	H1.2F3	Fluorochrome	Armenian hamster	FC	According to manufacturer's instructions	Biolegend /San Diego, USA)
<b>EpCam</b>	G8.8	Fluorochrome	Rat	FC	According to manufacturer's instructions	Biolegend /San Diego, USA)
<b>F4/80</b>	BM8	Fluorochrome	Rat	FC	According to manufacturer's instructions	Biolegend /San Diego, USA)

<b>Fc-Block</b>	.	-		FC	According to manufacturer's instructions	Biologend /San Diego, USA)
<b>Ki67</b>	SolA15	Fluorochrome	Rat	FC	According to manufacturer's instructions	eBioscience (San Diego, USA)
<b>CERS2</b>	-	-	Rabbit	FC WB	1:200 1:1000	[191]
<b>Actin</b>	Polyclonal	-	Rabbit	WB	1:2000	Sigma-Aldrich (St. Louis, USA)
<b>Phospho-p38</b>	Polyclonal	-	Rabbit	WB	1:1000	Cell Signaling (Danvers, USA)
<b>p38</b>	Polyclonal	-	Rabbit	WB	1:1000	Cell Signaling (Danvers, USA)
<b>Tubulin</b>	YL1/2	-	Rat	WB	1:2000	Merck Millipore (Darmstadt, Germany)
<b>Rabbit IgG</b>	Polyclonal	Fluorochrome	Donkey	FC	1:800	Jackson Immuno-research (West Grove, USA)
<b>Rabbit IgG</b>	Polyclonal	HRP	Goat	WB	1:5000	Santa Cruz (Dallas, USA)
<b>Rat IgG</b>	Polyclonal	HRP	Goat	WB	1:5000	Santa Cruz (Dallas, USA)

### 3.1.8 Primer for genotyping

Target locus	Primer name	Sequence (5'- ... -3')
<i>Cers2</i>	2_gen0_for	GTC AGT CTG CAT GCA GTT ACC TCT CC

<i>Cers2</i>	2_geno_rev	GAG ACA AGC ACA TCC CCA AAG CAC
<i>Cers2</i>	2_βneo	GGG ATC CAC TAG TTC TAG CCT CGA

### 3.1.9 Primer for RT-PCR

Target	Internal number	Sequence (5'- ... -3')
<i>Gapdh</i>	3	TCA CCA CCA TGG AGA AGG C
	4	GCT AAG CAG TTG GTG GTG CA
<i>Cers1</i>	73	GCC CTC TGT CTT CTA TGA CTG G
	74	GGC ATA GAT GGA GTG GCA GTA G
<i>Cers2</i>	11	GGC GCT AGA AGT GGG AAA C
	12	TCG AAT GAC GAG AAA GAG CAG G
<i>Cers3</i>	88	CAC TAT CTC GAG CCC TTC TTC
	89	CCT CTT CGT TGT CAC TCC TC
<i>Cers4</i>	67	CTG CGC ATG CTC TAC AGT TTC
	68	CCC TCG AGC CAT CCC ATT C
<i>Cers5</i>	77	TGA GAC AAC CCA CAA AAA CAA CC
	76	TGG CTT TAC AAG TCC CCT GC
<i>Cers6</i>	92	AGG GTT GAA CTG CTT CTG G
	93	GTT CCG TTG GTG GTT GTT G

## 3.1.10 Mice

Common strain name	Official strain name	Background	Description	References
<i>Cers2<sup>gt</sup></i>	<i>B6;129S4- Cers2Gt(S16-4B1)Sor/Cnrm</i>	C57BL/6J (Purity $\geq$ 98,4375%)	Derived from an ES cell clone in which the genomic locus of CERS2 was mutated by the insertion of the gene trap (gt) vector ROSAFARY. <i>Cers2<sup>+/+</sup></i> = wild type; <i>Cers2<sup>+/gt</sup></i> = heterozygous mutation; <i>Cers2<sup>gt/gt</sup></i> = homozygous mutation = CERS2-deficient.	[160, 166, 161]
<i>Cers4<sup><math>\Delta</math>neo</sup></i>	<i>Cers4<sup>tm1.1Kwi</sup>/Cnrm</i>	C57BL/6N (Purity ?)	Derived from an ES cell clone in which the genomic locus of CERS4 was mutated. <i>Cers4<sup>+/+</sup></i> = wild type; <i>Cers4<sup>+/<math>\Delta</math>neo</sup></i> = heterozygous mutation; <i>Cers4<sup><math>\Delta</math>neo/<math>\Delta</math>neo</sup></i> = homozygous mutation = CERS4-deficient.	[176]
<i>CD45.1<sup>+</sup></i>	<i>B6.SJL- Ptprc<sup>a</sup>Pepe<sup>b</sup>/BoyJ</i>	C57BL/6J (congenic)	This strain carries the differential pan leukocyte marker <i>Ptprc<sup>a</sup></i> , commonly known as CD45.1 or Ly5.1.	[192, 193, 194, 195, 196, 197, 198, 199]

## 3.2 Methods

### 3.2.1 Animal experimental methods

**3.2.1.1 Mouse breeding and husbandry** The *Cers2<sup>gt</sup>* and *Cers4<sup>Δneo</sup>* mouse strains were bred in IVCs (individually ventilated cages) under SPF-conditions (specific-pathogen free) in the animal facility of the LIMES Institute of the University of Bonn (LIMES GRC (genomic resource center)). The CD45.1<sup>+</sup> mouse strain was bred under the same conditions in the “Haus für experimentelle Therapie” (HET) of the University hospital of Bonn. All breedings and experimental procedures were approved by the LANUV NRW (Landesamt für Natur, Umwelt und Verbraucherschutz Nordrhein-Westfalen; approval numbers: 84-02.04.2011.A402 and 84-02.04.2015.A496) and conducted according to the respective institutional guidelines. In general, *Cers2<sup>+/gt</sup>* females were bred with *Cers2<sup>+/gt</sup>* males to produce *Cers2<sup>+/+</sup>* and *Cers2<sup>gt/gt</sup>* mice for experiments and analyses. The same breeding scheme was applied for the *Cers4<sup>Δneo</sup>* strain. Wild type and CERS-deficient mice of both genders (as indicated in the figure legends) were used for analyses at an age of 8 – 14 weeks. The heterozygous offspring was used for further breeding.

**3.2.1.2 Isolation of genomic DNA and genotyping of *Cers2<sup>gt/gt</sup>* mice** The genotype of mice from the *Cers2<sup>gt</sup>* strain was determined by PCR on genomic DNA from tail tips. To isolate genomic DNA, 200 µl lysis buffer plus 1 µl Proteinase K (Stock: 20 mg/ml) was added to each tail tip and samples were incubated for 3 - 4 h at 37° C under mild agitation. After the tail tip has been dissolved, samples were centrifuged for 10 min at 10000 x g and RT. The supernatant was decanted into a new 1.5 ml reaction tube, 500 µl 2-propanol were added to each sample and the tubes were inverted several times. Then, samples were centrifuged for 30 min at 12000 x g and 4° C. The supernatant was discarded and the pellet was rinsed once with 1 ml 70 % ethanol. After another centrifugation for 10 min at 10000 x g and 4° C, the supernatant was discarded and the pellet was air dried. Finally, the DNA was dissolved in 200 – 500 µl TE pH 8.0.

Lysis buffer	Component	Final concentration
	Tris-HCl	100 mM pH 8.0
	EDTA	5 mM
	SDS	0.5 %
	NaCl	200 mM
	A. bidest	

For genotyping of mice from the *Cers2<sup>gt</sup>* strain, a 3 primer strategy was applied, which generates an amplicon of 400 bp for the wild type allele and an amplicon of 564 bp for the *Cers2<sup>gt</sup>* allele (primer sequences can be found in 3.1.8). The following components and thermal cycler conditions were used:

<b>Reaction setup</b>	Component (concentration)		Volume for 1x reaction [ $\mu$ l]	
		A. bidest		12
		DMSO		0.8
		10x DreamTaq Buffer		2
		dNTP's (10 mM)		1
		2_genom_for (10 pmol/ $\mu$ l)		1
		2_kneo (10 pmol/ $\mu$ l)		1
		2_genom_rev (10 pmol/ $\mu$ l)		1
		DreamTaq		0.2
		DNA		1
		$\Sigma$		20

<b>Thermal cycler program</b>	Step	Temperature [ $^{\circ}$ C]	Time [mm:ss]	Cycles
	1	94	05:00	1x
	2	94	00:30	
	2	61	00:30	35x
	2	72	00:40	
	3	72	10:00	1x
	4	4	$\infty$	-

After the genotyping PCR was completed, amplicons were separated via agarose gel electrophoresis (2 %) to determine the genotype of the corresponding animals (see 3.2.2.1).

**3.2.1.3 Blood collection by cardiac puncture** To collect blood, mice were anesthetized with isoflurane, laid on their back and cleaned with 70 % ethanol. Without opening the abdomen or the thoracic cavity, the heart was directly punctured with a 27G needle on a 1 ml syringe and up to 1 ml blood was carefully withdrawn. Afterwards, the mice were sacrificed by cervical dislocation. To prevent coagulation, blood was either transferred into heparinized blood collection tubes (for isolation of plasma) or gently mixed with 0.5 M EDTA (up to 500  $\mu$ l blood per 50  $\mu$ l EDTA) in standard 1.5 ml reaction tubes (for isolation of PBMCs).

For the isolation of plasma, the anticoagulated blood was centrifuged in the heparinized tubes for 5 min at 2000 x g and 4 $^{\circ}$  C. Then, the plasma phase was harvested, transferred into a new 1.5 ml reaction tube and snap-frozen in liquid N<sub>2</sub>.

For the isolation of PBMCs, the anticoagulated blood was diluted with PBS containing 2 % FCS and 2 mM EDTA to a final volume of 1.2 ml and stored at RT until further processing (3.2.4.1).

**3.2.1.4 Dissection of thymi, spleens, lymph nodes and bones** To dissect lymphoid organs and bones, mice were sacrificed by cervical dislocation, laid on their back and cleaned with 70 % ethanol. First, the abdomen and the thoracic cavity were opened with

sterile dissection instruments to remove the thymus, the spleen and the inguinal lymph nodes. All organs were transferred into PBS containing 1.5 ml reaction tubes and stored on ice until further processing (3.2.4.2). Next, tibia and femur of each leg were dissected, carefully cleaned from connective and muscle tissue, transferred into 1.5 ml tubes containing PBS and stored on ice until further processing (3.2.4.5).

**3.2.1.5 Transcardial perfusion** In order to measure the precise tissue levels of different sphingolipids from whole organs by mass spectrometry, blood has to be cleared from the vessels of those organs, as it would corrupt the results by its own sphingolipid content. Therefore, mice were transcardially perfused with PBS prior to the dissection of organs for mass spectrometric analyses. First, mice were anesthetized with isoflurane, laid on their back, cleaned with 70 % ethanol and the thoracic cavity was opened. Then, a 21G butterfly needle tubed to a 50 ml syringe containing pre-chilled PBS was carefully inserted into the left ventricle and fixed, before the right atrium was incised with scissors. With gentle pressure, the mouse was perfused with PBS until the efflux from the atrium became transparent and organs like the lungs, liver and kidney turned pale. Afterwards, organs could be removed for mass spectrometric analyses.

**3.2.1.6 Generation of bone marrow chimeras** The generation of bone marrow chimeras was performed in cooperation with the Institute for Experimental Immunology (IEI) at the University hospital Bonn and conducted by Dr. Elisabeth Mettke. Therefore, this technique is just briefly described. Donor mice were sacrificed by cervical dislocation, bones were removed as described in 3.2.1.4 and bone marrow cells were isolated as described in 3.2.4.5. Recipient mice were anesthetized by an i.p. injection of ketamine (93.75 mg/kg body weight) and xylazine (6.225 mg/kg body weight) in 150  $\mu$ l saline, followed by an irradiation with 7 Gy from a Caesium-137 source for 4 min. After 4 h, recipient mice received  $0.5 - 1 \times 10^7$  bone marrow cells from the donor mice in 100  $\mu$ l saline via i.v. injection. 10 weeks post reconstitution, chimeric mice were analyzed.

**3.2.1.7 Thymus transplantation** Thymus transplantation experiments were performed in cooperation with the Institute for Experimental Immunology (IEI) at the University hospital Bonn and the surgeries were conducted by Katarzyna Jobin. Therefore, this technique is just briefly described. After neonatal donor mice were sacrificed by decapitation, the thymi were removed as described in 3.2.1.4, the lobes were separated and stored in pre-chilled PBS on ice until further processing. Male adult recipient mice were anesthetized with isoflurane and the kidney was accessed by a small incision in the right flank. Single thymus lobes of donor mice were gently transferred under the kidney capsule of the recipient. After the incision was closed, the recipients received tramal as analgesic for 2 further days. 4 to 5 weeks post transplantation, thymic grafts were analyzed.

### 3.2.2 Molecular biology

**3.2.2.1 Agarose gel electrophoresis** Nucleic acids were separated according to their size via agarose gel electrophoresis. First, agarose was added to TAE buffer (1 - 3 % (w/v), depending on the size of the nucleic acid that is to be separated) and solved via heating in a microwave. Afterwards, ethidium bromide was added (final concentration: 0.2  $\mu\text{g}/\text{ml}$ ) and the mixture was allowed to polymerize in special agarose gel cast chambers. Combs with defined numbers of teeth were inserted into the polymerizing gel to form pockets, in which the samples of interest could be loaded after the gel has hardened. Next, the polymerized gels were transferred into electrophoresis chambers, which contained TAE as running buffer, the combs were removed and the samples that have been previously mixed with 6x loading dye were loaded into the gel pockets. Additionally, a “DNA ladder”, a mixture of DNA fragments of defined sizes, was loaded into one pocket, enabling the determination of the size of the nucleic acids in the samples. Dependent on the size of the gels, electrophoretic separations were performed for 30 – 60 min at 60 - 120 V. Afterwards, nucleic acids were visualized in a transilluminator at a wavelength of 230 nm.

<b>1x TAE</b>	Component	Final concentration
	Tris	40 mM
	Acetic acid	40 mM
	EDTA	0.5 mM
	A. bidest	

<b>6x loading dye</b>	Component	Final concentration
	Bromphenol blue	0.25 %
	Xylene cyanol	0.25 %
	Glycerol	30 %
	A. bidest	

**3.2.2.2 Isolation of RNA** The isolation of RNA was performed using TRIzol reagent according to the manufacturer’s instructions. The cells of interest were harvested and pelleted by centrifugation (5 min at 300 x g and RT). The supernatant was discarded and the pellet was resuspended in TRIzol reagent to homogenize the cells (1 ml TRIzol for  $0.5 - 1 \times 10^7$  cells and 0.5 ml TRIzol for less than  $0.5 \times 10^7$  cells). Then, the samples were either stored at  $-80^\circ\text{C}$  to continue isolation at later time points or immediately processed by incubating them for 5 min at RT. Afterwards, chloroform was added to the samples (0.2 ml per 1 ml TRIzol) and the tubes were shaken for 15 s. After 3 min incubation at room temperature, samples were centrifuged for 1 min at 12000 x g and  $4^\circ\text{C}$ . The RNA-containing aqueous phase (upper phase) was transferred into a new 1.5 ml reaction tube and mixed with 2-propanol (0.5 ml per 1 ml TRIzol), followed by an incubation for 10 min at RT. The samples were centrifuged for 10 min at 12000 x g and  $4^\circ\text{C}$ , the supernatant was discarded and the RNA pellet was rinsed once by adding 70 % ethanol (1 ml per 1 ml TRIzol). After a

centrifugation for 5 min at 7500 x g and 4° C, the supernatant was discarded again and the RNA pellet was air dried. Finally, the RNA pellet was resuspended in 20 – 40 µl RNase-free water and the samples were incubated for 1 - 2 min at 55° C in heat block to dissolve the RNA. Isolated RNA samples were either further processed or stored at -80° C.

To extract RNA from tissues, freshly isolated or frozen samples were transferred into 2 ml micro tubes with an appropriate amount of acid-washed glass beads. 1 ml TRIzol per 50 - 100 mg sample weight was added to the tubes and samples were homogenized using a Precellys tissue homogenizer. The subsequent steps were carried out according to the above-mentioned protocol.

**3.2.2.3 DNaseI digestion of RNA samples** To remove contaminating genomic DNA in RNA preparations, samples were treated with DNaseI. Therefore, 2.4 µl 10x DNaseI buffer and 2 µl DNaseI were added to 20 µl of each RNA preparation and samples were incubated for 20 min at 37° C. Afterwards, 2 µl 50 mM EDTA was added (prevents RNA hydrolysis[200]) and samples were incubated for 10 min at 75° C to inactivate the DNaseI.

**3.2.2.4 Measuring RNA concentrations** The concentration of RNA was measured in a Nanodrop spectrophotometer. Based on the absorbance at 280 nm and on the ratio of the absorbance at 280 and 260 nm (280/260) the amount of RNA per µl and the purity of the sample were calculated, respectively.

**3.2.2.5 cDNA synthesis** Isolated RNA (up to 1 µg per sample) was transcribed into cDNA using the High-Capacity cDNA Reverse Transcription Kit from Applied Biosystems (Thermo Fischer). According to the manufacturer’s instructions, the following components and thermal cycler conditions were used:

Reaction setup	Component (concentration)	Volume for 1x reaction [µl]
	10x RT Buffer	2
	25x dNTP Mix (100 mM)	0.8
	10x RT Random Primers	2
	MultiScribe Reverse Transcriptase	1
	RNA	≤1 µg
	A. bidest	Ad 20
	Σ	20

Thermal cycler program	Step	Temperature [° C]	Time [hh:mm:ss]	Cycles
	1	25	00:10:00	1x
	2	37	02:00:00	1x
	3	85	00:05:00	1x
	4	4	∞	-

**3.2.2.6 RT-PCR with SYBR green** Gene expression was analyzed by SYBR green-based semi-quantitative real time PCR using the KAPA SYBR FAST qPCR Master Mix for Bio-Rad iCycler or the iTaq Universal SYBR Green Supermix from Bio-rad according to manufacturer’s instructions. These master mixes provided all essential components for RT-PCR except for the cDNA template and the primers which target the transcripts of interest. For one reaction, the reagents were mixed in the following ratios:

Reaction setup	Component (concentration)	Volume for 1x reaction [ $\mu$ l]
	cDNA	0.5
	Forward Primer (10 mM)	0.2
	Reverse Primer (10 mM)	0.2
	2x Master Mix	5
	A. bidest	4.1
	$\Sigma$	10

All RT-PCRs were performed in sealed 96-well plates in an CFX thermal cycler from Bio-Rad with the following conditions:

Thermal cycler program	Step	Temperature [ $^{\circ}$ C]	Time [mm:ss]	Cycles	Phase
	1	95	03:00	1x	Denaturation
	2	95	00:10		Denaturation
	2	58	00:30	40x	Annealing
	2	72	00:30		Elongation
	2	72	-		Measurement
	3	95 - 55	00:30 per step	1x	Melting Curve
	4	4	$\infty$	-	Hold

Relative expression of genes of interests was calculated in relation to the expression Gapdh as housekeeping gene on the basis of the  $2^{-\Delta\text{Ct}}$  method.

To detect the formation of unspecific amplicons, which would corrupt gene expression measurements, melting curve analyses were performed at the end of a successful RT-PCR run. Additionally, specificity of the RT-PCR was verified by loading the samples onto an agarose gel to analyze if the amplicons have the expected size.

### 3.2.3 Biochemistry

**3.2.3.1 Protein extraction** The cells of interest were harvested and centrifuged at 300 x g and 4 $^{\circ}$  C for 5 min. The supernatant was discarded and the cells were rinsed once with ice-cold PBS, followed by another centrifugation at 300 x g and 4 $^{\circ}$  C for 5 min. The supernatant was discarded again and the cells were resuspended in ice-cold RIPA lysis buffer containing pre-added phosphatase inhibitors and freshly added protease inhibitors (30 - 40  $\mu$ l lysis buffer per 2 x 10<sup>6</sup> cells (lymphocytes)). Samples were incubated for 5 min on ice, before they were sonicated (10 pulses at 35 - 70 %) and centrifuged for 5 min at

16000 x g and 4° C. Afterwards, the supernatant was transferred into a new 1.5 ml reaction tube and kept at 4° C for further processing or stored at -20° C. The pellet was discarded.

To isolate proteins from tissues, freshly isolated or frozen samples were minced with a small pestle in the presence of ice-cold RIPA lysis buffer containing pre-added phosphatase inhibitors and freshly added protease inhibitors within a 1.5 ml reaction tube. The subsequent steps were carried out according to the above-mentioned protocol.

<b>RIPA lysis buffer</b>	Component	Final concentration	
	NaCl	150 mM	
	Triton X-100	1 %	
	Sodiumdeoxycholate	0.5 %	
	SDS	0.1 %	
	Tris	50 mM	prepared
	Glycerol phosphate	10 mM	
	Sodium fluoride	50 mM	
	Sodium pyrophosphate	5 mM	
	Sodium orthovanadate	1 mM	
	Antipain	2 µg/ml	
	Aprotinin	10 µg/ml	freshly added
	Benzamidine	1 mM	phosphatase
	Leupeptin	10 µg/ml	inhibitors
	PMSF (saturated solution)	1:1000	

**3.2.3.2 Determination of protein concentration** The protein concentration of lysates was determined using the BCA Protein Assay Kit from Thermo Scientific according to manufacturer's instructions. This method is based on the linear dependence between the reduction of  $\text{Cu}^{2+}$  to  $\text{Cu}^{1+}$  by proteins in alkaline milieu and the subsequent colorimetric detection of  $\text{Cu}^{1+}$  by bicinchoninic acid, which can be photometrically determined by measuring the absorbance at 562 nm. In brief, 3 µl per sample were transferred into a 96-well plate, before 200 µl BCA reagent (50:1 Solution A:Solution B) was added to each well. Additionally, a BSA standard curve (0, 0.125, 0.25, 0.5, 1, 2, 4 mg/ml; 3 µl per standard) was also pipetted into the plate and mixed with 200 µl BCA reagent. After the plate was incubated for 10 min at 65° C, the absorbance at 562 nm was measured in a tecan plate reader and the protein concentration was calculated according to the BSA standard curve.

**3.2.3.3 Preparation of lysates for SDS-PAGE** After the protein concentration was successfully determined, the required volume was transferred into a new 1.5 ml reaction tube and an adequate amount of 5x sample buffer was added. Then, the samples were incubated for 5 min at 95° C to effectively denature the proteins, short spun to collect the lysates at the bottom of the tube and loaded onto an SDS gel.

5x sample buffer	Component	Final concentration
	Tris-HCl	100 mM
	SDS	4 %
	Bromphenol blue	0.1 %
	Glycerol	20 %
	DTT	200 mM

**3.2.3.4 SDS-PAGE** Via SDS-PAGE, proteins were electrophoretically separated according to their molecular weight. In contrast to nucleic acids, proteins can have complex superior structures (secondary, tertiary and quaternary) and a variable ratio of mass and charge. To enable an electrophoretic separation that only depends on the molecular weight, both of these factors need to be graded between the proteins in a lysate. SDS is an anionic detergent that performs either tasks. On the hand, it binds proteins in a direct proportionality to their mass (1.4 g SDS per g protein). Thus, the negative charge of the SDS masks the intrinsic charge of the protein, constituting a constant ratio of mass and charge. On the other hand, binding of SDS to proteins causes their denaturation, as the superior structures become unfolded. In this study discontinuous SDS gels were used for all experiments. These gels consist of an upper gel (stacking gel) with low pH (6.8) and low acrylamide concentration (5 %) and a lower gel (resolving gel) with a higher pH (8.8) and higher acrylamide concentration (8 - 12 %). Whereas the stacking gel concentrates the proteins in a sharp band, allowing their simultaneous entry into the resolving gel, the latter actually separates the proteins according to their molecular weight. Per sample, 10 or 20  $\mu$ g protein in sample buffer (3.2.3.3) were loaded onto the SDS gels. Electrophoresis was performed in running buffer at 80 V until the proteins reached the resolving gel and subsequently at 120 V until the dye front leaked into the buffer.

Discontinuous SDS-Gels	Component	Stacking Gel [ml]	Resolving Gel [ml]
	H <sub>2</sub> O	0.68	1.6 – 2.3
	Tris-HCl (1 M, pH 6.8)	0.13	-
	Tris-HCl (1.5 M, pH 8.8)	-	1.3
	Acrylamide/ Bisacrylamide (30 %)	0.17	1.3 – 2.0
	SDS 10%	0.01	0.05
	APS 10%	0.01	0.05
	TEMED	0.001	0.002
	$\Sigma$	1 ml	5 ml

10x running buffer	Component	Final concentration
	Tris	0.25 M
	Glycin	2.5 M
	SDS	1 %

**3.2.3.5 Western Blot** Separated proteins were transferred from SDS gels onto nitrocellulose membranes by Western Blotting. First, the SDS gel, a nitrocellulose membrane, 6 Whatman papers and two sponges were drenched in cooled transfer buffer. Then, the SDS gel and the nitrocellulose membrane were compressed against each other in a mini gel holder cassette by 3 Whatman papers and one sponge on each side. The cassette was placed into a blotting chamber filled with cooled transfer buffer and the transfer was performed for 2 h at 80 V and 6°C. The success of the transfer was verified by incubating the membrane for 1 - 2 min in Ponceau red solution. Ponceau S is a dye that reversibly stains proteins on nitrocellulose or PVDF membranes. After incubation in Ponceau red solution, the membrane was rinsed with TBST until an adequate contrast between the protein bands and the background was achieved.

<b>1x transfer buffer</b>	Component	Final concentration
	Glycin	192 mM
	Tris	25 mM
	Methanol	20 %
<b>1x TBST</b>	Component	Final concentration
	Tris	50 mM
	NaCl	150 mM
	Tween-20	0.05 %
<b>Ponceau Red</b>	Component	Final concentration
	Acetic acid	5 %
	Ponceau S	0.1 %

**3.2.3.6 Immunodetection of proteins** Specific proteins on nitrocellulose membranes were detected via a two-stage antibody staining and a subsequent chemoluminescence reaction. First, the membranes were rinsed once with TBST, followed by incubation with 5 % milk powder in TBST for 1 h at RT to block unspecific binding sites. Next, the blocked membranes were incubated overnight at 4°C with a primary antibody, which was diluted in 5 % milk powder in TBST and directed against the protein of interest. On the next day, the membranes were rinsed 3 times for 5 - 10 min with TBST and subsequently incubated for 1 h at RT with the secondary antibody that was coupled to HRP and directed against the host species of the primary antibody. Afterwards, the membranes were rinsed again 3 times for 5 - 10 min with TBST. Finally, the membranes were moistened with freshly prepared ECL solution (1:1 mixture of solution A and solution B) and placed in autoradiography cassettes. In the presence of H<sub>2</sub>O<sub>2</sub>, the HRP now catalyzed the oxidation of luminol (both components were included in the ECL solution), emitting chemoluminescent signals that were detected using photosensitive films. The exposure time was adjusted to the signal strength and films were developed manually or using a developing machine.

**3.2.3.7 Regeneration of membranes (Stripping)** In most cases, more than one protein was to be detected sequentially on a single nitrocellulose membrane. To remove primary and secondary antibodies from previous immunostainings, the membranes were covered with RT stripping buffer in a glass dish and placed on a heat plate that was adjusted to 150° C. After 15 - 20 min, the membranes were removed from the stripping buffer and intensively rinsed with TBST (5 - 10x for 5 - 10 min). Afterwards, membranes were ready to be blocked and stained again.

Stripping buffer (pH 6.8)	Component	Final concentration
	SDS	2 %
	Tris (pH 6.8)	62.5 mM
	$\beta$ -Mercaptoethanol	100 mM

**3.2.3.8 Extraction and mass spectrometric quantification of sphingolipids** The extraction and mass spectrometric quantification of sphingolipids was performed by Prof. Dr. Markus Gräler (Department of Anesthesiology and Intensive Care Medicine, Center for Sepsis Control and Care (CSCC), and the Center for Molecular Biomedicine (CMB), Jena University Hospital, Jena, Germany). In brief, tissue samples were mechanically homogenized and (sphingo-)lipids were isolated via methanol/chloroform extraction before they were quantified using liquid chromatography coupled to triple-quadrupole mass spectrometry (LC/MS/MS). A detailed description of the method can be found in [1, 201, 202].

### 3.2.4 Cell biology

**3.2.4.1 Isolation of PBMCs** PBMCs were isolated via density gradient centrifugation. The diluted blood (3.2.1.3) was carefully layered onto 3 ml lymphoprep density centrifugation medium in a 15 ml falcon tube and centrifuged for 20 min at 800 x g and RT. In order to protect the gradient during the deceleration process at the end of the centrifugation, the brakes of the centrifuge were switched off. The PBMC containing interphase was carefully harvested, transferred into a new 15 ml falcon tube, rinsed with 10 ml PBS and centrifuged for 10 min at 300 x g and 4° C. The supernatant was discarded and the pellet was resuspended in another 10 ml PBS, followed by a centrifugation for 10 min at 120 x g and 4° C. During this slow spin, the PBMCs were pelleted at the bottom of the tubes, whereas contaminating platelets, which were unintentionally co-harvested, remain in suspension for the most part. The (platelet-rich-)supernatant was discarded and the PBMCs were resuspended in 1 - 2 ml PBS and stored on ice until further processing.

**3.2.4.2 Isolation of lymphocytes from thymi, spleens and lymph nodes** Lymphocyte single cell suspensions from thymi, spleens and lymph nodes were prepared by placing the single organs in a 40  $\mu$ m cell strainer within a 10 cm cell culture dish that was filled with cooled PBS. Then, the organs were passed with gentle pressure through the cell

strainer using the plunger of a 10 ml syringe. The strainer was rinsed once with cooled PBS and the single cell suspension was transferred into new falcon tubes (15 ml for lymph nodes and 50 ml for thymi and spleens), followed by a centrifugation for 10 min at 300 x g and 4° C. Lymphocytes from thymi and lymph nodes were resuspended in cooled PBS and counted with a Neubauer chamber. Lymphocytes from spleens were resuspended in RBC lysis buffer (3 ml per spleen) and incubated for 2 min at RT. In this hypotonic buffer, erythrocytes, which constitute a large fraction in single cell suspensions from spleens, break, whereas the lymphocytes remain intact. Lysis was stopped by the addition of 45 ml cooled PBS. Cellular debris, which occurred during the mechanical disruption of the spleen and the subsequent RBC lysis, was removed by transferring the cell suspension through a 70 µm cell strainer into a new 50 ml falcon tube, followed by a centrifugation for 5 min at 300 x g and 4° C. After the supernatant was discarded, the cells were resuspended in cooled PBS and counted with a Neubauer chamber.

**3.2.4.3 Isolation of innate immune cells from the thymus** Thymic innate immune cells were isolated via enzymatic digestion of whole thymi applying the same protocol that was used for the isolation of TSCs (3.2.4.4).

**3.2.4.4 Isolation of thymic stromal cells (TSCs)** Isolation of TSCs was performed via enzymatic digestion of thymic tissue according to [203]. In brief, thymi were cut into small pieces and transferred in a new 50 ml falcon tube, filled with 20 ml pre-chilled RPMI. Thymocytes were released from the fragments via repeated resuspension with a 20 ml serological pipette. After the fragments had settled, the thymocyte rich supernatant was discarded and the fragments were transferred into a new 1.5 ml reaction tube containing 600 - 700 µl digestion medium (RPMI containing a mix of liberase (TM, 0.5 WU/ml) and DNaseI (50 - 375 U/ml)), followed by an incubation at 37° C for 10 - 15 min. Next, the fragments were gently agitated using a 1000 µl pipette tip. The fragments were allowed to settle and the supernatant was transferred into a 50 ml falcon tube containing 10 ml stopping buffer (PBS with 0.02 %BSA and 5 mM EDTA) to prevent further digestion. Then, fresh digestion medium was added to the remaining fragments and the cycle was repeated until the tissue was completely disaggregated (typically 2 - 3 times). The supernatants that were harvested in between, were all pooled in the 50 ml tube containing the stopping buffer. Eventually, cells were pelleted via a centrifugation at 500 x g for 5 min at 4° C and resuspended in fresh PBS. After counting the cells with a Neubauer chamber, TSCs were further enriched by depletion of CD45<sup>+</sup> cells via MACS (3.2.4.7).

**3.2.4.5 Isolation of bone marrow cells from tibia and femur** To isolate bone marrow cells from tibia and femur, the bones were opened at both ends with a bone scissors. Next, the bone marrow was flushed out of the bones into a 10 cm cell culture dish using a 10 ml syringe filled with cooled PBS and equipped with a 27G needle. The

bone marrow single cell suspension was transferred into a 50 ml falcon tube, rinsed with 20 - 30 ml cooled PBS and centrifuged for 10 min at 300 x g and 4° C. After the supernatant was discarded, the cells were resuspended in cooled PBS and counted with a Neubauer chamber.

**3.2.4.6 Cell counting and calculations** Cells in suspension were counted using a hemocytometer (Neubauer chamber). In a hemocytometer, a microscope slide with a grid and a cover slip form a space of specific volume that can be filled with a cell suspension of interest. The cells in the grid can be counted with a microscope and the number of cells per ml can be calculated via the known volume of the liquid column above the grid. The grid contains four large squares that are composed of 16 small squares, respectively. Generally, cells in 2 - 4 large squares were counted and the the cell number per ml was calculated according to the following formula:

$$N = \frac{n}{BS} \cdot \frac{1}{V_{BS}} \cdot D = \frac{n}{BS} \cdot \frac{1}{0.1mm^3} \cdot D = \frac{n}{BS} \cdot \frac{10^4}{1ml} \cdot D$$

N	Cell number [1/ml]
n	Counted cells
BS	Number of counted big squares
V <sub>BS</sub>	Volume of one big square (0.1 mm <sup>3</sup> )
D	Dilution factor

The numbers of lymphocyte subpopulations in thymus, spleen, lymph node, blood and bone marrow, were calculated from their relative frequencies, which were obtained by flow cytometric analyses (see 3.2.4.8), and the total cell numbers in the respective compartments, which were obtained by counting (see above).

**3.2.4.7 Magnetic activated cell sorting (MACS)** Via magnetic activated cell sorting, specific cell populations can be isolated out of single cell suspensions. In general, two different separation strategies can be applied. For positive selection, the cells of interest are stained with biotinylated antibodies and magnetic anti-biotin microbeads. Afterwards, the samples are transferred into MACS column that is placed into a magnetic field. Whereas all unstained stains pass through the column, the stained cells are retained in the magnetic field and can be flushed after the column has been removed from the magnetic field. For negative selection (depletion), all unwanted cells are stained with biotinylated antibodies and magnetic anti-biotin microbeads, followed by the same separation method as for the positive selection. In both cases, single cell suspensions were incubated with biotinylated antibodies according to manufacturer's instructions (generally  $\leq 0.25 \mu\text{g}$  per  $10^6$  cells in 100  $\mu\text{l}$  volume for 20 min at 4° C) to label the wanted/unwanted cells. Afterwards, cells were rinsed with 2 ml cooled MACS buffer per  $10^7$  cells and centrifuged for 5 min at 300 x g and 4° C. After the supernatant was discarded, cells were resuspended in 80  $\mu\text{l}$  cooled MACS

buffer per  $10^7$  cells and 20  $\mu$ l anti-Biotin microbeads per  $10^7$  cells were added to the samples, followed by an incubation for 10 min at 4° C. Cells were rinsed again with 2 ml cooled MACS buffer per  $10^7$  cells, centrifuged for 5 min at 300 x g and 4° C and resuspended in 500  $\mu$ l cooled MACS buffer per  $10^8$  cells. The subsequent magnetic separation was either performed manually or automatically using an autoMACS pro separator according to manufacturer’s instructions.

In some experiments, cells were prepared for magnetic separation by labelling them with magnetic microbeads that directly bind to specific surface markers (e.g. anti-CD45 microbeads). In these cases, the staining conditions, as well as the subsequent steps are comparable to the incubation with anti-Biotin microbeads.

MACS buffer	Component	Final concentration
	EDTA	2 mM
	BSA	0.5 %
	PBS	

**3.2.4.8 Flow cytometry** Via flow cytometry, various parameters (e.g. the size, the granularity or the (surface) expression of proteins) of single cells or other small particles can be analyzed simultaneously. In general, the cells of a single cell suspension become arranged in succession by a technique called hydrodynamic focusing, before they pass laser beams. Dependent on the size and the granularity of the cells, the light is differentially absorbed and scattered, which is measured by two detector systems. The forward scatter detector (FSC) is arranged in line with the laser beams and measures the light that passes through the cells. The bigger the cells are the less light reaches the detector. Thus, the FSC detector gives information about the cell size. Contrarily, the sideward scatter detector (SSC) is positioned in a defined angle to the laser beams and measures the light that is scattered by the cells. As this parameter is dependent on e.g. the amount of granules or other membrane compartments, the SSC detector gives information about the internal complexity of the cells. Furthermore, the lasers are able to excite several fluorochromes simultaneously, whose emission is separated from each other by specific band pass filters and finally measured by an additional set of detectors. Thus, extra- or intracellular proteins can be stained with fluorochrome-conjugated antibodies and their expression is subsequently analyzed via flow cytometry.

**3.2.4.9 Staining of cell surface proteins for flow cytometric analyses** To stain cell surface proteins for flow cytometric analyses,  $0.5 - 1 \times 10^6$  cells were harvested and transferred into special tubes for flow cytometry and rinsed with 1 ml cooled PBS. After a centrifugation for 5 min at 300 x g and 4° C, the supernatant was discarded and the cells were resuspended in 100  $\mu$ l PBS containing the antibodies against the proteins of interest (the amounts of antibodies were calculated according to the manufacturer’s instructions) and incubated for 20 min at 4° C in the dark. Next, cells were rinsed with 1 ml cooled PBS,

centrifuged for 5 min at 300 x g and 4° C, resuspended in 200 - 500 µl cooled PBS and stored briefly at 4° C until analysis on a Canto II or an LSR flow cytometer. In some experiments, PI (200 ng per sample) was added to the cells before they were measured. PI stains dead and dying cells as it passes through porous membranes and binds to DNA. Thus, it was possible to consider only living cells for analysis.

**3.2.4.10 Staining of intracellular proteins for flow cytometric analyses** Intracellular proteins were stained using the Foxp3/Transcription Factor Staining Buffer Set from eBioscience according to manufacturer's instructions. First,  $1 - 5 \times 10^6$  cells were surface stained as described above. After the final wash, the supernatant was discarded and the cells were pulse-vortexed in 1 ml PBS containing fixable viability dye from eBioscience (1:1000), followed by an incubation for 30 min at 4° C in the dark. Marking the dead cells with a fixable dye at this stage is absolutely important, as the subsequent fixation kills all cells, preventing the setting of a classical living gate by FSC/SSC characteristics during flow cytometric analysis. Next, cells were rinsed with 1 ml cooled PBS, centrifuged for 10 min at 300 x g and 4° C. After the supernatant was discarded, the cells were vortexed in the residual buffer while 1 ml FoxP3 fixation/permabilization working solution was simultaneously added. Cells were incubated for 45 min at 4° C in the dark, rinsed with 2 ml 1x permeabilization buffer and centrifuged for 10 min at 300 x g and 4° C. The supernatant was discarded and the cells were resuspended in 100 µl 1x permeabilization buffer containing the antibodies against the proteins of interest, followed by an incubation for 30 min at 4° C in the dark. If the antibody against the protein of interest was conjugated to a fluorochrome, the cells were rinsed two times with 2 ml 1x permeabilization buffer and centrifuged for 10 min at 300 x g and 4° C, before they were resuspended in 200 - 500 µl cooled PBS and stored briefly at 4° C until analysis on a Canto II or an LSR flow cytometer. If the antibody against the protein of interest was unconjugated, the cells were rinsed once with 2 ml 1x permeabilization buffer, centrifuged for 10 min at 300 x g and 4° C and resuspended in 100 µl 1x permeabilization buffer containing the secondary antibody, followed by an incubation for 30 min at 4° C in the dark. Finally, the cells were rinsed two times with 2 ml 1x permeabilization buffer and centrifuged for 10 min at 300 x g and 4° C, before they were also resuspended in 200 - 500 µl cooled PBS and stored briefly at 4° C until flow cytometric analysis.

**3.2.4.11 Annexin V staining** Apoptotic cells were detected using the Annexin V Apoptosis Detection kit from eBioscience according to manufacturer's instructions. First,  $1 - 5 \times 10^5$  cells were harvested, rinsed with 1 ml PBS and centrifuged for 5 min at 300 x g and RT. After the supernatant was discarded, the cells were washed again with 1 ml 1x binding buffer and centrifuged at the same conditions. Next, the cells were resuspended in 100 µl binding buffer containing 5 µl fluorochrome-conjugated Annexin V and incubated for 15 min at RT in the dark. Before the cells were analyzed in a flow cytometer, they were

rinsed with 2 ml 1x binding buffer, centrifuged for 5 min at 300 x g and 4° C and resuspended in 200 µl 1x binding buffer containing 5 µl PI.

## 4 Results

### 4.1 CERS2 facilitates S1P-mediated thymic egress of mature SP thymocytes into the circulation

To be able to induce effective immune responses against a broad range of pathogens, the adaptive immune system depends on an ever-changing peripheral TCR repertoire, which requires the constant production of new T cells in the thymus. After finishing their developmental program, mature SP thymocytes leave the thymus and enter the circulation along a chemoattractive S1P gradient to become part of the peripheral T cell pool. Although it is known that this S1P gradient results from low S1P levels in the thymus parenchyma and high S1P levels in the perivascular space and in the blood, its exact architecture as well as the regulatory mechanisms that control S1P-mediated thymic egress are insufficiently understood [26, 79].

We hypothesized that the CERS2-dependent regulation of the S1P precursor sphingosine might contribute to the maintenance of the S1P gradient between thymus and blood and thus facilitates the entry of terminally differentiated thymocytes into the periphery. In the first part of the present study, this hypothesis was tested by analyzing the shape of the thymic S1P gradient and the efficiency of thymic egress in wild type (*Cers2<sup>+/+</sup>*) and CERS2-deficient mice (*Cers2<sup>gt/gt</sup>*).

#### 4.1.1 Introductory remarks concerning the use of CERS2-deficient mice for the analysis of S1P-dependent thymic egress

The *Cers2<sup>gt</sup>* strain derives from an ES cell clone, in which the *Cers2* locus was mutated via random insertion of the gene trap vector ROSAFARY (see 3.1.10). Mice that are homozygous for this gene trap mutation (*Cers2<sup>gt/gt</sup>*) have no functional *Cers2* allele and totally lack expression of CERS2, as shown by RT-PCR and immunoblot analysis (Figure 4.1A - D). The *Cers2<sup>gt/gt</sup>* mice and the appropriate wild type controls (*Cers2<sup>+/+</sup>*) that were used in this study were generated by intercrossing *Cers2<sup>+ /gt</sup>* mice. CERS2-deficient mice exhibit severe phenotypes, such as decreased body size and increased mortality, which reduces the frequency of *Cers2<sup>gt/gt</sup>* mice within litters of *Cers2<sup>+ /gt</sup>* intercrossings already 3 weeks after birth from the expected 25 % (Mendelian ratio) to below 10 % (Figure 4.1E - G and [161]). However, a sufficient amount of *Cers2<sup>gt/gt</sup>* mice reached adulthood and could be analyzed in this study.

Worthy of note is that the reduced body size of *Cers2<sup>gt/gt</sup>* mice would skew the quantification of absolute cell numbers, which are integral parts of many analyses of the present study, towards generally fewer cells in CERS2-deficient mice. To overcome this bias, cell counts of *Cers2<sup>gt/gt</sup>* mice and of respective wild type controls are shown in two different ways throughout this manuscript. On the one hand, the results are presented as unmodified

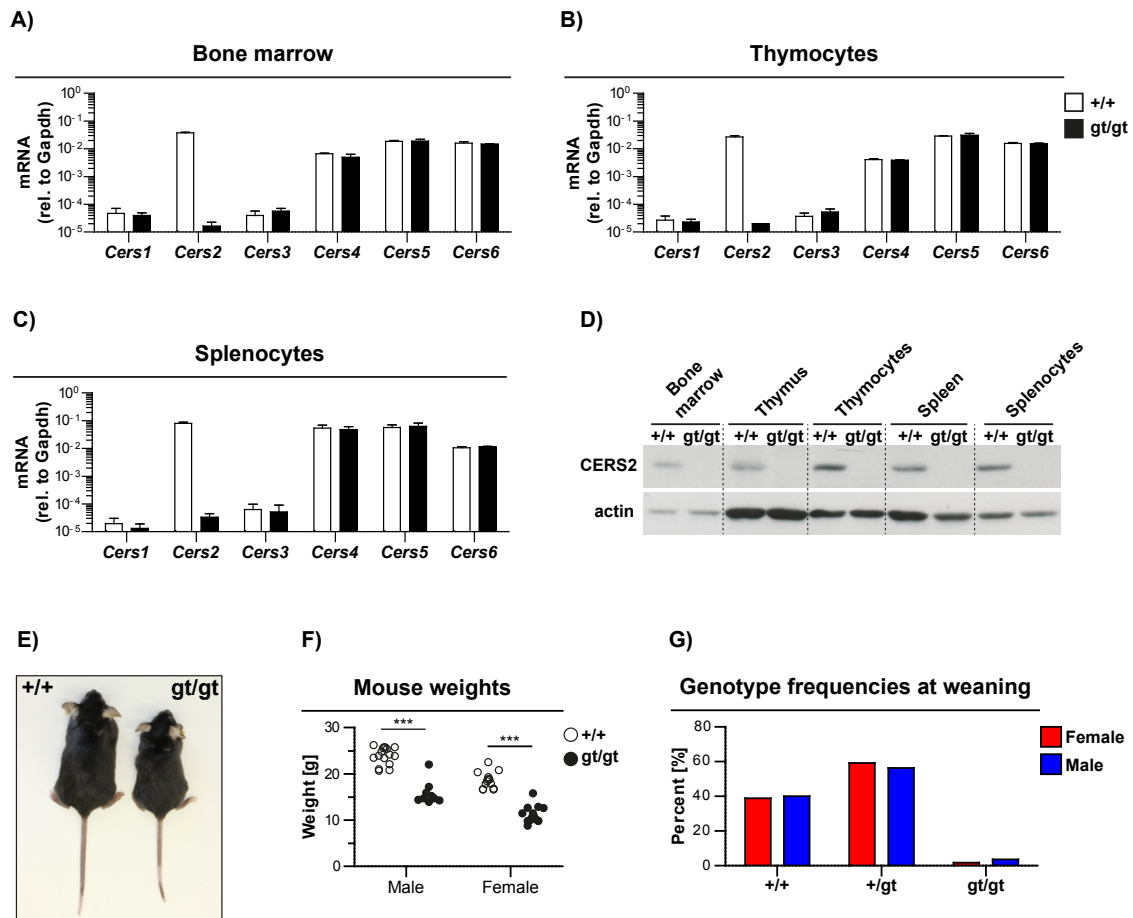


**Figure 4.1:** Basal characteristics of *Cers2*<sup>gt/gt</sup> mice. (A - C) Expression of *Cers1 - 6* in bone marrow (A), thymocytes (B) and splenocytes (C) of female wild type (+/+, white bars) and CERS2-deficient mice (gt/gt, black bars) was analyzed by RT-PCR (N = 3 mice per genotype). Expression is shown relative to that of Gapdh. Bar graphs represent means + SD. Data are pooled from 2 experiments, in which 1 - 2 mice per genotype were analyzed. (D) Levels of CERS2 and actin in lysates of bone marrow, thymus, thymocytes, spleen and splenocytes of one female wild type and one female CERS2-deficient mouse were determined by immunoblot-analysis. Data represent a single experiment. (E) Representative photo of an adult male wild type mouse and a CERS2-deficient litter mate. (F) Weights of female (N = 14 mice per genotype) and male (N = 9 - 16 mice per genotype) wild type (+/+, white dots) and CERS2-deficient (gt/gt, black dots) mice at young adulthood (8 - 14 weeks). Dots represent individual mice (Unpaired t-test; \*\*\*P < .001). Data are pooled from individual experiments, in which 1 - 2 mice per genotype were analyzed, respectively. (G) Frequencies of wild type (+/+), heterozygous (+/gt) and CERS2-deficient mice (gt/gt) at the age of weaning (3 - 4 weeks after birth), originating from heterozygous parental intercrossings (+/gt x +/gt). In total, 162 newborn female (red bars) and 190 newborn male (blue bars) mice were analyzed. Bar graphs represent the percentage of the genotypes within all females and males, respectively. The data of panel F were already published in [1].

numbers (shown as cell count and denoted as raw data). On the other hand, the results are presented as numbers that have been normalized to the average mouse weights of wild type and CERS2-deficient mice (shown as cell count per g mouse and denoted as weight corrected data). For weight correction, the following average weights were used: male wild type mice = 23.9 g, male CERS2-deficient mice = 15.8 g, female wild type mice = 18.6 g and female CERS2-deficient mice = 11.2 g (Figure 4.1F). The descriptions in the main text of the results part refer exclusively to the weight corrected data, unless indicated

otherwise. All figures, in which the results are shown in this dual manner can be found in the following list: Figure 4.2, Figure 4.4A and B, Figure 4.5A and B, Figure 4.6D and F, Figure 4.17B and C.

Additionally, it should be remarked that the thymi of female CERS2-deficient mice harboured generally fewer cells than their wild type controls, while the overall number of thymocytes in male CERS2-deficient mice was even slightly increased compared to male wild type controls (Figure 4.2). A similar gender-specific phenotype was not found in any other lymphoid or non-lymphoid organ of CERS2-deficient mice (data not shown). As a consequence of this thymus-specific sexual dimorphism, quantifications of thymocyte subpopulations from *Cers2<sup>gt/gt</sup>* mice, which are key read-outs for the present study, are shown separately for male and female mice throughout this manuscript (affected figures include Figure 4.4, Figure 4.5 and Figure 4.17). The results of all other analyses are not separated for genders.

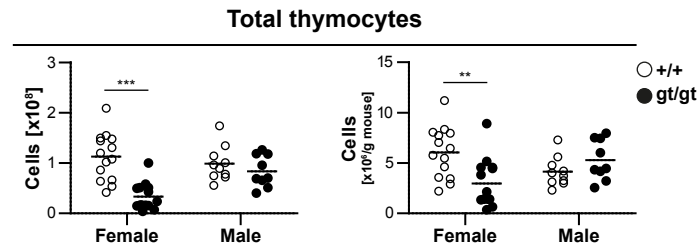


**Figure 4.2:** CERS2-deficiency reduces thymocyte numbers in female but not in male mice. Quantification of total thymocyte counts in thymi of female (N = 14 mice per genotype) and male (9 - 10 mice per genotype) wild type (+/+, white dots) and CERS2-deficient (gt/gt, black dots) mice. Results are shown as counts (left, raw data) and as counts per g mouse (right, weight corrected data). For weight correction, total counts were normalized to the average mouse weights of female and male wild type and CERS2-deficient mice, respectively, (see 4.1.1). Dots in scatter plots represent individual mice and black lines represent means (Unpaired t-test; \*\*P<.01, \*\*\*P<.001). Data are pooled from individual experiments, in which 1 - 2 mice per genotype were analyzed.

### 4.1.2 CERS2-deficiency impairs thymic egress

Based on several groundbreaking studies, thymic emigration along the S1P gradient is currently regarded as a two-stage process. First, terminally differentiated thymocytes are chemotactically recruited from the medulla into the perivascular space by the intrathymic part of the S1P gradient. Second, the thymocytes transmigrate from the perivascular space into the circulation in response to the steep S1P gradient that exists between thymus and blood [79].

To investigate if CERS2-deficiency affects emigration of terminally differentiated thymocytes into the periphery, frequencies and total numbers of immature and mature SP thymocytes in thymi of wild type and CERS2-deficient mice were determined by flow cytometry. Whereas immature cells are still in the process of negative selection and are consequently not allowed to leave the thymus, mature SP thymocytes have completed negative selection, express S1PR1 and are thus competent to emigrate via the S1P gradient into the circulation (see 1.3.2 and [89]). Immature and mature SP thymocytes were discriminated on the basis of differential surface expression of CD62L and CD69 (immature =  $CD62L^{\text{low}}/CD69^{\text{high}}$  and mature  $CD62L^{\text{high}}/CD69^{\text{intermediate}}$ ).

Flow cytometric analysis revealed that deficiency of CERS2 in male mice led to a significant increase in the frequencies and numbers of mature  $CD4^+/CD8^-$  and  $CD4^-/CD8^+$  thymocytes, but did not affect the numbers of immature SP thymocytes (Figure 4.3, Figure 4.4A and Figure 4.5A). The same observation was made in females, except that the difference in the numbers of mature SP thymocytes between *Cers2*<sup>+/+</sup> and *Cers2*<sup>gt/gt</sup> mice did not reach statistical significance (Figure 4.4B and Figure 4.5B). Most likely, the increase in the numbers of mature SP thymocytes in female CERS2-deficient mice is less robust than in males, because it is partially masked by the general reduction in thymic cellularity (Figure 4.2).

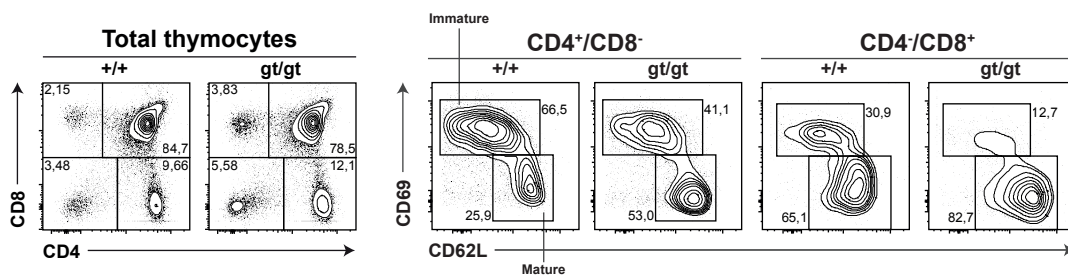


**Figure 4.3:** Representative pictures of flow cytometric identification of immature ( $CD62L^{\text{low}}/CD69^{\text{high}}$ ) and mature ( $CD62L^{\text{high}}/CD69^{\text{intermediate}}$ )  $CD4^+/CD8^-$  and  $CD4^-/CD8^+$  thymocytes in thymi of male wild type (+/+) and male CERS2-deficient mice (gt/gt). Numbers indicate percentages of subpopulations within the parental populations. This figure was taken from [1].

**Figure 4.4:** Selective accumulation of mature  $CD4^+/CD8^-$  thymocytes in thymi of CERS2-deficient mice. (A and B) Frequencies and counts of immature and mature  $CD4^+/CD8^-$  thymocytes in thymi of male (A; N = 7 - 8 mice per genotype) and female (B; N = 5 mice per genotype) wild type (+/+), white bars and dots) and CERS2-deficient (gt/gt, black bars and dots) mice were determined by flow cytometry. Results are shown as frequencies (upper panels), counts (middle panels, raw data) and counts per g mouse (lower panel, weight corrected data). For weight correction, total counts were normalized to the average mouse weights of female and male wild type and CERS2-deficient mice, respectively, (see 4.1.1). Results are separated for genders as described above (see 4.1.1). Dots in scatter plots represent individual mice and black lines represent means; bar graphs represent means + SD (Unpaired t-test; \* $P < .05$ , \*\* $P < .01$ , \*\*\* $P < .001$ ). Data are pooled from individual experiments, in which 1 - 2 mice per genotype were analyzed. The data of panel A were already published in [1]

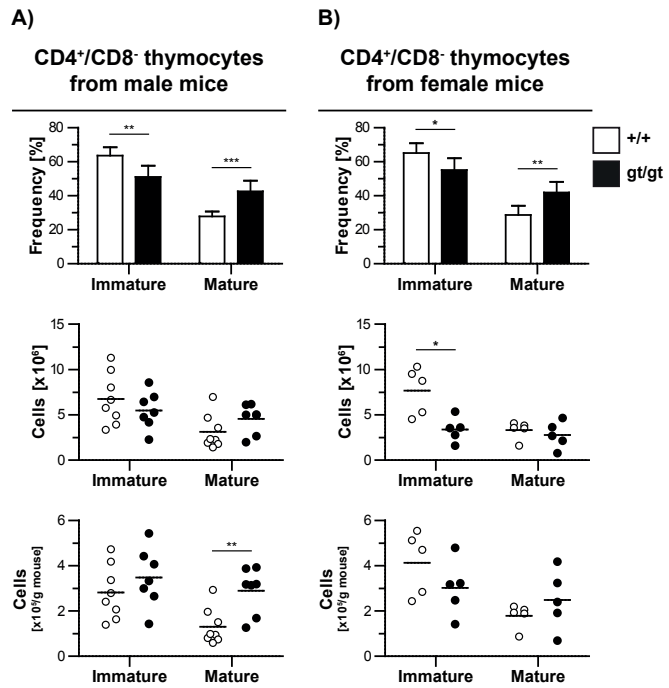
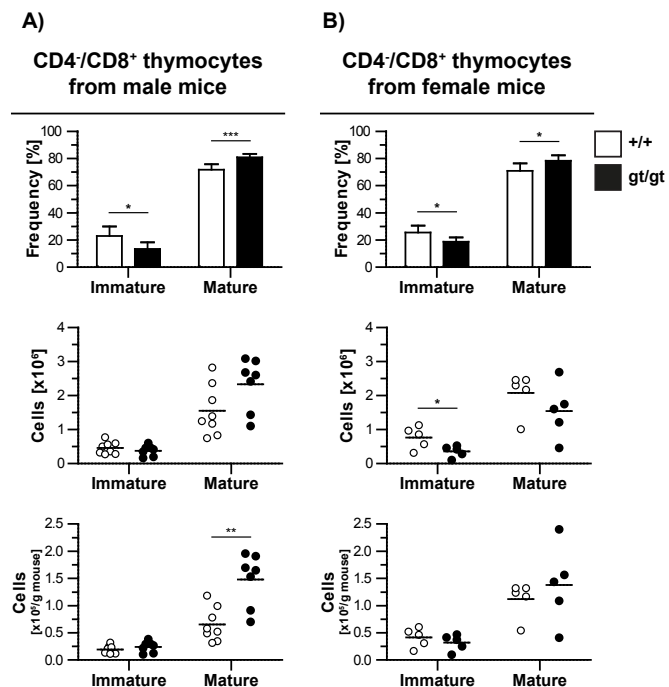


**Figure 4.5:** Selective accumulation of mature  $CD4^+/CD8^+$  thymocytes in thymi of CERS2-deficient mice. (A and B) Frequencies and counts of immature and mature  $CD4^+/CD8^+$  thymocytes in thymi of male (A; N = 7 - 8 mice per genotype) and female (B; N = 5 mice per genotype) wild type (+/+), white bars and dots) and CERS2-deficient (gt/gt, black bars and dots) mice were determined by flow cytometry. Results are shown as frequencies (upper panels), counts (middle panels, raw data) and counts per g mouse (lower panel, weight corrected data). For weight correction, total counts were normalized to the average mouse weights of female and male wild type and CERS2-deficient mice, respectively, (see 4.1.1). Results are separated for genders as described above (see 4.1.1). Dots in scatter plots represent individual mice and black lines represent means; bar graphs represent means + SD (Unpaired t-test; \* $P < .05$ , \*\* $P < .01$ , \*\*\* $P < .001$ ). Data are pooled from individual experiments, in which 1 - 2 mice per genotype were analyzed. The data of panel A were already published in [1].



In addition to the quantification of immature and mature SP thymocytes, we determined the numbers of CD4<sup>+</sup> and CD8<sup>+</sup> T cells in blood, spleen and lymph nodes of *Cers2*<sup>+/+</sup> and *Cers2*<sup>gt/gt</sup> mice, as it was demonstrated by numerous studies that alterations in thymic egress also affect the size of peripheral T cell populations [78, 89, 91, 93, 97]. Robustly reduced numbers of CD4<sup>+</sup> and CD8<sup>+</sup> T cells were found in blood and spleen of *Cers2*<sup>gt/gt</sup> mice, compared to wild type controls (Figure 4.6A and D). Surprisingly, the T cell numbers in lymph nodes were largely unaffected by ablation of CERS2 (Figure 4.6E and F).

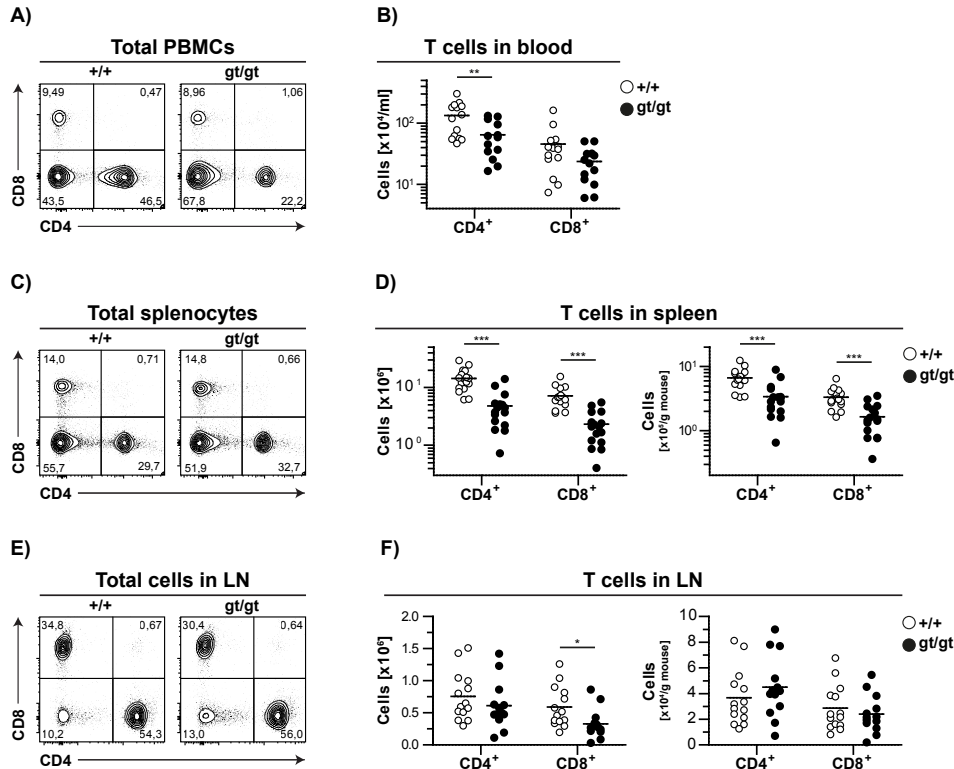


**Figure 4.6:** Reduced T cell numbers in blood and spleen of CERS2-deficient mice. (A and B) Numbers of CD4<sup>+</sup> and CD8<sup>+</sup> T cells in the blood of wild type (+/+, white dots) and CERS2-deficient mice (gt/gt, black dots) were determined by flow cytometry. (A) Representative pictures of flow cytometric identification of CD4<sup>+</sup> and CD8<sup>+</sup> T cells in the blood. (B) Results are shown as counts per ml blood; (N = 13 - 14, 5 female and 8 - 9 male mice per genotype). (C and D) Numbers of CD4<sup>+</sup> and CD8<sup>+</sup> T cells in the spleen of wild type and CERS2-deficient mice were determined by flow cytometry. (C) Representative pictures of flow cytometric identification of splenic CD4<sup>+</sup> and CD8<sup>+</sup> T cells. (D) Results are shown as counts (left panel, raw data) and counts per g mouse (right panel, weight corrected data); (N = 16 - 17; 8 female and 8 - 9 male mice per genotype). (E and F) Numbers of CD4<sup>+</sup> and CD8<sup>+</sup> T cells in the inguinal lymph nodes of wild type and CERS2-deficient mice were determined by flow cytometry. (E) Representative pictures of flow cytometric identification of CD4<sup>+</sup> and CD8<sup>+</sup> T cells in inguinal lymph nodes. (F) Results are shown as average counts of both inguinal lymph nodes (left panel, raw data) and average counts from both inguinal lymph nodes per g mouse (right panel, weight corrected data); (N = 13 - 14; 6 female and 7 - 8 male mice per genotype). (A - F) Numbers in dot plots indicate the percentages of CD4<sup>+</sup> and CD8<sup>+</sup> T cells within the parental populations. Dots in scatter plots represent individual mice and black lines represent means (Unpaired t-test, \*P<0.5, \*\*P<.01, \*\*\*P<.001). For weight correction, total counts were normalized to the average mouse weights of female and male wild type and CERS2-deficient mice, respectively, (see 4.1.1). Data are pooled from individual experiments, in which 1 - 3 mice per genotype were analyzed. Parts of panel B and D (male data) were already published in [1].

Worthy of note is that except for a reduced percentage of CD4<sup>+</sup> T cells within the PBMCs, the frequencies of CD4<sup>+</sup> and CD8<sup>+</sup> T cells were not significantly altered in all analyzed compartments of wild type and *Cers2<sup>gt/gt</sup>* mice, indicating that CERS2-deficiency only affects the cellularity but not the composition of peripheral lymphoid organs (Figure 4.6A, C, and E).

However, peripheral T cell homeostasis is not only dependent on stable thymic egress, but also on other processes, such as differentiation, proliferation or apoptosis [184, 204, 205, 206, 207]. Consequently, we investigated if these processes are altered in CERS2-deficient mice. First, the frequencies of naive, central memory and effector memory cells within the CD4<sup>+</sup> and CD8<sup>+</sup> T cell populations of blood and spleen from *Cers2<sup>+/+</sup>* and *Cers2<sup>gt/gt</sup>* mice were determined by flow cytometry to determine if CERS2-deficiency alters the differentiation of naive into memory T cells. T cell subsets were discriminated on the basis of differential surface expression of CD44 and CD62L (naive = CD44<sup>low</sup>/CD62L<sup>high</sup>; central memory = CD44<sup>high</sup>/CD62L<sup>high</sup>; effector memory = CD44<sup>high</sup>/CD62L<sup>low</sup>). Except for a slight but significant shift from more naive to less effector memory CD4 T cells in CERS2-deficient mice, no alterations in the frequencies of T cell subsets were observed in *Cers2<sup>gt/gt</sup>* mice compared to *Cers2<sup>+/+</sup>* mice (Figure 4.7).

Second, to examine if CERS2-deficiency increases the levels of cellular stress, which might e.g. impair (T cell) proliferation [208], the amounts of phosphorylated p38 in protein lysates of total spleens and of isolated splenocytes from wild type and CERS2-deficient mice were determined by immunoblot analysis. P38 is a MAP kinase, which is phosphorylated and activated by different upstream kinases in response to a diverse range of cellular stressors, like UV radiation, growth factors or certain ceramides [128, 209]. After activation, p38 can activate various downstream targets to induce repair or protective mechanisms [208]. *Cers2<sup>gt/gt</sup>* mice exhibited similar levels of phospho-p38 in total spleens and isolated splenocytes compared to *Cers2<sup>+/+</sup>* mice (Figure 4.8A and B).

Third, to explore if CERS2-deficiency affects the viability of peripheral T cells, the frequencies of living cells within splenic CD4<sup>+</sup> and CD8<sup>+</sup> T cells from *Cers2<sup>+/+</sup>* and *Cers2<sup>gt/gt</sup>* mice were determined by flow cytometry. Living cells were identified by the absence of Annexin 5 on the surface. Comparable frequencies of living cells within the T cell populations were found in *Cers2<sup>+/+</sup>* and *Cers2<sup>gt/gt</sup>* mice (Figure 4.8C and D).

Taken together, the combination of a selective accumulation of egress-competent mature SP thymocytes in the thymus with a robust peripheral T cell lymphopenia, which is not caused by alterations in differentiation, proliferation and apoptosis, clearly suggests that CERS2-deficiency leads to an impaired thymic egress.

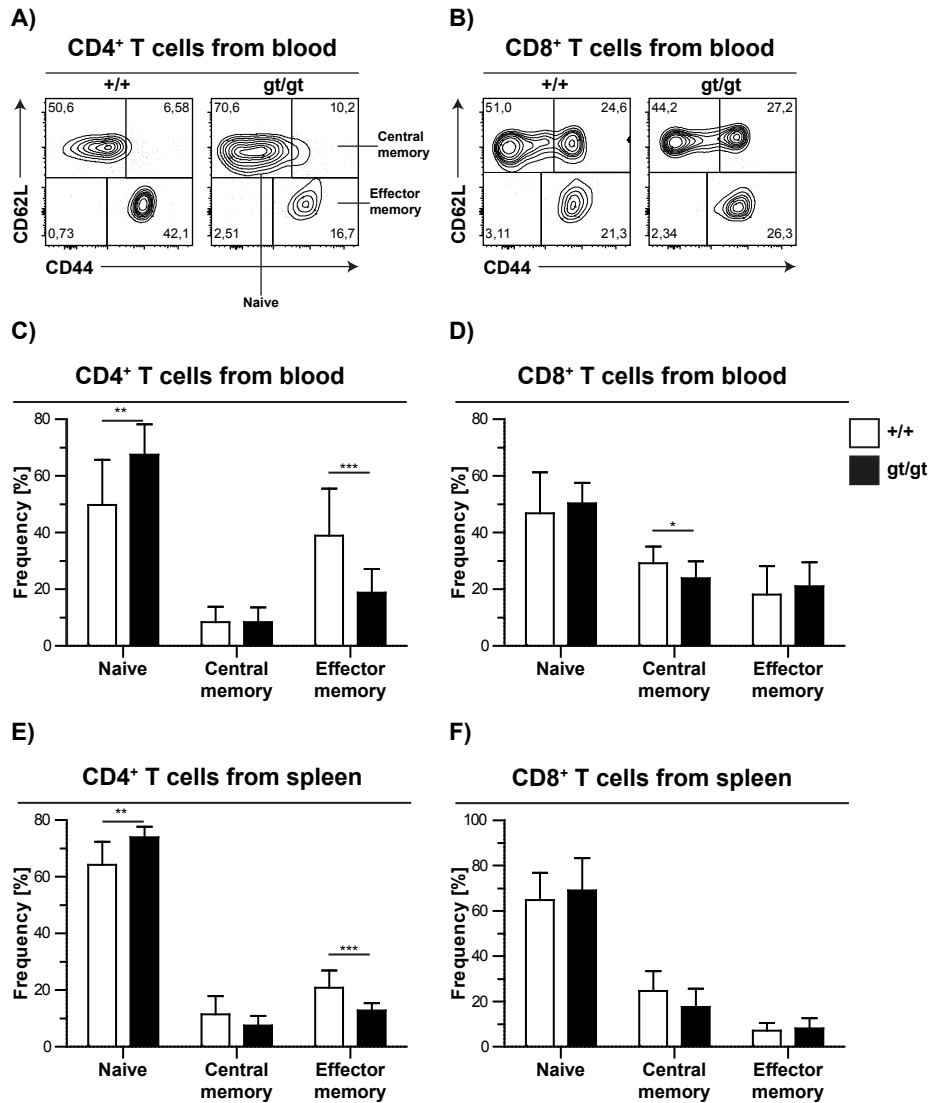


**Figure 4.7:** CERS2-deficiency has only minor effects on the differentiation of peripheral T cells. Percentages of naive, central memory and effector memory cells within CD4<sup>+</sup> and CD8<sup>+</sup> T cell populations in the blood and the spleen of wild type (+/+; white bars) and CERS2-deficient mice (gt/gt, black bars) were determined by flow cytometry. (A and B) Representative pictures of flow cytometric identification of naive (CD62L<sup>+</sup>/CD44<sup>-</sup>), central memory (CD62L<sup>+</sup>/CD44<sup>+</sup>) and effector memory (CD62L<sup>-</sup>/CD44<sup>+</sup>) cells within CD4<sup>+</sup> (A) and CD8<sup>+</sup> (B) T cell populations from blood. Numbers indicate the percentages of subpopulations within the parental populations. (C and D) Percentages of naive, central memory and effector memory cells within CD4<sup>+</sup> (C) and CD8<sup>+</sup> (D) T cell populations from blood (N = 13 - 14; 5 female and 8 - 9 male mice per genotype). (E and F) Percentages of naive, central memory and effector memory cells within CD4<sup>+</sup> (E) and CD8<sup>+</sup> (F) T cell populations from spleen (N = 11 - 12; 4 female and 7 - 8 male mice per genotype). Bar graphs represent means + SD (Unpaired t-test, \*P < .05, \*\*P < .01, \*\*\*P < .001). Data are pooled from individual experiments, in which 1 - 3 mice per genotype were analyzed.

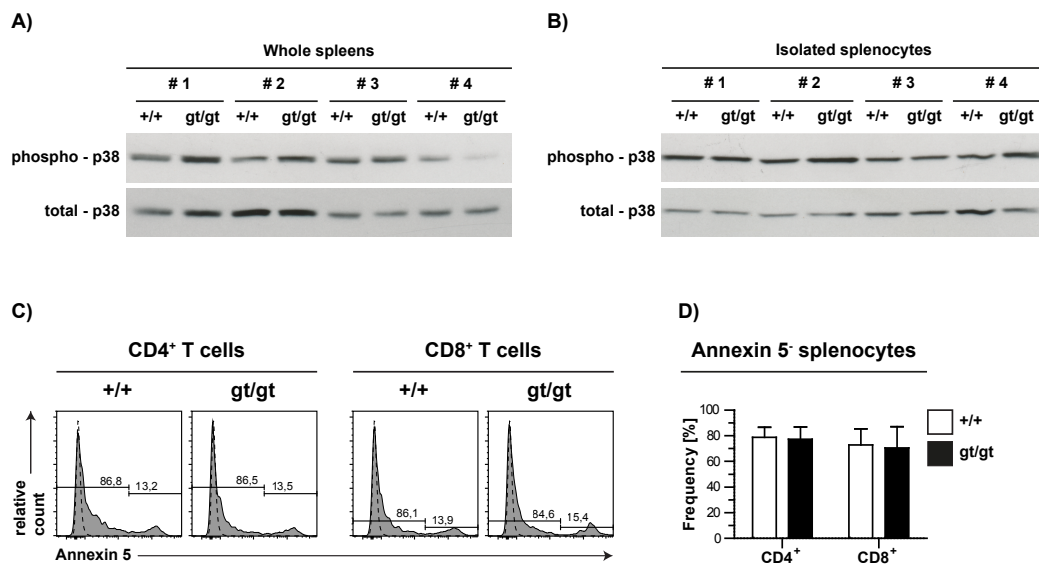


**Figure 4.8:** No aberrant cellular stress and cell death in splenocytes from CERS2-deficient mice. (A and B) Levels of phosphorylated and total p38 in lysates of whole spleens (A) and isolated splenocytes (B) of wild type (+/+) and CERS2-deficient (gt/gt) mice were determined by immunoblot-analysis (N = 4; 2 female (No. 1 - 2) and 2 male (No. 3 - 4) mice per genotype). Data are from a single experiment. (C and D) Viability of splenic CD4<sup>+</sup> and CD8<sup>+</sup> T cells from wild type (+/+, white bars) and CERS2-deficient (gt/gt, black bars) mice was investigated by Annexin 5 surface staining and flow cytometric analysis. (C) Representative pictures of flow cytometric identification of Annexin 5<sup>-</sup> CD4<sup>+</sup> and CD8<sup>+</sup> T cells. Numbers indicate the percentages of Annexin 5<sup>-</sup> and Annexin 5<sup>+</sup> cells within the parental populations; dashed curves represent unstained controls and grey-filled curves represent samples. (D) Percentages of Annexin 5<sup>-</sup> cells within the CD4<sup>+</sup> and CD8<sup>+</sup> T cell compartments (N = 4 female mice per genotype). Bar graphs represent means + SD. Data are pooled from individual experiments, in which 1 - 2 mice per genotype were analyzed.

### 4.1.3 CERS2-deficiency distorts the S1P gradient between thymus and blood

The functional S1P gradient that mediates the chemotactic emigration of terminally differentiated thymocytes into the circulation require tightly controlled S1P levels in the thymic interstitium, in the perivascular space (i. e. at the exit sites) and in the blood. Whereas the concentration of S1P must be relatively low in the thymic parenchyma, S1P levels need to be relatively high in the perivascular space and must finally peak in the blood stream [26, 79, 97]. To investigate if CERS2-deficiency affects the S1P gradient between thymus and blood, the levels of S1P (and DH-S1P, the phosphorylated form of dihydrosphingosine, which also binds to S1PR1 [210, 211]) in whole thymi, in plasma and in RBCs of *Cers2<sup>+/+</sup>* and *Cers2<sup>gt/gt</sup>* mice were determined by LC/MS/MS. Additionally, the concentration of certain ceramides, sphingomyelins and sphingoid bases were also measured in order to verify the findings of other studies, which demonstrate that ablation of CERS2 and the related loss of VLC (very long chain) sphingolipids lead to increased levels of LC (long chain) sphingolipids, sphingosine and dihydrosphingosine [160, 166, 188]. Mass spectrometric analysis revealed that the levels of S1P and DH-S1P are robustly elevated in all analyzed compartments of *Cers2<sup>gt/gt</sup>* mice compared to *Cers2<sup>+/+</sup>* mice (Figure 4.9A - C). In contrast to plasma and RBCs, however, the elevation of thymic S1P levels was less pronounced and did not reach statistical significance. Moreover, CERS2-deficiency resulted in an almost complete loss of VLC sphingolipids (e.g. C24:1 ceramide or C24:0 sphingomyelin), a compensatory increase in LC sphingolipids (e.g. C16:0 ceramide or C16:0 sphingomyelin) and an accumulation of sphingoid bases (sphingosine and dihydrosphingosine) in all analyzed compartments, entirely confirming the results of the above-cited studies.

Although S1P is synthesized in the cytoplasm and has proven intracellular functions, it must be exported into the extracellular space to form the S1P gradient and to stimulate (other) cells via their S1P receptors [59, 69, 73]. However, as the results of mass spectrometric measurements of whole thymic tissue reflect the combined amounts of intra- and extracellular S1P, we specifically analyzed if the S1P levels are elevated in the thymic interstitium of *Cers2<sup>gt/gt</sup>* mice (to further investigate the effect of CERS2-deficiency on the thymic S1P gradient). To this end, surface expression levels of CD69 on the mature SP thymocytes from *Cers2<sup>+/+</sup>* and *Cers2<sup>gt/gt</sup>* mice were reevaluated. CD69 is an appropriate indicator for the amounts of parenchymal S1P, as it is rapidly internalized from the plasma membrane upon signaling via the S1P-S1PR1 axis [89]. Compared to cells from wild type mice, mature CD4<sup>+</sup>/CD8<sup>-</sup> and CD4<sup>-</sup>/CD8<sup>+</sup> thymocytes from *Cers2<sup>gt/gt</sup>* mice had substantially reduced surface expression levels of CD69 (Figure 4.10A - C), suggesting that CERS2-deficiency leads to a dramatic increase of the S1P concentration in thymic parenchyma. S1P-independent causes for the diminished CD69 surface levels were excluded, as CD69 surface expression on immature SP thymocytes, which are inert to S1P stimulation, was not affected in *Cers2<sup>gt/gt</sup>* mice.

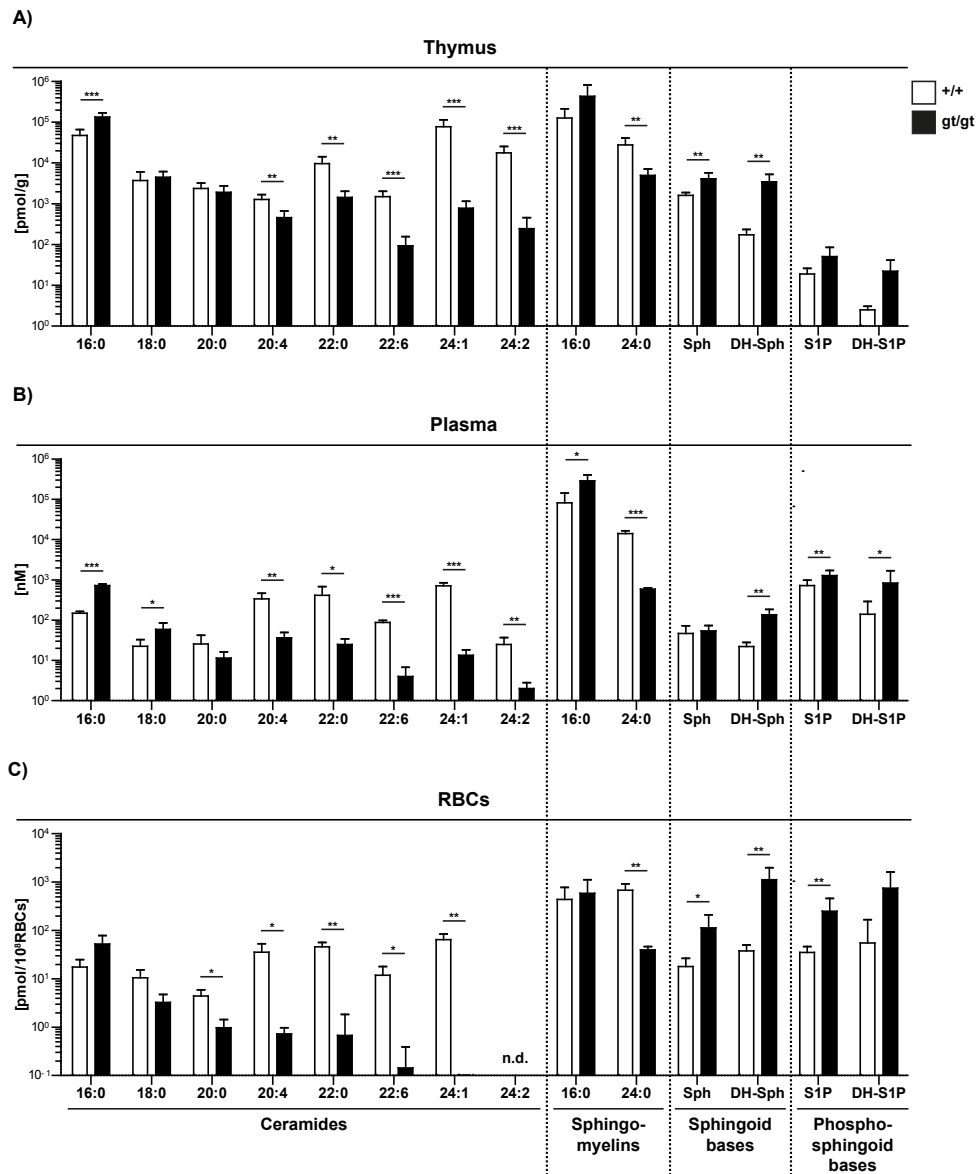


**Figure 4.9:** CERS2-deficient mice lack very long chain sphingolipids, but accumulate long chain sphingolipids, sphingoid bases and phosphorylated sphingoid bases in thymus, plasma and RBCs. (A - C) Amounts of common ceramides (C16:0, C18:0, C20:0, C22:0, C22:6, C24:1 and C24:2), sphingomyelins (C16:0 and C24:0), sphingoid bases (Sph = sphingosine and DH-Sph = dihydrosphingosine) and phosphorylated sphingoid bases (S1P = sphingosine-1-phosphate and DH-S1P = dihydrosphingosine-1-phosphate) in thymus (A, whole organs, shown as pmol/g tissue, N = 4 - 6, 2 - 4 female and 2 male mice per genotype), plasma (B, shown as nM, N = 4 - 12, 2 - 7 female and 2 - 5 male mice per genotype) and RBCs (C, shown as pmol/10<sup>8</sup>RBCs, N = 3 - 9, 3 - 6 female and 0 - 3 male mice per genotype) of wild type (+/+, white bars) and CERS2-deficient mice (gt/gt, black bars) were measured by mass spectrometry (n.d. = not determinable = below detection limit). Bar graphs represent means + SD (Unpaired t-test; \*P<.05, \*\*P<.01, \*\*\*P<.001). Data are pooled from individual experiments, in which 2 - 4 mice per genotype were analyzed. Mass spectrometric analysis was performed by Dr. Markus Gräler (Department of Anesthesiology and Intensive Care Medicine, Center for Sepsis Control and Care (CSCC), and the Center for Molecular Biomedicine (CMB), Jena University Hospital, Jena, Germany). Parts of this figure (S1P measurements) were already published in [1].

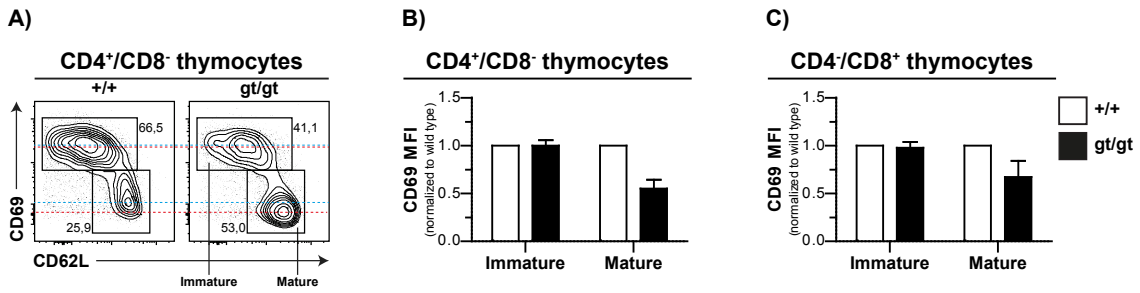


**Figure 4.10:** CERS2-deficiency leads to reduced surface expression of CD69 on mature SP thymocytes. CD69 surface expression on immature and mature  $CD4^+/CD8^-$  and  $CD4^+/CD8^+$  thymocytes from wild type (+/+, white bars) and CERS2-deficient (gt/gt, black bars) mice was analyzed by flow cytometry. (A) Representative pictures of flow cytometric analysis of CD69 surface expression on immature and mature  $CD4^+/CD8^-$  thymocytes. Blue dashed lines indicate the approximate CD69 MFIs of immature (upper) and mature (lower)  $CD4^+/CD8^-$  thymocytes from the wild type mouse. Red dashed lines indicate the approximate CD69 MFIs of immature (upper) and mature (lower)  $CD4^+/CD8^-$  thymocytes from the CERS2-deficient mouse. (B and C) CD69 MFIs (mean fluorescence intensities) of immature and mature  $CD4^+/CD8^-$  (B) and  $CD4^+/CD8^+$  (C) thymocytes were normalized to the respective wild type controls, which were set to 1 (N = 10, 5 male and 5 female mice per genotype). Bar graphs represent means + SD. Data are pooled from individual experiments, in which 1 - 2 mice per genotype were analyzed. Panels B and C were already published in [1].

Taken together, *Cers2<sup>gt/gt</sup>* mice exhibited substantially elevated levels of S1P in the plasma, in RBCs and in the thymic interstitium, besides the expected loss of VLC sphingolipids and the increased concentrations of LC sphingolipids and sphingoid bases. These findings indicate that ablation of CERS2 dramatically distorts the S1P gradient between thymus and blood.

#### 4.1.4 Summary

In the first part of this study we investigated via comparative analyses of *Cers2<sup>+/+</sup>* and *Cers2<sup>gt/gt</sup>* mice if the CERS2-dependent regulation of sphingosine levels is important for the stability of the thymic S1P gradient and thus for efficient emigration of terminally differentiated thymocytes into the circulation. We found that CERS2-deficiency did not only lead to an accumulation of sphingosine, but also to robustly elevated levels of S1P, which strongly distort the S1P gradient at the interface of thymus and blood. Consistently, thymic egress was impaired in *Cers2<sup>gt/gt</sup>* mice, which was indicated by an accumulation of egress-competent mature SP thymocytes in the thymus and a concomitant peripheral T cell lymphopenia. Based on these findings, we concluded that the regulation of sphingosine by CERS2 is an important mechanism to maintain the functional S1P gradient between thymus and blood and to facilitate efficient thymic egress.

## 4.2 S1P-mediated thymic egress is not regulated by CERS2 in thymic stromal or hematopoietic cells

The S1P gradient that facilitates the emigration of terminally differentiated thymocytes into the circulation result from low S1P levels in the thymic parenchyma but high S1P concentrations in the perivascular space and in the blood. Although its exact architecture is still incompletely understood, it was demonstrated that the thymic S1P gradient depends on many different cell types, including intrathymic hematopoietic cells (such as DCs or thymocytes), intrathymic non-hematopoietic cells (stroma cells, such as thymic epithelial cells (TECs), vascular endothelial cells (ECs) or neural crest-derived pericytes), extrathymic hematopoietic cells (such as erythrocytes or platelets) and extrathymic non-hematopoietic cells (such as vascular endothelial cells (ECs) or hepatocytes) [97, 92, 89, 91, 78, 98, 212]. Whereas DCs, thymocytes and TECs maintain low S1P levels in parenchyma via the expression of S1P lyase and LPP3 [89, 91], neural crest-derived pericytes keep up high S1P levels in the perivascular space, via the synthesis of S1P by SPHKs [92]. In contrast to these cell types, which exclusively regulate the intrathymic S1P micromilieu, the main role of erythrocytes, platelets and hepatocytes is to maintain the extremely high concentration of S1P in the blood [97, 99]. The function of endothelial cells is rather complex. On the one hand, it is assumed that these cells limit the amounts of S1P in the perivascular space via the expression of LPP3 to shape the S1P gradient on the abluminal side of the blood vessels [89]. On the other hand, ECs also contribute to the maintenance of the high S1P levels in the circulation by secreting considerable amounts of S1P into the blood, mediated by SPNS2 [78]. However, whereas the first described function of endothelial cells is of course restricted to those cells that form blood vessels within the thymus (intrathymic ECs), the second function is presumably fulfilled by all vascular ECs of the organism (extrathymic ECs).

In the first part of this study it was discovered that CERS2 is an additional factor that contributes to the maintenance of the thymic S1P gradient. In the second part, it was consequently investigated, in which cell types CERS2 is required to exert this function. To identify possible candidates, flow cytometric analysis was performed to measure CERS2 expression in all of the above-mentioned cell types. For technical reasons, erythrocytes and platelets were not included in this analysis. Furthermore, hepatocytes were also not considered, as the high expression of CERS2 in the liver was already proven by other studies [160, 166]. In return, macrophages were included, although a role of these cells for S1P-mediated thymic egress has not been documented yet. Flow cytometric analyses revealed that CERS2 is robustly expressed in all analyzed cell types (Figure 4.11A - D). This broad expression did not lead to the identification of possible candidates, in which CERS2 might be essential for the maintenance of thymic S1P gradients, but rather suggested that CERS2 could exert this function in any of the tested cell types. However, as investigations on the individual role of CERS2 in all of these cell types were beyond the scope of this study, it was decided to investigate alternatively if CERS2 is generally required in hematopoietic

or thymic stromal cells to maintain the chemoattractive S1P gradient between thymus and blood. To this end, bone marrow reconstitution and thymus transplantation experiments were performed.

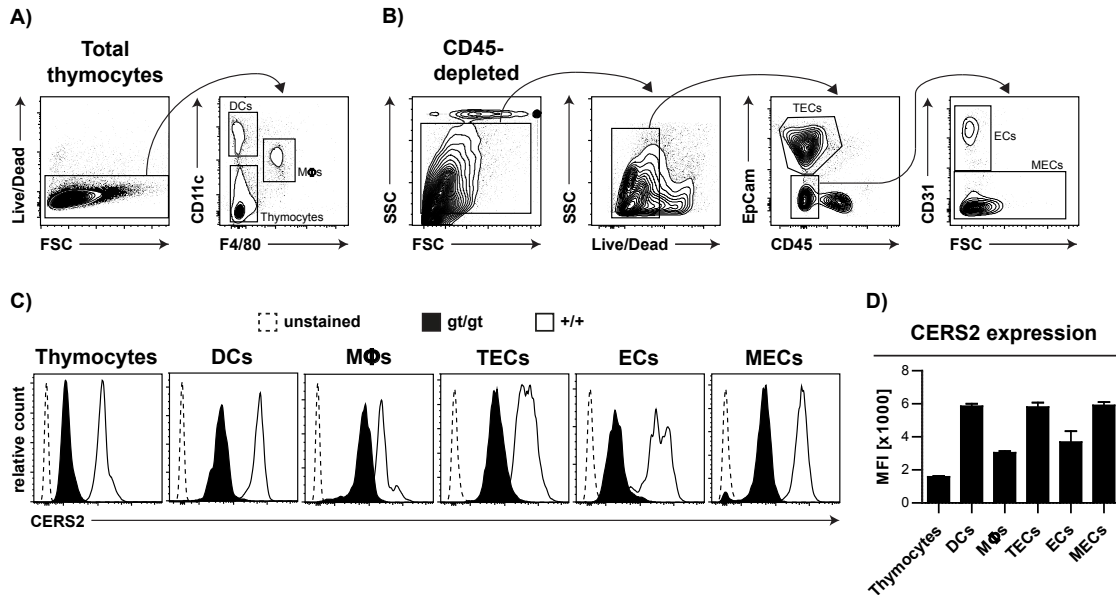


**Figure 4.11:** CERS2 is expressed in all major hematopoietic and non-hematopoietic cell types of the thymus. CERS2 expression in thymocytes, dendritic cells (DCs), macrophages (MΦs), thymic epithelial cells (TECs), vascular endothelial cells (ECs) and mesenchymal cells (MECs) was determined by intracellular staining and subsequent flow cytometric analysis. Before thymic stromal cells were stained against CERS2, they were pre-enriched by depletion of hematopoietic cells via MACS using CD45-microbeads (see 3.2.4.4, 3.2.4.7 and 3.2.4.10). (A) Gating strategy for flow cytometric identification of thymocytes ( $CD11c^-/F4/80^-$ ), thymic dendritic cells (DCs,  $CD11c^+/F4/80^-$ ) and macrophages (MΦs,  $CD11c^{intermediate}/F4/80^+$ ), according to [213]. (B) Gating strategy for flow cytometric discrimination between thymic epithelial cells (TECs,  $CD45^+/EpCam^+$ ), vascular endothelial cells (ECs,  $CD45^-/EpCam^-/CD31^+$ ) and neural crest-derived mesenchymal cells (MECs,  $CD45^-/EpCam^-/CD31^-$ ); with minor modifications according to [214]. (C) Representative pictures of flow cytometric quantification of CERS2 expression in all analyzed cell types. Cells from wild type mice (+/+), continuous lines) were used to investigate CERS2 expression. Cells from CERS2-deficient mice (gt/gt, black, filled curves) were used as specificity control for the CERS2 staining. Unstained cells (dashed lines) were used as negative control for the CERS2 staining. (D) CERS2 expression in all analyzed cell types. Results are shown as MFIs (mean fluorescence intensities); (N = 3 male wild type mice for quantification and 1 CERS2-deficient mouse as specificity control). Bar graphs represent means + SD. Data are from a single experiment. This figure was taken from [1] and modified.

#### 4.2.1 CERS2 in hematopoietic cells is dispensable for S1P-mediated thymic egress

Bone marrow reconstitution allows the complete replacement of the hematopoietic system of recipient mice with that of donor mice. Initially, recipients are myeloablated by a lethal irradiation via a gamma ray source. Shortly thereafter, freshly isolated bone marrow cells from donor mice are transplanted into the irradiated recipients. Within a few weeks, donor HSCs (hematopoietic stem cells) populate the empty niches in the bone marrow and start to reconstitute the whole hematopoietic system. Mice, whose hematopoietic system has been replaced via bone marrow reconstitution, are termed bone marrow chimeras, as their hematopoietic cells have a another genetic origin than the rest of their cells. It is commom practice to use recipient and donor mice from strains, which carry different alleles of pan leukocyte surface markers, such as CD45 (CD45.1/CD45.2) or CD90 (CD90.1/CD90.2), respectively. Thus, remaining host cells and donor-derived cells are distinguishable, e.g. by flow cytometry, and the success of engraftment can be easily monitored ([215, 216] and 3.1.10).

In the present study, bone marrow reconstitution experiments were performed to examine if CERS2 is required in hematopoietic cells to maintain the chemoattractive S1P gradient between thymus and blood. For this purpose, irradiated wild type recipients (CD45.1<sup>+</sup>) were reconstituted with bone marrow from either *Cers2<sup>gt/gt</sup>* or *Cers2<sup>+/+</sup>* mice (both CD45.2<sup>+</sup>), to generate chimeras with a CERS2-deficient hematopoietic system (gt/gt → +/+) and control chimeras with a wild type hematopoietic system (+/+ → +/+). Ten weeks post reconstitution, replacement of the hematopoietic system was verified and S1P-mediated thymic egress was analyzed.

To control the reconstitution of the hematopoietic system by donor bone marrow, the frequencies of host- (CD45.1<sup>+</sup>) and donor-derived cells (CD45.2<sup>+</sup>) within total bone marrow cells, total thymocytes and total splenocytes of wild type and CERS2-deficient chimeras were determined by flow cytometry (Figure 4.12A - D). In all analyzed compartments, more than 80 % of the cells were found to be CD45.2<sup>+</sup>, clearly demonstrating a successful engraftment of the donor cells. The genotypes of the reconstituted hematopoietic cells were confirmed on a functional level by demonstrating via mass spectrometry that donor-derived thymocytes from *Cers2<sup>gt/gt</sup>* chimeras lack C24:0 ceramides and accumulate C16:0 ceramides in comparison to donor-derived thymocytes from *Cers2<sup>+/+</sup>* chimeras (Figure 4.12E). Although the analysis of wild type and *Cers2<sup>gt/gt</sup>* mice revealed that also sphingomyelins are affected by ablation of CERS2 (see 4.1.3), no alteration in the levels of C16:0 or C24:0 sphingomyelins were detected between donor-derived thymocytes from *Cers2<sup>+/+</sup>* and *Cers2<sup>gt/gt</sup>* chimeras, suggesting that the wild type environment of the recipients might be able to counterbalance the aberrant turnover of complex sphingolipids in CERS2-deficient thymocytes.

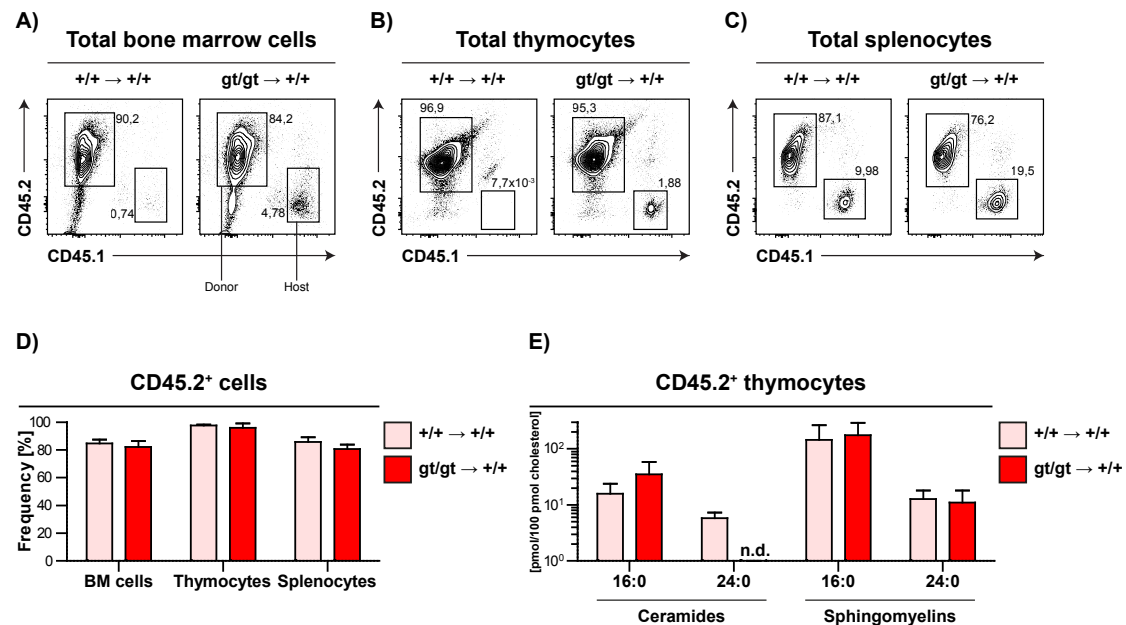


**Figure 4.12:** Successful engraftment of wild type and CERS2-deficient bone marrow into lethally irradiated wild type mice. Bone marrow chimeras were generated by reconstitution of lethally irradiated female wild type mice (CD45.1<sup>+</sup>) with bone marrow from female wild type ( $+/+ \rightarrow +/+$ , light red bars) or CERS2-deficient ( $gt/gt \rightarrow +/+$ , dark red bars) mice (both CD45.2<sup>+</sup>). 10 weeks post reconstitution, recipient mice were analyzed for successful engraftment of donor bone marrow. (A - D) Frequencies of host (CD45.1<sup>+</sup>) and donor-derived (CD45.2<sup>+</sup>) cells were determined by flow cytometry. Representative pictures of flow cytometric identification of host and donor-derived cells within bone marrow cells (A), thymocytes (B) and splenocytes (C). Numbers indicate the percentages of host and donor cells within parental populations. (D) Percentages of donor-derived cells (CD45.2<sup>+</sup>) within bone marrow cells, thymocytes and splenocytes (N = 6 chimeras per donor genotype). (E) Donor-derived thymocytes (CD45.2<sup>+</sup>) from wild type ( $+/+ \rightarrow +/+$ ) and CERS2-deficient ( $gt/gt \rightarrow +/+$ ) chimeras were negatively isolated by MACS (= depletion of CD45.1<sup>+</sup> thymocytes) and analyzed for the amounts of ceramide (16:0 and 24:0) and sphingomyelin (16:0 and 24:0) species by mass spectrometry (N = 5 - 6 chimeras per donor genotype). Results were normalized to the respective cholesterol contents and shown as pmol of ceramide or sphingomyelin per 100 pmol cholesterol. Bar graphs represent means + SD (n.d. = not determinable = below detection limit). Data are pooled from 2 - 4 independent experiments, in which 1 - 2 recipients were reconstituted with bone marrow from 1 donor mouse per genotype, respectively. Generation of bone marrow chimeras was performed in cooperation with the group of Dr. Christian Kurts (Institute for Experimental Immunology, University Hospital Bonn, Germany). Mass spectrometric analysis was performed by Dr. Markus Gräler (Department of Anesthesiology and Intensive Care Medicine, Center for Sepsis Control and Care (CSCC), and the Center for Molecular Biomedicine (CMB), Jena University Hospital, Jena, Germany). The data of panel B and parts of the data of panel D (thymocyte data) were already published in [1].

After confirming the successful reconstitution, the same key parameters of efficient S1P-mediated thymic egress that have been analyzed in the initial characterization of wild type and *CERS2*-deficient mice (see 4.1.2 and 4.1.3) were examined in *Cers2<sup>+/+</sup>* and *Cers2<sup>gt/gt</sup>* chimeras. Wild type and *CERS2*-deficient chimeras had equal concentrations of S1P in the plasma, similar frequencies and numbers of mature SP thymocytes in the thymus and comparable counts of T cells in blood and spleen (Figure 4.13A - E), collectively indicating that the functional S1P gradient is presumably not dependent on *CERS2* in the hematopoietic compartment.

Worthy of note is that the mature SP thymocytes in *Cers2<sup>gt/gt</sup>* chimeras had a decreased surface expression of CD69 compared to *Cers2<sup>+/+</sup>* chimeras, which indicates an excessive stimulation via the S1P-S1PR1 axis (Figure 4.13D and E). Consequently, it was assumed that *CERS2*-deficiency in hematopoietic cells might alter the S1P microenvironment in the thymus without disrupting the S1P gradient and the corresponding emigration of terminally differentiated thymocytes into the periphery.

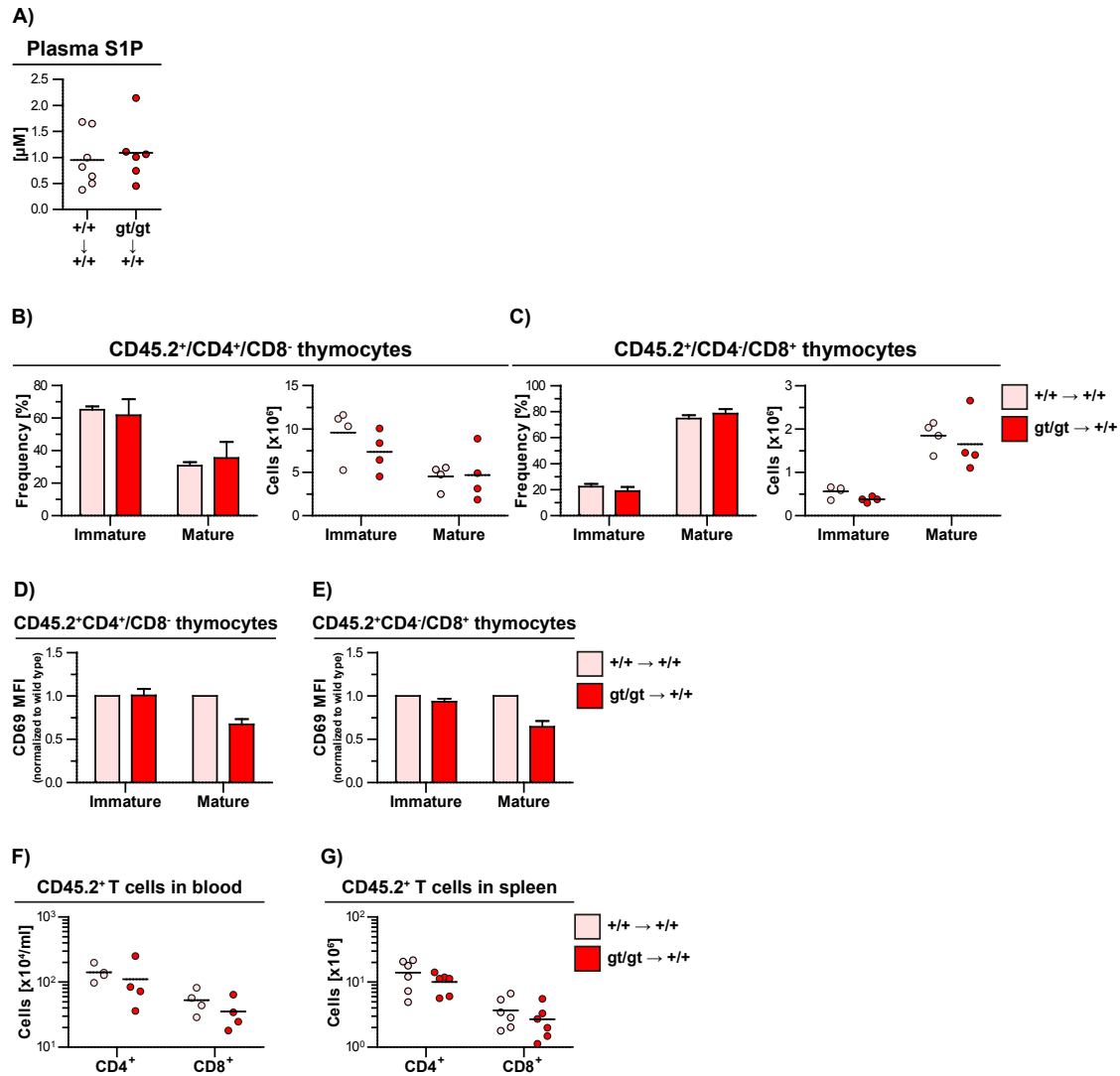


**Figure 4.13:** Deficiency of CERS2 in hematopoietic cells has no effect on thymic egress. (A) Concentration of plasma S1P from wild type and CERS2-deficient chimeras was measured by mass spectrometry (N = 6 - 7 chimeras per genotype). (B and C) Percentages (left) and counts (right) of donor-derived (CD45.2<sup>+</sup>) immature (CD62L<sup>low</sup>/CD69<sup>high</sup>) and mature (CD62L<sup>high</sup>/CD69<sup>intermediate</sup>) CD4<sup>+</sup>/CD8<sup>-</sup> (B) and CD4<sup>-</sup>/CD8<sup>+</sup> (C) thymocytes from wild type (+/+  $\rightarrow$  +/+, light red bars and dots) and CERS2-deficient chimeras (gt/gt  $\rightarrow$  +/+, dark red bars and dots) were determined by flow cytometry (N = 4 chimeras per genotype). (D and E) Flow cytometric analysis of CD69 surface expression on immature and mature CD4<sup>+</sup>/CD8<sup>-</sup> (D) and CD4<sup>-</sup>/CD8<sup>+</sup> (E) thymocytes from wild type and CERS2-deficient chimeras. Results are shown as CD69 MFIs. Data were normalized to wild type chimeras, which were set to 1 (N = 4 chimeras per genotype). (F) Total counts of donor-derived CD4<sup>+</sup> and CD8<sup>+</sup>T cells per ml blood from wild type and CERS2-deficient chimeras were determined by flow cytometry (N = 4 chimeras). (G) Total counts of donor-derived CD4<sup>+</sup> and CD8<sup>+</sup> T cells in the spleens of wild type and CERS2-deficient chimeras were determined by flow cytometry (N = 6 chimeras per genotype). Dots in scatter plots represent individual chimeras and black lines represent means; bar graphs represent means + SD. Data are pooled from 2 - 4 independent experiments, in which 1 - 2 recipients were reconstituted with bone marrow from 1 donor mouse per genotype, respectively. Generation of bone marrow chimeras was performed in cooperation with the group of Dr. Christian Kurts (Institute for Experimental Immunology, University Hospital Bonn, Germany). Mass spectrometric analysis was performed by Dr. Markus Gräler (Department of Anesthesiology and Intensive Care Medicine, Center for Sepsis Control and Care (CSCC), and the Center for Molecular Biomedicine (CMB), Jena University Hospital, Jena, Germany). The data of panels A - E were already published in [1].

#### 4.2.2 CERS2 in thymic stromal cells is dispensable for S1P-mediated thymic egress

In a thymus transplantation, thymi from fetal or neonatal donor mice are grafted under the kidney capsule of recipient mice. Within 3 - 4 weeks, the thymocytes (and other hematopoietic cells) from the donor are replaced by cells from the host, while the donor stroma remains unaltered [217]. At the end of this process, thymic grafts consist of hematopoietic cells from the host and of stroma cells from the donor, allowing the subsequent analysis of stroma-specific functions. As described for the generation of bone marrow chimeras (see 4.2.1), the donor and recipient mice that are used for thymus transplantation studies are often derived from strains, which differentially express CD45.1 and CD45.2 or CD90.1 and CD90.2. Thus, the exchange of the donor cells by hematopoietic cells from the host can be easily controlled by flow cytometry.

In this study, thymus transplantation experiments were performed to examine if CERS2 is required in thymic stromal cells to maintain the chemoattractive S1P gradient between thymus and blood. To this end, thymus lobes from neonatal *Cers2*<sup>+/+</sup> and *Cers2*<sup>gt/gt</sup> mice (both CD45.2<sup>+</sup>) were co-transplanted under the kidney capsule of wild type recipients (CD45.1<sup>+</sup>) (Figure 4.14A). The presence of a wild type (+/+ → +/+) and a CERS2-deficient thymic graft (gt/gt → +/+) in the same recipient ensured a high degree of comparability, as both lobes were populated with wild type TSPs (thymic seeding progenitor) from the same origin. Four to five weeks post transplantation, the exchange of the hematopoietic cells in the grafts was verified and S1P-mediated emigration of mature SP thymocytes into the periphery was analyzed.

To verify the replacement of hematopoietic cells from the donor by cells from the recipient, the frequencies of host- (CD45.1<sup>+</sup>) and donor-derived cells (CD45.2<sup>+</sup>) within total thymocytes in wild type and CERS2-deficient thymic grafts were determined by flow cytometry (Figure 4.14B and C). Close to 100 % of all thymocytes in both thymic grafts were found to be CD45.1<sup>+</sup>, indicating that cells from the host have completely displaced the hematopoietic cells from the donor.

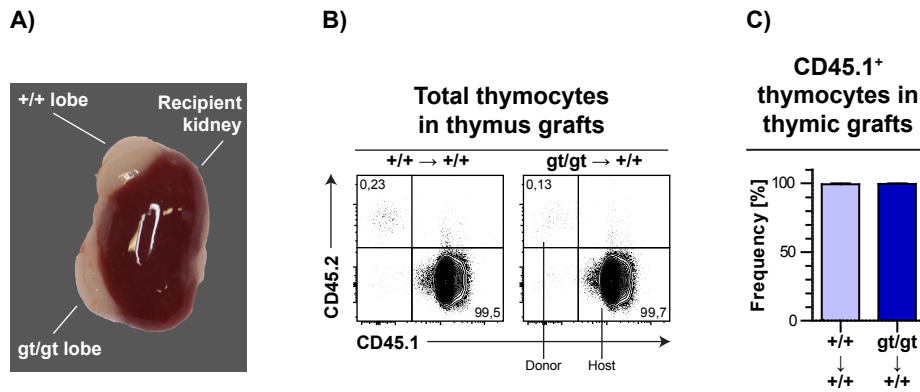
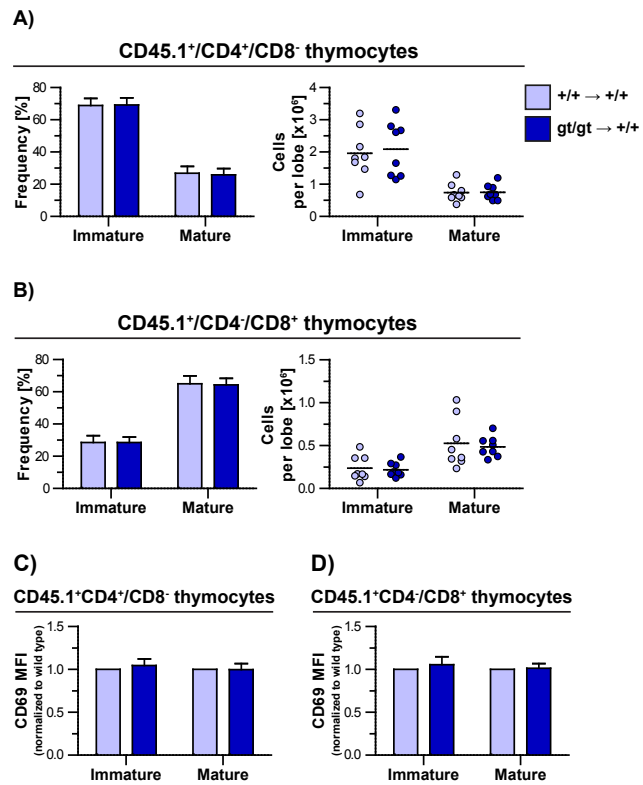


**Figure 4.14:** Successful transplantation of wild type and *CERS2*-deficient thymus lobes under the kidney capsule of wild type recipients. Lobes of wild type (+/+) and *CERS2*-deficient (*gt/gt*) thymi from neonatal mice (both  $CD45.2^+$ ) were transplanted under the kidney capsule of male wild type recipients ( $CD45.1^+$ ). 4-5 weeks after the transplantation, engraftment of donor lobes and successful replacement of donor thymocytes by cells from the host was investigated by flow cytometry. (A) Representative photo of renal grafts from wild type and *CERS2*-deficient mice 4 weeks after transplantation. The original image background was replaced with a grey area to increase contrast. (B and C) Percentages of host- ( $CD45.1^+$ ) and donor-derived ( $CD45.2^+$ ) cells in wild type (+/+  $\rightarrow$  +/+, light blue bars) and *CERS2*-deficient thymic grafts (*gt/gt*  $\rightarrow$  +/+, dark blue bars) were determined by flow cytometry. (B) Representative pictures of flow cytometric identification of host- and donor-derived cells within the thymocyte fraction. Numbers indicate the percentages of host and donor cells within the parental populations. (C) Percentages of host cells ( $CD45.1^+$ ) within the thymocyte fraction ( $N = 8$  lobes per donor genotype). Data are pooled from 4 independent experiments, in which the two thymic lobes of a wild type and a *Cers2*<sup>gt/gt</sup> lobe per recipient), respectively. Bar graphs represent means + SD. Thymus transplantation experiments were performed in cooperation with the group of Dr. Christian Kurts (Institute for Experimental Immunology, University Hospital Bonn, Germany). The data of panels B and C were already published in [1].

It was observed that wild type and *CERS2*-deficient thymic grafts harbored the same quantities of mature SP thymocytes (Figure 4.15A and B). Likewise, the surface levels of CD69 on mature SP thymocytes were comparable between both grafts (Figure 4.15C and D). These findings indicate that the functional S1P gradient is presumably also not dependent on *CERS2* in the thymic stromal compartment. Unfortunately, it was not feasible to verify this hypothesis by analyzing other key parameters of efficient thymic egress, such as the numbers of  $CD4^+$  and  $CD8^+$  T cells in blood and spleen, as all peripheral T cells in the recipients carry host signature and it is therefore impossible to determine from which thymus they entered the periphery (endogenous thymus, wild type thymus graft, *CERS2*-deficient thymus graft).

**Figure 4.15:** Deficiency of CERS2 in thymic stromal cells has no effect on thymic egress. (A and B) Frequencies (left) and counts per lobe (right) of host (CD45.1<sup>+</sup>) immature (CD62L<sup>low</sup>/CD69<sup>high</sup>) and mature (CD62L<sup>high</sup>/CD69<sup>intermediate</sup>) CD4<sup>+</sup>/CD8<sup>-</sup> (A) and CD4<sup>+</sup>/CD8<sup>+</sup> (B) thymocytes in wild type (+/+ → +/+, light blue bars and dots) and CERS2-deficient thymic grafts (gt/gt → +/+, dark blue bars and dots) were determined by flow cytometry (N = 8 lobes per genotype). (C and D) Flow cytometric analysis of CD69 surface expression on immature and mature CD4<sup>+</sup>/CD8<sup>-</sup> (C) and CD4<sup>+</sup>/CD8<sup>+</sup> (D) thymocytes from wild type and CERS2-deficient thymic grafts. Results are shown as CD69 MFIs. Data were normalized to wild type grafts, which were set to 1 (N = 8 lobes per genotype). Dots in scatter plots represent individual lobes and black lines represent means; bar graphs represent means + SD. Data are pooled from 4 independent experiments, in which the two thymic lobes of a wild type and a CERS2-deficient mouse were separated and transplanted into 2 wild type recipients (1 wild type and 1 CERS2-deficient lobe per recipient), respectively. Thymus transplantation experiments were performed in cooperation with the group of Dr. Christian Kurts (Institute for Experimental Immunology, University Hospital Bonn, Germany). The data of this figure were already published in [1].



### 4.2.3 Summary

In the second part of the present study, it was investigated if CERS2 is required in hematopoietic or thymic stromal cells to maintain the chemoattractive S1P gradient between thymus and blood. To address this issue, it was analyzed if mice, which lack CERS2 specifically in the hematopoietic or in the thymic stromal compartment, exhibit the same impairments in thymic emigration as *Cers2*<sup>gt/gt</sup> mice. Surprisingly, CERS2-deficiency in neither of both compartments affected S1P-mediated emigration of mature SP thymocytes into the circulation, clearly indicating that the thymic S1P gradient is independent of CERS2 in hematopoietic or thymic stromal cells. As discussed later, it was consequently assumed that the thymic S1P gradient requires CERS2 in non-hematopoietic extrathymic cell types, such as hepatocytes or vascular endothelial cells, as these are the only known regulators of the thymic S1P gradient, which were not covered by the bone marrow reconstitution and thymus transplantation experiments.

### 4.3 S1P-mediated thymic egress is independent of CERS4

The first two parts of this study suggest that the CERS2-dependent regulation of sphingosine is essential for the maintenance of the chemoattractive S1P gradient at the interface of thymus and blood. Apart from CERS2, however, the family of ceramide synthases comprises five other members (CERS1, CERS3 - 6), which also use sphingosine as substrate for the synthesis of different ceramides species. In the third part of this study, it was therefore investigated if the regulation of S1P-mediated thymic egress is an exclusive feature of CERS2 or if other ceramide synthases also contribute to the stabilization of the thymic S1P gradient.

To address this issue, S1P-mediated thymic egress was comparatively investigated in wild type (*Cers4*<sup>+/+</sup>) and CERS4-deficient mice (*Cers4* <sup>$\Delta$ neo/ $\Delta$ neo</sup>, see 3.1.10). CERS4 appeared to be the most promising candidate for having a similar function as CERS2, since it is the second most abundant ceramide synthase family member, with a robust expression in many of the tissues and organs that are known to be relevant for the maintenance of the thymic S1P gradient, such as the liver or the thymus [155]. In contrast to that, the other ceramide synthases are either weakly expressed (CERS5 and CERS6) or restricted to particular organs, e.g. to the brain (CERS1) or to the testes (CERS3) [155].

Levels of S1P in thymus and plasma, frequencies and numbers of mature SP thymocytes in the thymus and numbers of CD4<sup>+</sup> and CD8<sup>+</sup> T cells in blood and in spleen were comparable in wild type and CERS4-deficient mice (Figure 4.16A - D, G and H). Likewise, also the surface expression of CD69 on mature SP thymocytes was unaffected by ablation of CERS4 (Figure 4.16E and F). These findings consistently indicate that S1P-mediated thymic egress is independent of CERS4. Consequently, it was assumed that the regulation of the thymic S1P gradient is not a general function of all ceramide synthases, but is most likely specific for CERS2. However, a contribution of CERS1, CERS3, CERS5 and CERS6 to the stabilization of the gradient can not be excluded.

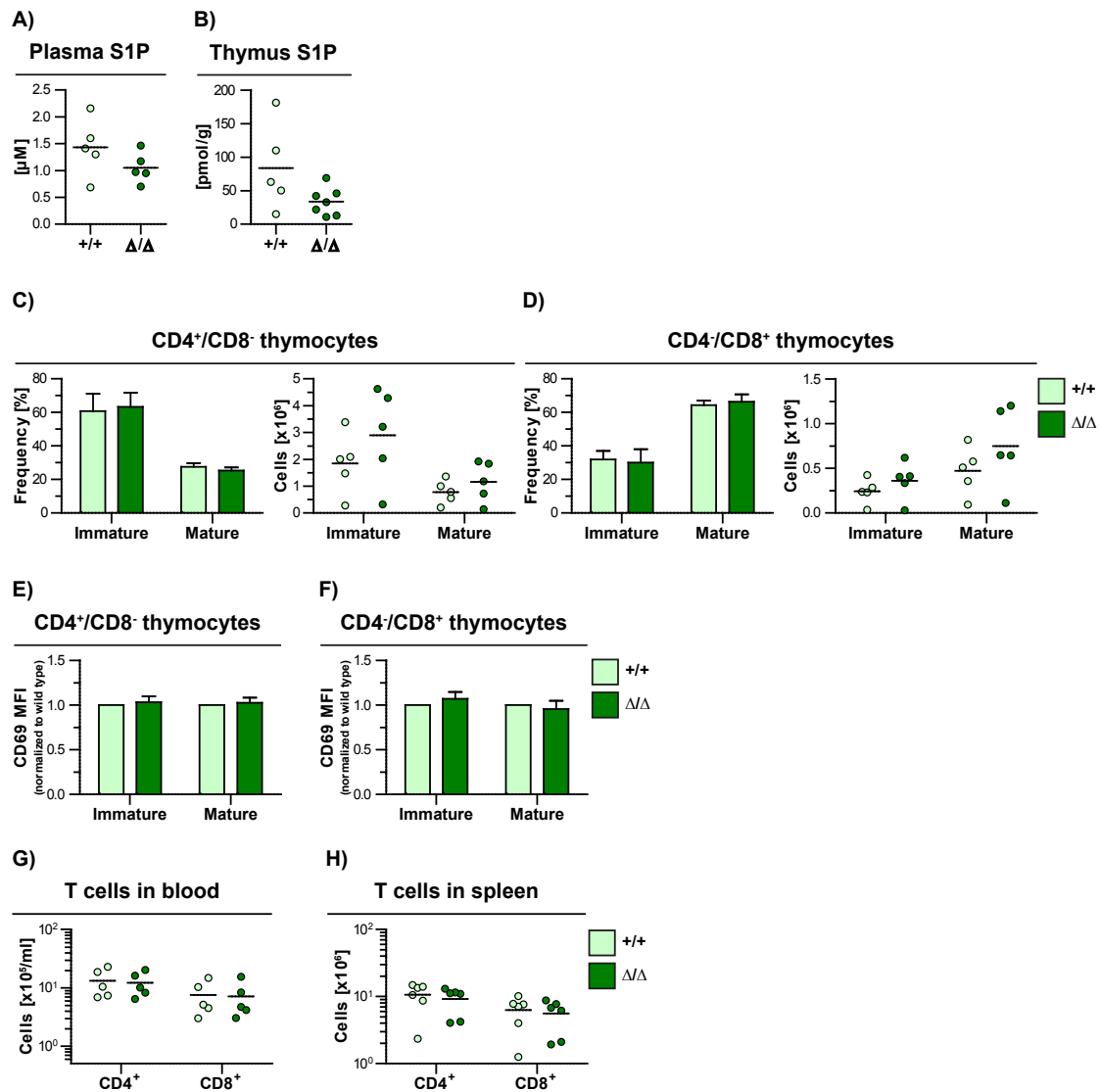


**Figure 4.16:** Deficiency of CERS4 has no effect on thymic egress. (A) Concentration of plasma S1P from wild type and CERS4-deficient mice was measured by mass spectrometry (N = 5 male mice per genotype). (B) Mass spectrometric measurement of S1P levels in thymi (whole organ) of wild type and CERS4-deficient mice, shown as pmol per g tissue (N = 5 – 7 male mice per genotype). (C and D) Frequencies (left) and counts (right) of immature (CD62L<sup>low</sup>/CD69<sup>high</sup>) and mature (CD62L<sup>high</sup>/CD69<sup>intermediate</sup>) CD4<sup>+</sup>/CD8<sup>-</sup> (C) and CD4<sup>-</sup>/CD8<sup>+</sup> (D) thymocytes from wild type (+/+, light green bars and dots) and CERS4-deficient mice ( $\Delta/\Delta$ , dark green bars and dots) were determined by flow cytometry (N = 5 male mice per genotype). (E and F) Flow cytometric analysis of CD69 surface expression on immature and mature CD4<sup>+</sup>/CD8<sup>-</sup> (E) and CD4<sup>-</sup>/CD8<sup>+</sup> (F) thymocytes from wild type and CERS4-deficient mice. Results are shown as CD69 MFIs. Data were normalized to wild type mice, which were set to 1 (N = 5 male mice per genotype). (G) Total counts of CD4<sup>+</sup> and CD8<sup>+</sup>T cells per ml blood from wild type and CERS4-deficient mice were determined by flow cytometry (N = 4 male mice per genotype). (H) Total counts of CD4<sup>+</sup> and CD8<sup>+</sup> T cells in the spleens of wild type and CERS4-deficient mice were determined by flow cytometry (N = 6 male mice per genotype). Dots in scatter plots represent individual mice and black lines represent means; bar graphs represent means + SD. Data are pooled from individual experiments, in which 1 - 2 mice per genotype were analyzed. Mass spectrometric analysis was performed by Dr. Markus Gräler (Department of Anesthesiology and Intensive Care Medicine, Center for Sepsis Control and Care (CSCC), and the Center for Molecular Biomedicine (CMB), Jena University Hospital, Jena, Germany). The data of this figure were already published in [1].

#### 4.4 Excursus: Early T cell development in female mice depends on CERS2

In previous analyses, it was discovered that CERS2-deficiency leads to a selective reduction of the total thymocyte numbers in female mice (see 4.1.1), demonstrating that CERS2 has a gender-specific function for T cell development, in addition to its role as regulator of efficient S1P-mediated thymic egress.

Interestingly, it was shown by flow cytometry that ablation of CERS2 in female mice leads to a significant reduction in the frequencies and numbers of DN1 thymocytes, which represent the initial precursor population, from which all other thymocytes derive (Figure 4.17A and B). Consequently, it was assumed that the thymic atrophy in female CERS2-deficient mice is caused by impairments in the earliest stages of T cell development. Consistent with this hypothesis, female *Cers2<sup>gt/gt</sup>* mice exhibited decreased thymocyte counts throughout all developmental stages that follow the DN1 phase (DN2 to SP). Worthy of note is that the reduction in the numbers of DN3, DN4 and CD8SP thymocytes was comparably weak and did not reach statistical significance. Surprisingly, CERS2-deficiency also led to diminished frequencies of DN1 thymocytes in male mice. Compared to female mice, however, this reduction was smaller and not accompanied by decreased thymocyte numbers in any developmental stage (Figure 4.17C). These findings indicate that ablation of CERS2 selectively affects early T cell development in female mice.

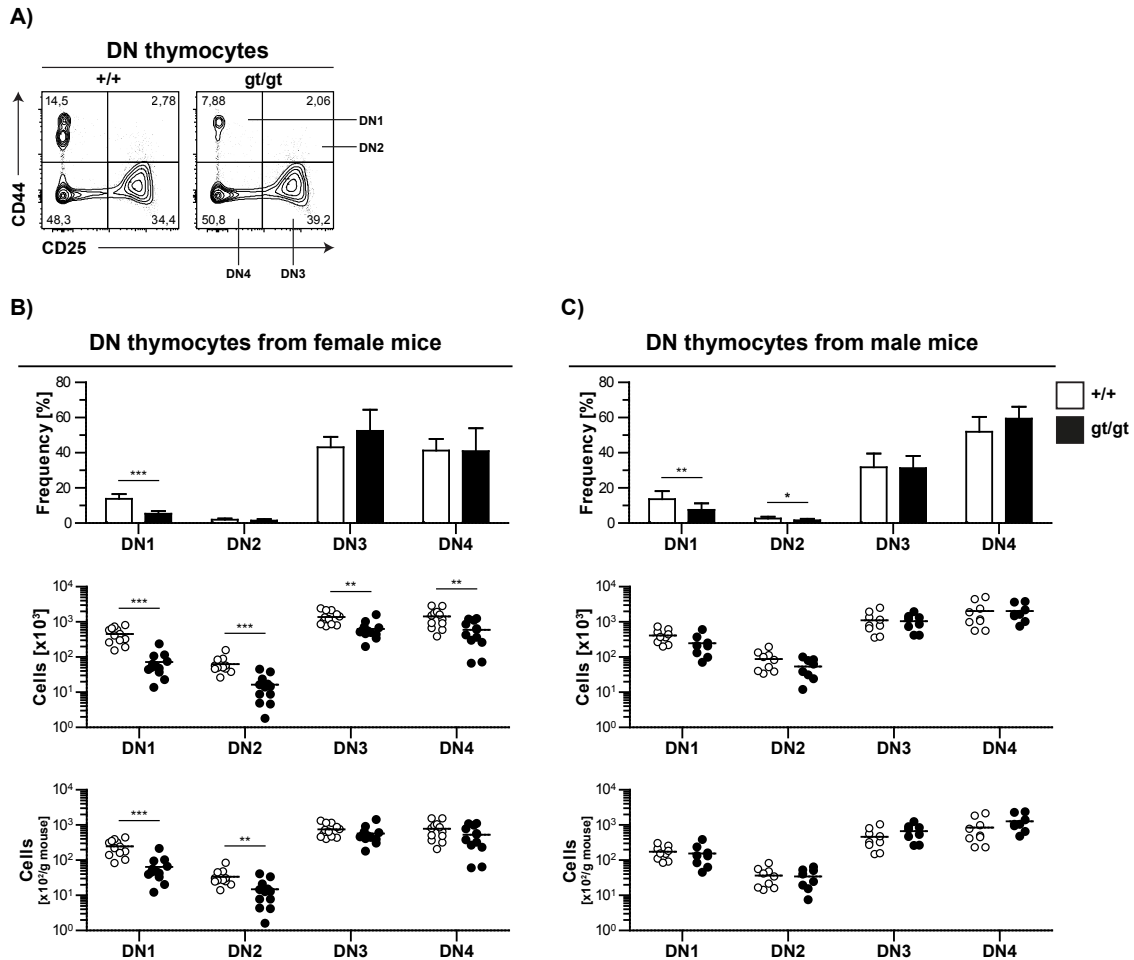


**Figure 4.17:** Reduced numbers of DN1 and DN2 thymocytes in the thymi of female *CERS2*-deficient mice. Percentages and counts of DN thymocyte subpopulations in the thymi of wild type (+/+; white bars and dots) and *CERS2*-deficient (*gt/gt*; black bars and dots) mice were determined by flow cytometry. (A) Representative pictures of flow cytometric identification of DN thymocyte subpopulations (DN1 (CD44<sup>+</sup>/CD25<sup>-</sup>), DN2 (CD44<sup>+</sup>/CD25<sup>+</sup>), DN3 (CD44<sup>-</sup>/CD25<sup>+</sup>) and DN4 (CD44<sup>-</sup>/CD25<sup>-</sup>)). Numbers indicate the percentages of subpopulations within the parental populations. (B) Percentages (upper panel), counts (middle panel, raw data) and counts per g mouse (lower panel, weight corrected data) of DN thymocyte subpopulations in the thymi of female mice (N = 12 mice per genotype). (C) Percentages (upper panel), counts (middle panel, raw data) and counts per g mouse (lower panel, weight corrected data) of DN thymocyte subpopulations in the thymi of male mice (N = 8 - 9 mice per genotype). For weight correction, total counts were normalized to the average mouse weights of female and male wild type and *CERS2*-deficient mice, respectively, (4.1.1). Dots in scatter plots represent individual mice and black lines represent means; bar graphs represent means + SD (Unpaired t-test; \*P < .05, \*\*P < .01, \*\*\*P < .001). Data are pooled from individual experiments, in which 1 - 2 mice per genotype were analyzed.

At several stages of thymic development, thymocyte populations are shaped by apoptosis and proliferation. To examine if alterations in these processes contribute to the reduced thymic cellularity in female *CERS2*-deficient mice, the frequencies of Annexin 5<sup>-</sup> and Ki67<sup>+</sup> cells within the DN, the DP and the SP thymocyte populations of female *Cers2*<sup>+/+</sup> and *Cers2*<sup>gt/gt</sup> mice were determined by flow cytometry. Whereas Annexin 5 labels apoptotic/necrotic cells and serves thus as viability marker, the expression of Ki67 identifies non G0 cells and serves thus as marker for proliferation. *CERS2*-deficiency did not affect the percentages of Annexin 5<sup>-</sup> and Ki67<sup>+</sup> cells in the analyzed thymocyte subpopulations, suggesting that the thymic atrophy in female *CERS2*-deficient mice is predominantly caused by the developmental defects in the DN1 stage and not by aberrant apoptosis or proliferation (Figure 4.18 and 4.19).

Taken together, these findings indicate that *CERS2* supports T cell development in female thymi by regulating the earliest steps of thymocyte differentiation.

**Figure 4.18:** Deficiency of *CERS2* has no impact on the percentage of viable cells in female thymi. Viability of major thymocyte subpopulations from female wild type (+/+), with bars) and *CERS2*-deficient (gt/gt, black bars) mice was investigated by Annexin 5 surface staining and flow cytometric analysis. (A) Representative pictures of flow cytometric identification of Annexin 5<sup>-</sup> DN (CD4<sup>-</sup>/CD8<sup>-</sup>), DP (CD4<sup>+</sup>/CD8<sup>+</sup>), CD4<sup>+</sup>/CD8<sup>-</sup> and CD4<sup>-</sup>/CD8<sup>+</sup> thymocytes. Numbers indicate the percentages of Annexin 5<sup>-</sup> and Annexin 5<sup>+</sup> cells within the parental populations; dashed curves represent unstained controls and grey curves represent samples. (B) Percentages of Annexin 5<sup>-</sup> cells within the DN, DP, CD4<sup>+</sup>/CD8<sup>-</sup> and CD4<sup>-</sup>/CD8<sup>+</sup> compartments (N = 4 female mice per genotype). Bar graphs represent means + SD. Data are pooled from individual experiments, in which 1 - 2 mice per genotype were analyzed.

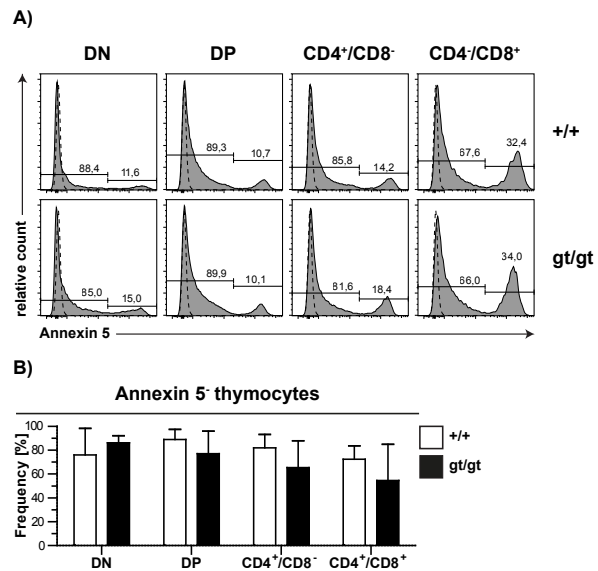
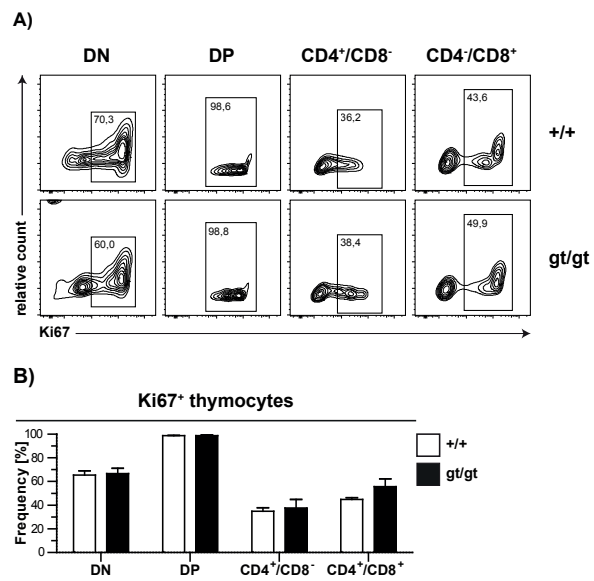


**Figure 4.19:** Deficiency of CERS2 has no impact on the percentage of proliferating cells in female thymi. The frequencies of proliferating cells within the major thymocyte subpopulations from female wild type (+/+), with bars) and CERS2-deficient (gt/gt, black bars) mice was investigated by an intracellular Ki67 staining and flow cytometric analysis. (A) Representative pictures of flow cytometric identification of Ki67<sup>+</sup> DN (CD4<sup>-</sup>/CD8<sup>-</sup>), DP (CD4<sup>+</sup>/CD8<sup>+</sup>), CD4<sup>+</sup>/CD8<sup>-</sup> and CD4<sup>-</sup>/CD8<sup>+</sup> thymocytes. Numbers indicate the percentages of Ki67<sup>+</sup> cells within the parental populations. (B) Percentages of Ki67<sup>+</sup> cells within the DN, DP, CD4<sup>+</sup>/CD8<sup>-</sup> and CD4<sup>-</sup>/CD8<sup>+</sup> compartments (N = 4 female mice per genotype). Bar graphs represent means + SD. Data are pooled from individual experiments, in which 1 - 2 mice per genotype were analyzed.



## 5 Discussion

The process of thymic egress is of fundamental importance for the adaptive immune system and thus for the protection against various invading pathogens, as it constantly replenishes the peripheral TCR repertoire with new specificities [19, 26]. The main driver of thymic emigration is a chemoattractive gradient of the lipid mediator S1P, which extends from the thymic parenchyma into the blood stream [99]. While passing negative selection, SP thymocytes develop from an egress-incompetent (immature) into an egress-competent (mature) state, as they induce surface expression of S1PR1, which enables them to sense the directional information of the S1P gradient and to exit chemotactically into the circulation [26, 89]. Despite its importance, the exact architecture of the thymic S1P gradient, as well as the regulatory mechanisms that maintain the functional differences in S1P concentration are still insufficiently understood [79].

In this study, we hypothesized that CERS2, as regulator of the S1P precursor sphingosine, might be important for S1P production and thus for the maintenance of the chemoattractive S1P gradient between thymus and blood. To verify this hypothesis we comparatively analyzed the shape of the thymic S1P gradient and the efficiency of thymic egress in wild type and CERS2-deficient mice. We observed that ablation of CERS2 did not only lead to the expected severe alterations in the turnover of sphingosine, but also to a distortion of the S1P gradient and a consistent impairment of the emigration of terminally differentiated thymocytes into the circulation. However, by performing bone marrow reconstitution and thymus transplantation experiments, we found that these phenotypes are neither due to the deficiency of CERS2 in hematopoietic cells nor caused by the absence of CERS2 in thymic stromal cells. Based on these findings, we concluded that CERS2 is required in non-hematopoietic extrathymic cells to maintain the functional S1P gradient between thymus and blood and to facilitate efficient thymic egress of terminally differentiated thymocytes into the circulation.

### 5.1 CERS2 in vascular endothelial cells maintains the thymic S1P gradient and facilitates efficient thymic egress by limiting the levels of S1P in the blood

Although their exact architecture has still not been resolved, it is assumed that the S1P gradient between thymus and circulation results from low S1P levels in the whole parenchyma but high S1P levels in the perivascular space (where the mature SP thymocytes cross the endothelium and enter the circulation) and in the blood [26, 78, 79]. According to the current understanding, these functional differences in S1P concentration are the result of local imbalances in S1P production, export and degradation. Whereas the low parenchymal S1P concentration is maintained by TECs and DCs, which degrade S1P via LPP3 or S1P lyase, it was demonstrated that neural crest-derived pericytes foster the high S1P levels at the exit sites by SPHK-dependent S1P production and subsequent export [89, 91, 92].

The high S1P amounts in the blood, which are even higher than those in the perivascular space, most likely result from several mechanisms. First, multiple cell types (vascular endothelial cells, hepatocytes, erythrocytes and platelets) contribute to the production, secretion and stabilization of S1P in the plasma [78, 98, 99, 212]. Second, circulatory S1P is bound to carrier proteins (albumin or HDL), which presumably increase its stability [218]. Third, erythrocytes, which represent the major blood cell population, lack expression of S1P lyase, SPPs and LPPs. Consequently, blood has low S1P degrading capacities [99]. Although the importance of high S1P levels in the blood for efficient thymic egress has been demonstrated in several studies, the underlying mechanisms remain elusive [78, 79].

We observed that CERS2-deficiency distorts the thymic S1P gradient, indicated by elevated S1P levels in the thymic parenchyma and in the blood (Figure 4.9 and 4.10). Concomitantly, mature SP thymocytes accumulated in the thymus of *Cers2<sup>gt/gt</sup>* mice, while the periphery exhibited a significant T cell lymphopenia, which suggests a considerable impairment in thymic egress (Figure 4.4, 4.5 and 4.6). It was demonstrated in several publications that even small alterations in S1P levels of thymus or blood can readily compromise the functionality of the S1P gradient and thus impair efficient emigration of newly formed T cells into the circulation. Interestingly, this holds true for lowering and for elevating the S1P concentration in any of the relevant compartments [78, 92, 89, 91]. It could, for instance, be shown that deficiency of SPHKs in neural crest-derived pericytes, which leads to decreased S1P levels at the exit sites, or ablation of SPNS2 in vascular endothelial cells, which causes a reduction of the S1P concentration in the blood, weakens the attraction of the gradient and thus interferes with thymic egress [78, 92]. Likewise, it was demonstrated that deletion of LPP3 in TECs or ablation of S1P lyase in DCs, which results in a robust elevation in the interstitial S1P concentration, also impairs efficient exit into the periphery. In this situation, however, the elevated S1P levels lead to an internalization of S1PR1 from the cell surface, which desensitizes the newly formed T cells before they have entered the circulation and thus causes their sequestration in the thymus [89, 91]. In the light of these findings, it is most likely that the increased concentration of S1P in the thymic interstitium of CERS2-deficient mice might also exceed the threshold of desensitization and thus lead to a slowed egress of the mature SP thymocytes into the periphery. Measuring the surface expression of S1PR1 on mature SP thymocytes from CERS2-deficient and wild type mice, would be a straightforward way to substantiate this hypothesis. Although several publications describe flow cytometric assays to detect surface S1PR1, we were not successful in establishing these protocols in our laboratory. Therefore, the comparative analysis of S1PR1 surface expression on mature SP thymocytes from *Cers2<sup>+/+</sup>* and *Cers2<sup>gt/gt</sup>* mice remains a future endeavour. Nonetheless, our findings collectively indicate that CERS2 is important for the S1P gradient and efficient thymic egress, as it contributes to the limitation of S1P levels in thymus and blood. Thus, CERS2 has a similar, but not redundant function as the S1P degrading enzymes LPP3 or S1P lyase.

Although CERS2 is ubiquitously expressed in thymic cells, we surprisingly found that

the exclusive ablation of CERS2 in all hematopoietic or all thymic stromal cells did not phenocopy the impaired thymic egress that was observed in *Cers2<sup>gt/gt</sup>* mice (Figure 4.13 and 4.15). Therefore, we concluded that CERS2 is mainly required in non-hematopoietic extrathymic cell types to facilitate S1P-mediated thymic emigration. As these cell types predominantly influence the concentration of S1P in the blood [78, 98], it must be assumed that CERS2 maintains the functional thymic S1P gradient and efficient egress exclusively via limiting the levels of circulatory S1P. The need for high and stable S1P levels in the blood was initially described by Pappu et al., who demonstrated that circulatory S1P (alone) is able to promote the emigration of mature SP thymocytes into the circulation [97]. In the corresponding study, mice were generated, which lack both SPHKs in many different tissues (such as the hematopoietic system, vascular endothelium, lymphatic endothelium, the liver and additional organs), resulting in reduced S1P levels in the blood and in all lymphoid organs. Consequently, thymic egress was abrogated. However, exclusive reconstitution of plasma S1P, via the transfusion of wild type erythrocytes, restored thymic egress to more than 50 %, compared to wild type mice. Despite these findings, it remains elusive how circulatory S1P can affect the intrathymic microenvironment and stimulate mature SP thymocytes, although the endothelium is a diffusion barrier. One potential explanation bases upon investigations of Bode and Sensken et al., who demonstrated that S1P from the blood can principally access lymphoid organs via transcellular transport through endothelial cells [219, 220]. Thus, the high amount of S1P in the circulation could directly shape the gradient on the abluminal side of the blood vessel. Another theory favors a model, in which the high levels of circulatory S1P do not only affect the thymocytes directly, but contribute to thymic egress by regulating the permeability of the endothelium. This hypothesis was developed, as it was shown in different studies that S1P signaling is important for vascular integrity [26, 79, 221].

Assuming that CERS2 regulates thymic egress mainly via limiting the amounts of circulatory S1P, the increased concentration of S1P in the thymic interstitium of *Cers2<sup>gt/gt</sup>* mice, which eventually leads to the desensitization and the subsequent sequestration of mature SP thymocytes, are presumably not due to intrathymic alterations in S1P turnover, but must be caused predominantly by the elevated levels of S1P in the blood. Perhaps, large quantities of the accumulated S1P in the circulation are indeed transported into the thymus via the transcytosis mechanism that was proposed by Bode and Sensken et al. [219, 220]. It should be noted that mice with an exclusive ablation of CERS2 in the hematopoietic system also exhibited signs of elevated S1P amounts in the thymic interstitium (Figure 4.13D and E). Although these alterations were obviously not potent enough to impair thymic egress on their own, they might aggravate the blood-dependent block in thymic egress in the *Cers2<sup>gt/gt</sup>* mice. As mentioned above, circulatory S1P is also important for the maintenance of vascular integrity. Consequently, it is conceivable that the increased levels of S1P in the circulation of *Cers2<sup>gt/gt</sup>* mice impair thymic egress not only by raising the intrathymic S1P concentration, but also by altering the permeability of the

vascular endothelium.

Until now, the only identified non-hematopoietic regulators of blood S1P are vascular endothelial cells and hepatocytes. Whereas vascular endothelial cells directly secrete S1P into the plasma, hepatocytes contribute to the stabilization of circulatory S1P via the production of apoM, which is the carrier of S1P in HDL [78, 98]. Both cell types robustly express CERS2 (Figure 4.11 and [155]). However, it was demonstrated in a study of Pewzner-Jung et al. that CERS2-deficiency had no effect on the S1P levels in the liver [161]. Moreover, Liu et al. showed that chemical inhibition of ceramide synthases in primary hepatocytes had no effect on the intracellular levels and on the secretion of S1P *in vitro* [212]. Therefore, we finally concluded that CERS2 must be required in vascular endothelial cells to limit the levels of circulatory S1P and to maintain thus the S1P gradient in the thymus. The generation and subsequent analysis of reverse bone marrow chimeras (i.e. the reconstitution of irradiated *Cers2<sup>gt/gt</sup>* mice with wild type bone marrow (and CERS2-deficient bone marrow as control)) would be a simple way to verify this hypothesis. However, these experiments could not be performed, as the CERS2-deficient mice would most likely not survive the rough irradiation procedure because of their limited viability (Figure 4.1 and [161]). Another and more elegant way to test our assumption would be the specific deletion of CERS2 in vascular endothelial cells. This would require the generation of a conditional *Cers2* knockout mouse (e.g. via flanking essential exons of the *Cers2* gene with LoxP sites) and the subsequent crossing with a vascular endothelial cell-specific driver line (e.g. *Tie2-Cre* [222]).

Taken together, we discovered that CERS2 is a crucial factor for efficient S1P-mediated thymic emigration of newly formed T cells into the periphery. On the basis of our data, we propose a model, in which CERS2 in vascular endothelial cells maintains the thymic S1P gradient and facilitates thymic exit by limiting the levels of S1P in the circulation (Figure 5.1). By the identification of CERS2 as a novel factor of S1P-dependent thymic egress, our study expands the knowledge on the maintenance of functional S1P gradients *in vivo* and presents CERS2 as important regulator of peripheral T cell homeostasis and thus of effective protection against invading pathogens.

## 5.2 CERS2 regulates S1P-mediated egress of circulating lymphocytes from lymph nodes into efferent lymphatics

Apart from the regulation of emigration from the thymus into the blood, S1P gradients also mediate the egress of circulating lymphocytes from lymph nodes into the efferent lymphatics. Based on several studies, it is generally assumed that, like in the thymus, the S1P gradients in the lymph nodes also result from low S1P levels in the parenchyma, but high S1P levels at the cortical sinuses, which are the presumable exit sites into the periphery [26]. Circulating lymphocytes enter lymph nodes as fully desensitized cells, which is a consequence of the high S1P levels in the blood [15]. In response to the low S1P levels

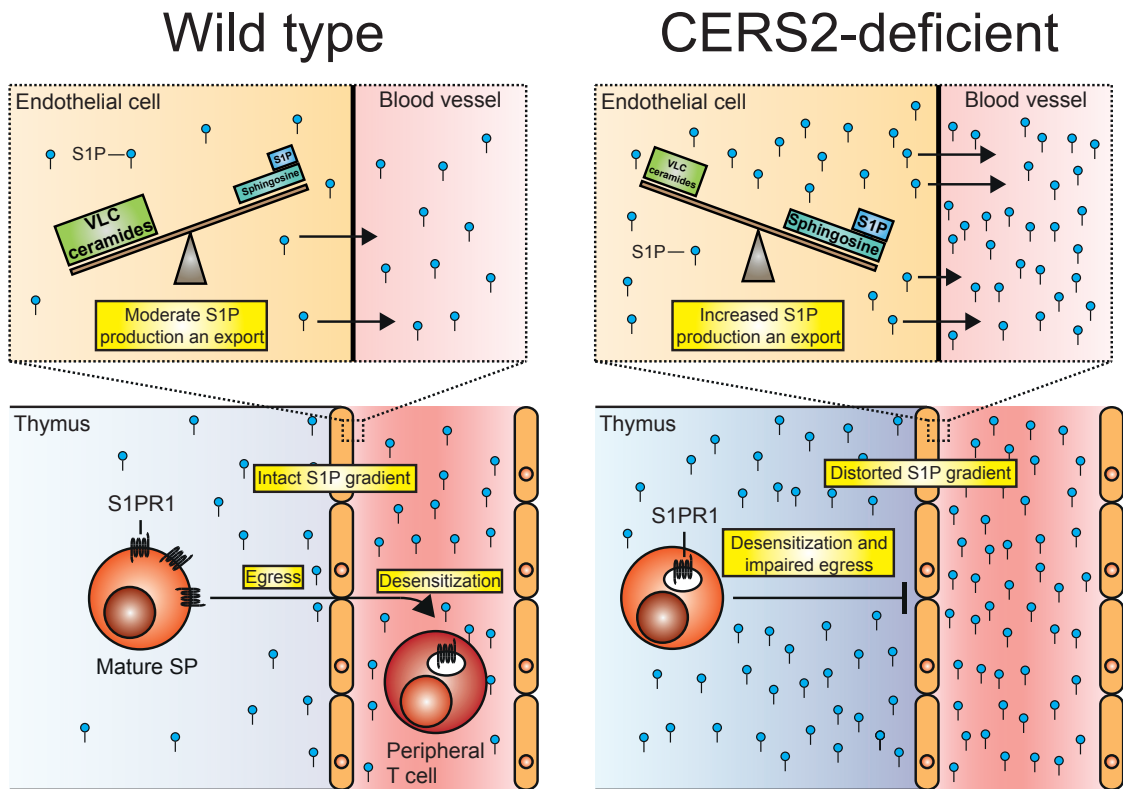


**Figure 5.1:** Working model how CERS2 in vascular endothelial cells maintains the S1P gradient in the thymus and facilitates efficient thymic egress of mature SP thymocytes into the circulation. The layout of this figure is based on the graphics of [1, 59, 79].

in the lymph node parenchyma, however, they start to reexpress S1PR1 on their surface while screening APCs for cognate antigens. After a dwell time of 6 - 24 hours without being activated, the lymphocytes are completely resensitized and leave the lymph nodes along the S1P gradient into the efferent lymphatics ([26] and 1.3.3). The importance of S1P signaling for efficient emigration from lymph nodes was proven in various studies. For instance, S1PR1-deficient lymphocytes, which had been adoptively transferred into wild type recipients, readily accumulated in lymph nodes [17]. Moreover, specific ablation of Sphks in lymphatic endothelial cells, which led to a reduction of lymph S1P and thus to a disruption of the gradient, efficiently blocked lymph node egress [223]. Similar impairments were observed after chemical inhibition of S1P lyase, which caused an elevation of the S1P concentration inside the lymph nodes. Thus, the lymphocytes were desensitized and eventually sequestered in the lymph nodes [102]. Likewise, treatment with FTY720, the most prominent functional antagonist of S1PR1, also resulted in a robust desensitization and a slowed emigration of lymphocytes from the lymph nodes into the efferent lymphatics, which is the basis for the use of FTY720 as drug in the treatment of autoimmune diseases, such as multiple sclerosis [107].

Consistent with an impaired egress from the thymus, *Cers2<sup>gt/gt</sup>* mice exhibited a robust T cell lymphopenia in blood and spleen (Figure 4.6B and D). We observed, however, that the

numbers of T cells in the lymph nodes were not affected by CERS2-deficiency (Figure 4.6F). Concerning the important role of S1P signaling for lymph node egress and the newly identified function of CERS2 as potent regulator of S1P levels, we hypothesized that ablation of CERS2 might not only impair emigration from the thymus, but also the S1P-dependent reentry of circulating lymphocytes from the lymph nodes into the efferent lymphatics. Under this assumption, the few T cells, which managed to overcome thymic sequestration and started circulating through the periphery, will eventually be sequestered in the lymph nodes. Thus, the peripheral T cell lymphopenia, which would normally affect all lymphoid compartments to a similar extent, is masked in the lymph nodes and simultaneously aggravated in blood and spleen. Importantly, as the entirety of all lymph nodes is a much larger compartment than blood and spleen, an S1P-dependent redistribution of peripheral lymphocytes is generally easier to detect by reduced lymphocyte counts in blood and spleen than by an increased cellularity in individual lymph nodes, as it was discussed in the study of Matloubian et al. [93]. As it was shown that plasma S1P does not contribute to the S1P gradients in the lymphatic system, we expect that the impaired lymph node egress in CERS2-deficient mice is not caused by the elevated levels of S1P in the blood [26]. With regard to the almost ubiquitous expression of CERS2 [155], however, it is quite possible that absence of CERS2 in lymphatic endothelial cells or in the lymph node stroma might lead to a local elevation of the S1P levels, which, in turn, desensitize the lymphocytes and thus attenuate their exit into the efferent lymphatics. To verify this hypothesis, the generation and subsequent analysis of lymphatic endothelial cell-specific CERS2-deficient mice would be an essential requirement (e.g. by using conditional *Cers2* knockout mice and a *Lyve-1* driver line [103]). As already described for the mature SP thymocytes (see 5.1), the putative desensitization of T cells in the lymph nodes of CERS2-deficient mice could also be verified by measuring the surface levels of S1PR1. Moreover, a detailed quantification of peripheral B cell populations in wild type and CERS2-deficient mice would also be of interest, as the S1P gradients in the lymph nodes do not only mediate T cell but also B cell egress into the efferent lymphatics [223].

Taken together, these findings suggest that CERS2 is not only important to regulate S1P-mediated egress from the thymus, but also to facilitate S1P-dependent emigration of T cells from the lymph nodes back into the circulation.

### 5.3 CERS2 is a multifunctional enzyme in basal sphingolipid metabolism

On a biochemical level, *Cers2* is a key enzyme of sphingolipid anabolism, which generates VLC (dihydro-)ceramides (mainly C24) by N-acylation of sphingoid bases with VLC fatty acids. Interestingly, deficiency of CERS2, however, did not only lead to a loss of VLC sphingolipids, but also to a compensatory increase in LC sphingolipids and an accumulation of sphingoid bases [160, 166]. While VLC ceramides are generally regarded as protective and anti-apoptotic lipids, LC ceramides and sphingoid bases are suspected lipotoxic mediators, which promote cell stress or apoptosis [224, 225, 226]. Consequently, a working model was

developed, in which CERS2 maintains physiological integrity by producing protective VLC sphingolipids while simultaneously preventing the accumulation of cytotoxic LC ceramides and sphingoid bases.

As mentioned before, we observed that CERS2-deficiency did not only lead to the expected alterations in the sphingolipid profile (loss of VLC SLs, increase of LC SLs and accumulation of sphingoid bases), but also to robustly increased concentrations of S1P in the thymus and in the blood, which distorted the chemotactic gradient and impaired thymic egress of newly formed T cells into the circulation (see 4.1 and 5.1). Although we cannot exclude that ablation of CERS2 affects the activity of the SPHKs via a regulatory feedback mechanism, we assume that the elevated S1P levels directly result from the massive accumulation of sphingosine, which shifts the biochemical equilibrium to an enhanced S1P synthesis. This assumption is supported by the results of several other studies, which investigated the physiological role of ceramidases and also demonstrated that the amounts of sphingosine are a key determinant for the production of S1P [227]. It was, for instance, shown that ablation of ACER3 (acid ceramides 3) leads to a decrease in the levels of sphingosine and a concomittant reduction of S1P in the lungs [228]. Consistently, overexpression of ACER1 (acid ceramidase 1) in HEK cells resulted in a co-elevation of sphingosine and S1P [229]. The huge impact of sphingosine on S1P synthesis might in particular be explained by the fact that the concentration of sphingosine is generally 100 fold higher than that of S1P. Thus, even small alterations in the levels of sphingosine can have a strong effect on the production of S1P, which might not always be compensated by counterregulatory mechanisms[114].

Importantly, correlations between the expression of CERS2 and the amounts of S1P were already found in previous studies. Choi et al. found that increased levels of S1P were associated with a reduced CERS2 expression in aged gastric smooth muscle cells [189]. Consistently, overexpression of CERS2 was sufficient to prevent an accumulation of S1P in neurons, which lack CERS1 [190]. Nonetheless, physiological consequences for S1P-dependent processes of a putative CERS2-S1P axis have not been analyzed in these studies.

Additionally, it should be noted that Liu and Pewzner-Jung et al. demonstrated that ablation of CERS2-function had no effect on the levels of S1P in the liver, inspite of a significantly increased concentration of sphingosine [166, 212]. Spatial differences in the expression and/or activities of S1P degrading enzymes might be an explanation why the absence of CERS2 can lead to an elevation of S1P in the blood (Figure 4.9) but not in the liver. Generally, most tissues (not only the thymus) exhibit a low concentration of S1P, which is, among other mechanisms, maintained by the activites of 6 different S1P-degrading enzymes [26, 85, 89]. Consequently, the accumulation of sphingosine in CERS2-deficient livers might indeed lead to an enhanced S1P synthesis, but this could be readily compensated by the superiority of the degrading enzymes. On the contrary, the blood exhibits a high S1P concentration, which results from the low expression of S1P degrading enzymes in circulating cells and the binding of S1P to carrier proteins, which are thought

to provide protection from degradation [99, 218, 230]. Therefore, the elevated levels of sphingosine in vascular endothelial cells of CERS2-deficient mice might induce an increased S1P production and export into the blood, where it is not efficiently degraded and can thus accumulate (compare 5.1).

Taken together, by showing that ablation of CERS2 alters the levels of S1P and thus impairs S1P-mediated lymphocyte egress, we demonstrate for the first time on a functional level that CERS2 maintains physiological integrity not only by synthesizing VLC ceramides and preventing the accumulation of LC sphingolipids and sphingoid bases, but also by limiting the production of the potent lipid mediator S1P. Thus, our study adds a further facet to the multifunctional character of CERS2. With regard to the magnitude of already identified intra- and extracellular functions of S1P, such as regulating histone accessibility, controlling the vascular tone or supporting growth, proliferation and differentiation (see 1.3.1), it might be worthwhile to investigate if CERS2 is also important for other S1P-dependent processes than lymphocyte trafficking.

#### **5.4 The regulation of S1P-mediated thymic egress is a specific function of CERS2**

Although investigations on the pleiotropic functions of CERS2 still dominate the current literature, the other members of the ceramide synthase family gained more and more attention from the research community in the last years. Thus, several pioneering studies, in which different CERS-deficient mouse models were analyzed, revealed that each CERS has unique physiological functions. While it could be shown that CERS1 is important for cerebellar development, it was found that CERS3 is crucial for cytokinesis during male meiosis and for the maintenance of the skin barrier [158, 174, 175]. Studies of Ebel and Peters et al. demonstrate that CERS4 is involved in the regulation of stem cell homeostasis in the skin, hair follicle cycling and sebum composition [176, 177]. Moreover, it was discovered that CERS5 and CERS6 play important roles in energy metabolism [167, 178].

Generally, this high degree of functional diversity has two reasons. First, all members of the CERS family exhibit an individual expression pattern. CERS1, for example, is the dominant CERS in the central nervous system and in skeletal muscles, but is absent in most other tissues. Likewise, CERS3 is highly abundant in reproductive tissues, but close to the detection limit in the rest of the organism [155].

Second, each CERS can only use fatty acids of a defined chain length for (dihydro-)ceramide synthesis. Whereas CERS5 and CERS6, for instance, are restricted to the use of LC fatty acids as substrates, CERS3 is limited to use VLC and ULC fatty acids [146]. Thus, each CERS produces ceramides with different acyl chain lengths, which are known to have highly specific cellular functions [225].

Despite these differences, all ceramide synthases have in common that they use sphingosine (and dihydrosphingosine) as substrate for the synthesis of (dihydro-)ceramides [129]. Consequently, we were interested if the consumption of sphingosine by other ceramide synthases than CERS2 is also important for S1P production and thus for S1P-dependent thymic egress (compare 5.1, 5.2 and 5.3). Importantly, a potential involvement of CERS1 and CERS3 was excluded a priori, as their expression is almost exclusively restricted to tissues, which are most likely unimportant for the thymic S1P gradient, such as the central nervous system, the skeletal muscles and the testes [155]. We hypothesized that CERS4 is the most probable candidate for having a similar impact on S1P-mediated egress processes as CERS2, since it is, in contrast to CERS5 and CERS6, also highly expressed in a variety of organs, tissues and cell types, which are known to be involved in the global or local regulation of the thymic S1P gradient, such as the thymus, the liver or immune cells in general (see 5.1 and [155]). Interestingly, we found that the thymic S1P gradient and efficient egress of terminally differentiated thymocytes into the periphery were unaffected in *CERS4*-deficient mice, indicating that the consumption of sphingosine by CERS4 is not important for the regulation of S1P synthesis (see 4.3). Although CERS4 can be found in various different tissues, its expression is mostly lower than that of CERS2 [155]. Therefore, we hypothesized that CERS4, in contrast to CERS2, is not abundant enough to compete effectively with the SPHKs for sphingosine to influence the production of S1P in cells, which are important for the maintenance of functional S1P gradients. Assuming that the impact of CERS2 on the production of S1P exclusively depends on its high expression levels, we moreover speculate that the consumption of sphingosine by CERS5 and CERS6 is presumably also not essential for the regulation of S1P synthesis, as both enzymes are expressed on even lower levels than CERS4 in most tissues [155]. However, analyses of CERS5- and CERS6-deficient mice need to be done in order to verify this hypothesis. Taken together, these findings suggest that the thymic S1P gradient is exclusively regulated by CERS2 and not by any other CERS. Thus, our study further substantiates the outstanding role of CERS2 within the ceramide synthase family.

### 5.5 CERS2 as putative pharmacological target

By identifying the impact of CERS2 on S1P gradients, our study presents CERS2 as potential novel pharmacological target. Based on our findings, we hypothesize that administration of a CERS2 antagonist could mimic the sequestration of lymphocytes in lymphoid organs, which is observed after FTY720 treatment, and might thus also be useful in the medication of autoimmune diseases or other immunological disorders (see 1.3.3). Interestingly, a chemical inhibitor that selectively targets CERS2 and not the other members of the CERS family was already characterized in an *in vitro* study of Schiffmann et al. [231]. However, as it is known from *Cers2<sup>gt/gt</sup>* mice that the organism-wide ablation of CERS2 can lead to serious phenotypes, the main challenge of targeting CERS2 for clinical purposes will be to avoid severe secondary effects [160, 161, 166]. Delivery strategies, which

target only the specific cell types/tissues/organs of interest and not the whole organism are absolutely required to address this issue, as they are currently developed for other critical drugs, such as anti-cancer agents [232].

## 5.6 Concluding remarks on the role of CERS2 in early T cell development in female mice

The thymus is of fundamental importance for adaptive immunity, as it provides a unique microenvironment, which is required for T cell development [27]. In the course of thymic T cell development, bone marrow-derived ETPs (early thymic progenitors) are induced by thymic stromal cells to undergo several steps of differentiation and proliferation, in which they stochastically rearrange the segments of their  $\beta$ - and  $\alpha$ -chains to diversify the TCR repertoire, on the one hand, and become committed to the CD4 or the CD8 lineage, on the other hand. After the cells with non-functional (unable to recognize peptide:MHC complexes) or autoreactive TCRs have been filtered out by extensive selection procedures, the remaining thymocytes, which express functional and self-tolerant TCRs, are allowed to complete thymic T cell development, enter the circulation and become part of the peripheral T cell pool, which protects the organism from invading pathogens (see 1.2).

Surprisingly, we observed that ablation of CERS2 led to a significant reduction in thymic cellularity in female mice, but not in males (Figure 4.2). Although this reduction was detectable in all thymocyte subsets, cells of the DN1 stage were affected the most (Figure 4.17). Interestingly, several independent studies revealed that thymic involution, the age-dependent reduction in thymic mass, cellularity and output, is partially mediated by sex hormones [28, 233, 27, 234, 235]. It could, for instance, be shown that androgen ablation (i. e. castration) in aged mice and rats is sufficient to regenerate a fully functional thymus [236, 237, 238]. Consistently, it was found that estrogen-treated mice exhibit a reduction of thymic cellularity by 80 % [239]. Strikingly, it was demonstrated in studies of Heng and Zoller et al. that sex hormones limit thymic cellularity predominantly by impairing T cell differentiation already at the ETP/DN1 stage and not by inducing apoptosis in later stages [239, 240].

With regard to the female-specific reduction in thymic cellularity in *Cers2<sup>gt/gt</sup>* mice and the huge impact of sex hormones on early T cell development, we assume that CERS2-deficiency interferes with the estrogen-dependent control of thymic involution. We speculate that the reduced numbers of ETPs and the atrophic thymi in female *Cers2<sup>gt/gt</sup>* mice are either caused by an increased production of estrogen in the ovaries or by defects in estrogen-receptor signaling in the thymus. In support of the first speculation is a study by Pieper et al, in which it was demonstrated that downregulation of CERS2 stimulates the secretory pathway (vesicle trafficking at the ER-Golgi interface) in chinese hamster ovary cells (CHO) [241]. Consequently, it is conceivable that deficiency of CERS2 might also amplify vesicle trafficking in the ovaries and thus lead to an enhanced estrogen secretion.

In sum, these findings indicate that CERS2 regulates thymic T cell development not only

by facilitating the egress of terminally differentiated T cells along the S1P gradient, but most likely also by preventing a premature estrogen-induced thymus involution. However, the verification of a potential involvement of CERS2 in the regulation of hormone-driven processes warrants further investigations, first of all quantifications of estrogen levels in female (and male) CERS2-deficient mice.

## 6 Summary

A key element for effective adaptive immunity against invading pathogens is an ever-changing peripheral TCR repertoire, which requires the constant release of newly formed T cells from the thymus. The process of thymic egress into the circulation is of chemotactic nature and is mediated by a soluble gradient of the lipid mediator sphingosine-1-phosphate (S1P), which results from low S1P levels in the thymic interstitium, but high S1P levels at the thymic exit sites and in the blood. Despite its importance for peripheral T cell homeostasis, the exact architecture of the thymic S1P gradient, as well as the underlying mechanisms, which maintain the spatial differences in S1P concentration are incompletely understood.

In the present study, we investigated if ceramide synthase 2 (CERS2), as regulator of the S1P precursor sphingosine, is involved in the maintenance of the thymic S1P gradient. We found that CERS2-deficient mice not only exhibited increased amounts of sphingosine, but also elevated levels of S1P within the thymic parenchyma, in the plasma and in RBCs, which resulted in a robust distortion of the S1P gradient between thymus and blood. Consistently, thymic egress was impaired in CERS2-deficient mice, indicated by a selective accumulation of egress-competent mature SP thymocytes in the thymus and a corresponding T cell lymphopenia in the periphery. We, therefore, concluded that the CERS2-dependent regulation of sphingosine is an important mechanism to facilitate efficient thymic egress of newly formed T cells into the periphery, as it prevents aberrant S1P synthesis by the sphingosine kinases (SPHKs) and thus stabilizes the chemoattractive S1P gradient between thymus and blood. CERS2 is ubiquitously expressed in the hematopoietic and non-hematopoietic cells of the thymus. However, we observed that neither the exclusive ablation of CERS2 in hematopoietic cells, nor the specific absence of CERS2 in thymic stromal cells could phenocopy the impaired S1P-dependent thymic egress, which was observed in CERS2-deficient mice. These results indicate that CERS2 shapes the thymic S1P gradient not by regulating S1P production in the thymus itself, but in extrathymic non-hematopoietic cells and thus exclusively by limiting the levels of S1P in the circulation. Based on our CERS2 expression data and the current understanding how S1P levels in blood are regulated, we hypothesize that vascular endothelial cells are the most promising cell type, in which CERS2 might be required to compete with the SPHKs to limit the production and secretion of S1P into the plasma.

Taken together, our study establishes for the first time a requirement of CERS2 for S1P gradient regulation between thymus and blood. Thus, we advance the understanding how egress from primary lymphoid organs and peripheral lymphocyte homeostasis are regulated *in vivo*. Consequently, CERS2 might be a promising pharmacological target to treat autoimmune diseases or other immunological disorders by manipulating lymphocyte trafficking.

---

## References

- [1] Michael Rieck, Christiane Kremser, Katarzyna Jobin, Elisabeth Mettke, Christian Kurts, Markus Graler, Klaus Willecke, and Waldemar Kolanus. Ceramide synthase 2 facilitates S1P-dependent egress of thymocytes into the circulation in mice. *European journal of immunology*, 47(4):677–684, 2017.
- [2] Bruce Alberts, Alexander Johnson, Julian Lewis, David Morgan, Martin Raff, Keith Roberts, Peter Walter, John Wilson, and Tim Hunt. *Molecular biology of the cell*. Garland Science Taylor and Francis Group, New York, NY, sixth edition edition, 2015.
- [3] Kenneth P. Murphy, Charles A. Janeway, Paul Travers, Mark Walport, Allan Mowat, and Casey T. Weaver. *Janeway’s immunobiology*. Garland Science, London, 8. ed. edition, 2012.
- [4] Harvey Lodish, Arnold Berk, and Chris A. Kaiser. *Molecular cell biology*. 8th revised edition edition, 2016.
- [5] Xuetao Cao. Self-regulation and cross-regulation of pattern-recognition receptor signalling in health and disease. *Nature reviews. Immunology*, 16(1):35–50, 2016.
- [6] David Nemazee. Receptor editing in lymphocyte development and central tolerance. *Nature reviews. Immunology*, 6(10):728–740, 2006.
- [7] David G. Schatz and Yanhong Ji. Recombination centres and the orchestration of V(D)J recombination. *Nature reviews. Immunology*, 11(4):251–263, 2011.
- [8] Stephen L. Nutt, Philip D. Hodgkin, David M. Tarlinton, and Lynn M. Corcoran. The generation of antibody-secreting plasma cells. *Nature reviews. Immunology*, 15(3):160–171, 2015.
- [9] Michel DuPage and Jeffrey A. Bluestone. Harnessing the plasticity of CD4(+) T cells to treat immune-mediated disease. *Nature reviews. Immunology*, 16(3):149–163, 2016.
- [10] Ian A. Parish and Susan M. Kaech. Diversity in CD8(+) T cell differentiation. *Current opinion in immunology*, 21(3):291–297, 2009.
- [11] Nikhil S. Joshi and Susan M. Kaech. Effector CD8 T cell development: a balancing act between memory cell potential and terminal differentiation. *Journal of immunology (Baltimore, Md. : 1950)*, 180(3):1309–1315, 2008.
- [12] Misty R. Jenkins and Gillian M. Griffiths. The synapse and cytolytic machinery of cytotoxic T cells. *Current opinion in immunology*, 22(3):308–313, 2010.

- 
- [13] Matthew A. Williams and Michael J. Bevan. Effector and memory CTL differentiation. *Annual review of immunology*, 25:171–192, 2007.
- [14] Nathan D. Pennock, Jason T. White, Eric W. Cross, Elizabeth E. Cheney, Beth A. Tamburini, and Ross M. Kedl. T cell responses: naive to memory and everything in between. *Advances in physiology education*, 37(4):273–283, 2013.
- [15] Jean-Philippe Girard, Christine Moussion, and Reinhold Forster. HEVs, lymphatics and homeostatic immune cell trafficking in lymph nodes. *Nature reviews. Immunology*, 12(11):762–773, 2012.
- [16] Taku Kambayashi and Terri M. Laufer. Atypical MHC class II-expressing antigen-presenting cells: can anything replace a dendritic cell? *Nature reviews. Immunology*, 14(11):719–730, 2014.
- [17] Trung H. M. Pham, Takaharu Okada, Mehrdad Matloubian, Charles G. Lo, and Jason G. Cyster. S1P1 receptor signaling overrides retention mediated by G alpha i-coupled receptors to promote T cell egress. *Immunity*, 28(1):122–133, 2008.
- [18] Donna L. Farber, Naomi A. Yudanin, and Nicholas P. Restifo. Human memory T cells: generation, compartmentalization and homeostasis. *Nature reviews. Immunology*, 14(1):24–35, 2014.
- [19] T. P. Arstila. A Direct Estimate of the Human T Cell Receptor Diversity. *Science*, 286(5441):958–961, 1999.
- [20] Jorg J. A. Calis and Brad R. Rosenberg. Characterizing immune repertoires by high throughput sequencing: strategies and applications. *Trends in immunology*, 35(12):581–590, 2014.
- [21] Menno C. van Zelm, Mirjam van der Burg, Anton W. Langerak, and Jacques J. M. van Dongen. PID comes full circle: applications of V(D)J recombination excision circles in research, diagnostics and newborn screening of primary immunodeficiency disorders. *Frontiers in immunology*, 2:12, 2011.
- [22] Kristin A. Hogquist, Troy A. Baldwin, and Stephen C. Jameson. Central tolerance: learning self-control in the thymus. *Nature reviews. Immunology*, 5(10):772–782, 2005.
- [23] Jacy Gameiro, Patricia Nagib, and Liana Verinaud. The thymus microenvironment in regulating thymocyte differentiation. *Cell Adhesion & Migration*, 4(3):382–390, 2014.
- [24] Yousuke Takahama. Journey through the thymus: stromal guides for T-cell development and selection. *Nature reviews. Immunology*, 6(2):127–135, 2006.

- 
- [25] Ellen V. Rothenberg, Jonathan E. Moore, and Mary A. Yui. Launching the T-cell-lineage developmental programme. *Nature reviews. Immunology*, 8(1):9–21, 2008.
- [26] Jason G. Cyster and Susan R. Schwab. Sphingosine-1-phosphate and lymphocyte egress from lymphoid organs. *Annual review of immunology*, 30:69–94, 2012.
- [27] Thomas Boehm and Jeremy B. Swann. Thymus involution and regeneration: two sides of the same coin? *Nature reviews. Immunology*, 13(11):831–838, 2013.
- [28] Kenneth Dorshkind, Encarnacion Montecino-Rodriguez, and Robert A. J. Signer. The ageing immune system: is it ever too old to become young again? *Nature reviews. Immunology*, 9(1):57–62, 2009.
- [29] D. I. Godfrey, J. Kennedy, T. Suda, and A. Zlotnik. A developmental pathway involving four phenotypically and functionally distinct subsets of CD3-CD4-CD8- triple-negative adult mouse thymocytes defined by CD44 and CD25 expression. *Journal of immunology (Baltimore, Md. : 1950)*, 150(10):4244–4252, 1993.
- [30] Ute Koch and Freddy Radtke. Mechanisms of T cell development and transformation. *Annual review of cell and developmental biology*, 27:539–562, 2011.
- [31] J. Jeremiah Bell and Avinash Bhandoola. The earliest thymic progenitors for T cells possess myeloid lineage potential. *Nature*, 452(7188):764–767, 2008.
- [32] Ute Koch, Emma Fiorini, Rui Benedito, Valerie Besseyrias, Karin Schuster-Gossler, Michel Pierres, Nancy R. Manley, Antonio Duarte, H. Robson Macdonald, and Freddy Radtke. Delta-like 4 is the essential, nonredundant ligand for Notch1 during thymic T cell lineage commitment. *The Journal of experimental medicine*, 205(11):2515–2523, 2008.
- [33] Helen E. Porritt, Kristie Gordon, and Howard T. Petrie. Kinetics of steady-state differentiation and mapping of intrathymic-signaling environments by stem cell transplantation in nonirradiated mice. *The Journal of experimental medicine*, 198(6):957–962, 2003.
- [34] Howard T. Petrie and Juan Carlos Zuniga-Pflucker. Zoned out: functional mapping of stromal signaling microenvironments in the thymus. *Annual review of immunology*, 25:649–679, 2007.
- [35] F. Livak, M. Tourigny, D. G. Schatz, and H. T. Petrie. Characterization of TCR gene rearrangements during adult murine T cell development. *Journal of immunology (Baltimore, Md. : 1950)*, 162(5):2575–2580, 1999.
- [36] M. Capone, R. D. Hockett, JR, and A. Zlotnik. Kinetics of T cell receptor beta, gamma, and delta rearrangements during adult thymic development: T cell receptor rearrangements are present in CD44(+)CD25(+) Pro-T thymocytes. *Proceedings of*

- the National Academy of Sciences of the United States of America*, 95(21):12522–12527, 1998.
- [37] J. Kang, A. Volkmann, and D. H. Raulet. Evidence that gammadelta versus alpha-beta T cell fate determination is initiated independently of T cell receptor signaling. *The Journal of experimental medicine*, 193(6):689–698, 2001.
- [38] Adrian Hayday and Robert Tigelaar. Immunoregulation in the tissues by gammadelta T cells. *Nature reviews. Immunology*, 3(3):233–242, 2003.
- [39] Pierre Vantourout and Adrian Hayday. Six-of-the-best: unique contributions of gammadelta T cells to immunology. *Nature reviews. Immunology*, 13(2):88–100, 2013.
- [40] Harald von Boehmer. Unique features of the pre-T-cell receptor alpha-chain: not just a surrogate. *Nature reviews. Immunology*, 5(7):571–577, 2005.
- [41] Tom Taghon, Mary A. Yui, Rashmi Pant, Rochelle A. Diamond, and Ellen V. Rothenberg. Developmental and molecular characterization of emerging beta- and gammadelta-selected pre-T cells in the adult mouse thymus. *Immunity*, 24(1):53–64, 2006.
- [42] M. Egerton, K. Shortman, and R. Scollay. The kinetics of immature murine thymocyte development in vivo. *International immunology*, 2(6):501–507, 1990.
- [43] C. Penit, B. Lucas, and F. Vasseur. Cell expansion and growth arrest phases during the transition from precursor (CD4-8-) to immature (CD4+8+) thymocytes in normal and genetically modified mice. *Journal of immunology (Baltimore, Md. : 1950)*, 154(10):5103–5113, 1995.
- [44] M. R. Tourigny, S. Mazel, D. B. Burtrum, and H. T. Petrie. T cell receptor (TCR)-beta gene recombination: dissociation from cell cycle regulation and developmental progression during T cell ontogeny. *The Journal of experimental medicine*, 185(9):1549–1556, 1997.
- [45] H. T. Petrie, M. Pearse, R. Scollay, and K. Shortman. Development of immature thymocytes: initiation of CD3, CD4, and CD8 acquisition parallels down-regulation of the interleukin 2 receptor alpha chain. *European journal of immunology*, 20(12):2813–2815, 1990.
- [46] H. T. Petrie, F. Livak, D. G. Schatz, A. Strasser, I. N. Crispe, and K. Shortman. Multiple rearrangements in T cell receptor alpha chain genes maximize the production of useful thymocytes. *The Journal of experimental medicine*, 178(2):615–622, 1993.
- [47] C. Penit. Localization and phenotype of cycling and post-cycling murine thymocytes studied by simultaneous detection of bromodeoxyuridine and surface antigens. *The*

- journal of histochemistry and cytochemistry : official journal of the Histochemistry Society*, 36(5):473–478, 1988.
- [48] Ronald N. Germain. T-cell development and the CD4-CD8 lineage decision. *Nature reviews. Immunology*, 2(5):309–322, 2002.
- [49] Timothy K. Starr, Stephen C. Jameson, and Kristin A. Hogquist. Positive and negative selection of T cells. *Annual review of immunology*, 21:139–176, 2003.
- [50] Ludger Klein, Maria Hinterberger, Gerald Wirnsberger, and Bruno Kyewski. Antigen presentation in the thymus for positive selection and central tolerance induction. *Nature reviews. Immunology*, 9(12):833–844, 2009.
- [51] Graham Anderson and Yousuke Takahama. Thymic epithelial cells: working class heroes for T cell development and repertoire selection. *Trends in immunology*, 33(6):256–263, 2012.
- [52] Mark S. Anderson and Maureen A. Su. AIRE expands: new roles in immune tolerance and beyond. *Nature reviews. Immunology*, 16(4):247–258, 2016.
- [53] J. Derbinski, A. Schulte, B. Kyewski, and L. Klein. Promiscuous gene expression in medullary thymic epithelial cells mirrors the peripheral self. *Nature immunology*, 2(11):1032–1039, 2001.
- [54] Ludger Klein, Bruno Kyewski, Paul M. Allen, and Kristin A. Hogquist. Positive and negative selection of the T cell repertoire: what thymocytes see (and don’t see). *Nature reviews. Immunology*, 14(6):377–391, 2014.
- [55] Ming O. Li and Alexander Y. Rudensky. T cell receptor signalling in the control of regulatory T cell differentiation and function. *Nature reviews. Immunology*, 16(4):220–233, 2016.
- [56] Eric Camerer, Jean B. Regard, Ivo Cornelissen, Yoga Srinivasan, Daniel N. Duong, Daniel Palmer, Trung H. Pham, Jinny S. Wong, Rajita Pappu, and Shaun R. Coughlin. Sphingosine-1-phosphate in the plasma compartment regulates basal and inflammation-induced vascular leak in mice. *The Journal of clinical investigation*, 119(7):1871–1879, 2009.
- [57] A. Olivera and S. Spiegel. Sphingosine-1-phosphate as second messenger in cell proliferation induced by PDGF and FCS mitogens. *Nature*, 365(6446):557–560, 1993.
- [58] O. Cuvillier, G. Pirianov, B. Kleuser, P. G. Vanek, O. A. Coso, S. Gutkind, and S. Spiegel. Suppression of ceramide-mediated programmed cell death by sphingosine-1-phosphate. *Nature*, 381(6585):800–803, 1996.
- [59] Sarah Spiegel and Sheldon Milstien. The outs and the ins of sphingosine-1-phosphate in immunity. *Nature reviews. Immunology*, 11(6):403–415, 2011.

- 
- [60] Richard L. Proia and Timothy Hla. Emerging biology of sphingosine-1-phosphate: its role in pathogenesis and therapy. *The Journal of clinical investigation*, 125(4):1379–1387, 2015.
- [61] Michael Maceyka, Kuzhuvelil B. Harikumar, Sheldon Milstien, and Sarah Spiegel. Sphingosine-1-phosphate signaling and its role in disease. *Trends in cell biology*, 22(1):50–60, 2012.
- [62] Hongying Shen, Francesca Giordano, Yumei Wu, Jason Chan, Chen Zhu, Ira Milosevic, Xudong Wu, Kai Yao, Bo Chen, Tobias Baumgart, Derek Sieburth, and Pietro de Camilli. Coupling between endocytosis and sphingosine kinase 1 recruitment. *Nature cell biology*, 16(7):652–662, 2014.
- [63] Stuart M. Pitson, Paul A. B. Moretti, Julia R. Zebol, Helen E. Lynn, Pu Xia, Mathew A. Vadas, and Binks W. Wattenberg. Activation of sphingosine kinase 1 by ERK1/2-mediated phosphorylation. *The EMBO journal*, 22(20):5491–5500, 2003.
- [64] C. R. Thompson, S. S. Iyer, N. Melrose, R. VanOosten, K. Johnson, S. M. Pitson, L. M. Obeid, and D. J. Kusner. Sphingosine Kinase 1 (SK1) Is Recruited to Nascent Phagosomes in Human Macrophages: Inhibition of SK1 Translocation by *Mycobacterium tuberculosis*. *The Journal of Immunology*, 174(6):3551–3561, 2005.
- [65] Nobuaki Igarashi, Taro Okada, Shun Hayashi, Toshitada Fujita, Saleem Jahangeer, and Shun-ichi Nakamura. Sphingosine kinase 2 is a nuclear protein and inhibits DNA synthesis. *The Journal of biological chemistry*, 278(47):46832–46839, 2003.
- [66] Guo Ding, Hirofumi Sonoda, Huan Yu, Taketoshi Kajimoto, Sravan K. Goparaju, Saleem Jahangeer, Taro Okada, and Shun-ichi Nakamura. Protein kinase D-mediated phosphorylation and nuclear export of sphingosine kinase 2. *The Journal of biological chemistry*, 282(37):27493–27502, 2007.
- [67] Graham M. Strub, Melanie Paillard, Jie Liang, Ludovic Gomez, Jeremy C. Allegood, Nitai C. Hait, Michael Maceyka, Megan M. Price, Qun Chen, David C. Simpson, Tomasz Kordula, Sheldon Milstien, Edward J. Lesnefsky, and Sarah Spiegel. Sphingosine-1-phosphate produced by sphingosine kinase 2 in mitochondria interacts with prohibitin 2 to regulate complex IV assembly and respiration. *FASEB journal : official publication of the Federation of American Societies for Experimental Biology*, 25(2):600–612, 2011.
- [68] Nitai C. Hait, Andrea Bellamy, Sheldon Milstien, Tomasz Kordula, and Sarah Spiegel. Sphingosine kinase type 2 activation by ERK-mediated phosphorylation. *The Journal of biological chemistry*, 282(16):12058–12065, 2007.
- [69] Nitai C. Hait, Jeremy Allegood, Michael Maceyka, Graham M. Strub, Kuzhuvelil B. Harikumar, Sandeep K. Singh, Cheng Luo, Ronen Marmorstein, Tomasz Kordula,

- Sheldon Milstien, and Sarah Spiegel. Regulation of histone acetylation in the nucleus by sphingosine-1-phosphate. *Science (New York, N. Y.)*, 325(5945):1254–1257, 2009.
- [70] Steffen E. Schnitzer, Andreas Weigert, Jie Zhou, and Bernhard Brune. Hypoxia enhances sphingosine kinase 2 activity and provokes sphingosine-1-phosphate-mediated chemoresistance in A549 lung cancer cells. *Molecular cancer research : MCR*, 7(3):393–401, 2009.
- [71] Bradley K. Wacker, Tae Sung Park, and Jeffrey M. Gidday. Hypoxic preconditioning-induced cerebral ischemic tolerance: role of microvascular sphingosine kinase 2. *Stroke*, 40(10):3342–3348, 2009.
- [72] Ana Olivera, Christoph Eisner, Yoshiaki Kitamura, Sandra Dillahunt, Laura Allende, Galina Tuymetova, Wendy Watford, Francoise Meylan, Susanne C. Diesner, Lingli Li, Jurgen Schnermann, Richard L. Proia, and Juan Rivera. Sphingosine kinase 1 and sphingosine-1-phosphate receptor 2 are vital to recovery from anaphylactic shock in mice. *The Journal of clinical investigation*, 120(5):1429–1440, 2010.
- [73] Sergio E. Alvarez, Kuzhuvelil B. Harikumar, Nitai C. Hait, Jeremy Allegood, Graham M. Strub, Eugene Y. Kim, Michael Maceyka, Hualiang Jiang, Cheng Luo, Tomasz Kordula, Sheldon Milstien, and Sarah Spiegel. Sphingosine-1-phosphate is a missing cofactor for the E3 ubiquitin ligase TRAF2. *Nature*, 465(7301):1084–1088, 2010.
- [74] Ana Olivera, Kiyomi Mizugishi, Anastassia Tikhonova, Laura Ciaccia, Sandra Odom, Richard L. Proia, and Juan Rivera. The sphingosine kinase-sphingosine-1-phosphate axis is a determinant of mast cell function and anaphylaxis. *Immunity*, 26(3):287–297, 2007.
- [75] Naoki Kobayashi, Nobuyoshi Kobayashi, Akihito Yamaguchi, and Tsuyoshi Nishi. Characterization of the ATP-dependent sphingosine 1-phosphate transporter in rat erythrocytes. *The Journal of biological chemistry*, 284(32):21192–21200, 2009.
- [76] Poulami Mitra, Carole A. Oskeritzian, Shawn G. Payne, Michael A. Beaven, Sheldon Milstien, and Sarah Spiegel. Role of ABCC1 in export of sphingosine-1-phosphate from mast cells. *Proceedings of the National Academy of Sciences of the United States of America*, 103(44):16394–16399, 2006.
- [77] Koichi Sato, Enkhzol Malchinkhuu, Yuta Horiuchi, Chihiro Mogi, Hideaki Tomura, Masahiko Tosaka, Yuhei Yoshimoto, Atsushi Kuwabara, and Fumikazu Okajima. Critical role of ABCA1 transporter in sphingosine 1-phosphate release from astrocytes. *Journal of neurochemistry*, 103(6):2610–2619, 2007.
- [78] Shigetomo Fukuhara, Szandor Simmons, Shunsuke Kawamura, Asuka Inoue, Yasuko Orba, Takeshi Tokudome, Yuji Sunden, Yuji Arai, Kazumasa Moriwaki, Junji Ishida,

- Akiyoshi Uemura, Hiroshi Kiyonari, Takaya Abe, Akiyoshi Fukamizu, Masanori Hirashima, Hirofumi Sawa, Junken Aoki, Masaru Ishii, and Naoki Mochizuki. The sphingosine-1-phosphate transporter Spns2 expressed on endothelial cells regulates lymphocyte trafficking in mice. *The Journal of clinical investigation*, 122(4):1416–1426, 2012.
- [79] Keisuke Yanagida and Timothy Hla. Vascular and Immunobiology of the Circulatory Sphingosine 1-Phosphate Gradient. *Annual review of physiology*, 2016.
- [80] Hugh Rosen and Jiayu Liao. Sphingosine 1-phosphate pathway therapeutics: a lipid ligand-receptor paradigm. *Current opinion in chemical biology*, 7(4):461–468, 2003.
- [81] Hugh Rosen, Pedro J. Gonzalez-Cabrera, M. Germana Sanna, and Steven Brown. Sphingosine 1-phosphate receptor signaling. *Annual review of biochemistry*, 78:743–768, 2009.
- [82] Alexander D. Borowsky, Padmavathi Bandhuvula, Ashok Kumar, Yuko Yoshinaga, Mikhail Nefedov, Loren G. Fong, Meng Zhang, Brian Baridon, Lisa Dillard, Pieter de Jong, Stephen G. Young, David B. West, and Julie D. Saba. Sphingosine-1-phosphate lyase expression in embryonic and adult murine tissues. *Journal of lipid research*, 53(9):1920–1931, 2012.
- [83] Mika Ikeda, Akio Kihara, and Yasuyuki Igarashi. Sphingosine-1-phosphate lyase SPL is an endoplasmic reticulum-resident, integral membrane protein with the pyridoxal 5'-phosphate binding domain exposed to the cytosol. *Biochemical and biophysical research communications*, 325(1):338–343, 2004.
- [84] David K. Breslow and Jonathan S. Weissman. Membranes in balance: mechanisms of sphingolipid homeostasis. *Molecular cell*, 40(2):267–279, 2010.
- [85] Christopher R. Gault, Lina M. Obeid, and Yusuf A. Hannun. An overview of sphingolipid metabolism: from synthesis to breakdown. *Advances in experimental medicine and biology*, 688:1–23, 2010.
- [86] S. M. Mandala. Sphingosine-1-phosphate phosphatases. *Prostaglandins & other lipid mediators*, 64(1-4):143–156, 2001.
- [87] Herve Le Stunff, Ismael Galve-Roperh, Courtney Peterson, Sheldon Milstien, and Sarah Spiegel. Sphingosine-1-phosphate phosphohydrolase in regulation of sphingolipid metabolism and apoptosis. *The Journal of cell biology*, 158(6):1039–1049, 2002.
- [88] Julie D. Saba and Timothy Hla. Point-counterpoint of sphingosine 1-phosphate metabolism. *Circulation research*, 94(6):724–734, 2004.

- [89] Beatrice Breart, Willy D. Ramos-Perez, Alejandra Mendoza, Abdelghaffar K. Salous, Michael Gobert, Yong Huang, Ralf H. Adams, Juan J. Lafaille, Diana Escalante-Alcalde, Andrew J. Morris, and Susan R. Schwab. Lipid phosphate phosphatase 3 enables efficient thymic egress. *The Journal of experimental medicine*, 208(6):1267–1278, 2011.
- [90] Audrey Baeyens, Victoria Fang, Cynthia Chen, and Susan R. Schwab. Exit Strategies: S1P Signaling and T Cell Migration. *Trends in immunology*, 36(12):778–787, 2015.
- [91] Jesus Zamora-Pineda, Ashok Kumar, Jung H. Suh, Meng Zhang, and Julie D. Saba. Dendritic cell sphingosine-1-phosphate lyase regulates thymic egress. *The Journal of experimental medicine*, 213(12):2773–2791, 2016.
- [92] Marcus A. Zachariah and Jason G. Cyster. Neural crest-derived pericytes promote egress of mature thymocytes at the corticomedullary junction. *Science (New York, N.Y.)*, 328(5982):1129–1135, 2010.
- [93] Mehrdad Matloubian, Charles G. Lo, Guy Cinamon, Matthew J. Lesneski, Ying Xu, Volker Brinkmann, Maria L. Allende, Richard L. Proia, and Jason G. Cyster. Lymphocyte egress from thymus and peripheral lymphoid organs is dependent on S1P receptor 1. *Nature*, 427(6972):355–360, 2004.
- [94] Iwao Yamashita, Taeko Nagata, Tomlo Tada, and Toshinori Nakayama. CD69 cell surface expression identifies developing thymocytes which audition for T cell antigen receptor-mediated positive selection. *International Immunology*, 5(9):1139–1150, 1993.
- [95] Kensuke Takada, Xiaodan Wang, Geoffrey T. Hart, Oludare A. Odumade, Michael A. Weinreich, Kristin A. Hogquist, and Stephen C. Jameson. Kruppel-like factor 2 is required for trafficking but not quiescence in postactivated T cells. *Journal of immunology (Baltimore, Md. : 1950)*, 186(2):775–783, 2011.
- [96] Corey M. Carlson, Bart T. Endrizzi, Jinghai Wu, Xiaojie Ding, Michael A. Weinreich, Elizabeth R. Walsh, Maqsood A. Wani, Jerry B. Lingrel, Kristin A. Hogquist, and Stephen C. Jameson. Kruppel-like factor 2 regulates thymocyte and T-cell migration. *Nature*, 442(7100):299–302, 2006.
- [97] Rajita Pappu, Susan R. Schwab, Ivo Cornelissen, Joao P. Pereira, Jean B. Regard, Ying Xu, Eric Camerer, Yao-Wu Zheng, Yong Huang, Jason G. Cyster, and Shaun R. Coughlin. Promotion of lymphocyte egress into blood and lymph by distinct sources of sphingosine-1-phosphate. *Science (New York, N.Y.)*, 316(5822):295–298, 2007.
- [98] Christina Christoffersen, Hideru Obinata, Sunil B. Kumaraswamy, Sylvain Galvani, Josefin Ahnstrom, Madhumati Sevvana, Claudia Egerer-Sieber, Yves A. Muller, Tim-

- othy Hla, Lars B. Nielsen, and Bjorn Dahlback. Endothelium-protective sphingosine-1-phosphate provided by HDL-associated apolipoprotein M. *Proceedings of the National Academy of Sciences of the United States of America*, 108(23):9613–9618, 2011.
- [99] Juan Rivera, Richard L. Proia, and Ana Olivera. The alliance of sphingosine-1-phosphate and its receptors in immunity. *Nature reviews. Immunology*, 8(10):753–763, 2008.
- [100] Charles G. Lo, Ying Xu, Richard L. Proia, and Jason G. Cyster. Cyclical modulation of sphingosine-1-phosphate receptor 1 surface expression during lymphocyte recirculation and relationship to lymphoid organ transit. *The Journal of experimental medicine*, 201(2):291–301, 2005.
- [101] Tal I. Arnon, Ying Xu, Charles Lo, Trung Pham, Jinping An, Shaun Coughlin, Gerald W. Dorn, and Jason G. Cyster. GRK2-dependent S1PR1 desensitization is required for lymphocytes to overcome their attraction to blood. *Science (New York, N.Y.)*, 333(6051):1898–1903, 2011.
- [102] Susan R. Schwab, Joao P. Pereira, Mehrdad Matloubian, Ying Xu, Yong Huang, and Jason G. Cyster. Lymphocyte sequestration through S1P lyase inhibition and disruption of S1P gradients. *Science (New York, N.Y.)*, 309(5741):1735–1739, 2005.
- [103] Trung H. M. Pham, Peter Baluk, Ying Xu, Irina Grigorova, Alex J. Bankovich, Rajita Pappu, Shaun R. Coughlin, Donald M. McDonald, Susan R. Schwab, and Jason G. Cyster. Lymphatic endothelial cell sphingosine kinase activity is required for lymphocyte egress and lymphatic patterning. *The Journal of experimental medicine*, 207(1):17–27, 2010.
- [104] Marc Bajenoff, Jackson G. Egen, Lily Y. Koo, Jean Pierre Laugier, Frederic Brau, Nicolas Glaichenhaus, and Ronald N. Germain. Stromal cell networks regulate lymphocyte entry, migration, and territoriality in lymph nodes. *Immunity*, 25(6):989–1001, 2006.
- [105] Lawrence R. Shiow, David B. Rosen, Nadezda Brdickova, Ying Xu, Jinping An, Lewis L. Lanier, Jason G. Cyster, and Mehrdad Matloubian. CD69 acts downstream of interferon-alpha/beta to inhibit S1P1 and lymphocyte egress from lymphoid organs. *Nature*, 440(7083):540–544, 2006.
- [106] Calliope A. Dendrou, Lars Fugger, and Manuel A. Friese. Immunopathology of multiple sclerosis. *Nature reviews. Immunology*, 15(9):545–558, 2015.
- [107] Volker Brinkmann, Andreas Billich, Thomas Baumruker, Peter Heining, Robert Schmouder, Gordon Francis, Shreeram Aradhya, and Pascale Burtin. Fingolimod (FTY720): discovery and development of an oral drug to treat multiple sclerosis. *Nature reviews. Drug discovery*, 9(11):883–897, 2010.

- 
- [108] Volker Brinkmann, Michael D. Davis, Christopher E. Heise, Rainer Albert, Sylvain Cottens, Robert Hof, Christian Bruns, Eva Prieschl, Thomas Baumruker, Peter Hiestand, Carolyn A. Foster, Markus Zollinger, and Kevin R. Lynch. The immune modulator FTY720 targets sphingosine 1-phosphate receptors. *The Journal of biological chemistry*, 277(24):21453–21457, 2002.
- [109] Suzanne Mandala, Richard Hajdu, James Bergstrom, Elizabeth Quackenbush, Jenny Xie, James Milligan, Rosemary Thornton, Gan-Ju Shei, Deborah Card, CarolAnn Keohane, Mark Rosenbach, Jeffrey Hale, Christopher L. Lynch, Kathleen Rupprecht, William Parsons, and Hugh Rosen. Alteration of lymphocyte trafficking by sphingosine-1-phosphate receptor agonists. *Science (New York, N.Y.)*, 296(5566):346–349, 2002.
- [110] Jeffrey A. Cohen, Frederik Barkhof, Giancarlo Comi, Hans-Peter Hartung, Bhupendra O. Khatry, Xavier Montalban, Jean Pelletier, Ruggero Capra, Paolo Gallo, Guillermo Izquierdo, Klaus Tiel-Wilck, Ana de Vera, James Jin, Tracy Stites, Stacy Wu, Shreeram Aradhya, and Ludwig Kappos. Oral fingolimod or intramuscular interferon for relapsing multiple sclerosis. *The New England journal of medicine*, 362(5):402–415, 2010.
- [111] Ludwig Kappos, Ernst-Wilhelm Radue, Paul O’Connor, Chris Polman, Reinhard Hohlfeld, Peter Calabresi, Krzysztof Selmaj, Catherine Agoropoulou, Malgorzata Leyk, Lixin Zhang-Auberson, and Pascale Burtin. A placebo-controlled trial of oral fingolimod in relapsing multiple sclerosis. *The New England journal of medicine*, 362(5):387–401, 2010.
- [112] Alfred H. Merrill, JR. Sphingolipid and glycosphingolipid metabolic pathways in the era of sphingolipidomics. *Chemical reviews*, 111(10):6387–6422, 2011.
- [113] Besim Ogretmen and Yusuf A. Hannun. Biologically active sphingolipids in cancer pathogenesis and treatment. *Nature reviews. Cancer*, 4(8):604–616, 2004.
- [114] Yusuf A. Hannun and Lina M. Obeid. Principles of bioactive lipid signalling: lessons from sphingolipids. *Nature reviews. Molecular cell biology*, 9(2):139–150, 2008.
- [115] Michael Maceyka and Sarah Spiegel. Sphingolipid metabolites in inflammatory disease. *Nature*, 510(7503):58–67, 2014.
- [116] E. C. Mandon, I. Ehses, J. Rother, G. van Echten, and K. Sandhoff. Subcellular localization and membrane topology of serine palmitoyltransferase, 3-dehydrosphinganine reductase, and sphinganine N-acyltransferase in mouse liver. *The Journal of biological chemistry*, 267(16):11144–11148, 1992.
- [117] David K. Breslow, Sean R. Collins, Bernd Bodenmiller, Ruedi Aebersold, Kai Simons, Andrej Shevchenko, Christer S. Ejsing, and Jonathan S. Weissman. Orm family proteins mediate sphingolipid homeostasis. *Nature*, 463(7284):1048–1053, 2010.

- [118] Akio Kihara and Yasuyuki Igarashi. FVT-1 is a mammalian 3-ketodihydrosphingosine reductase with an active site that faces the cytosolic side of the endoplasmic reticulum membrane. *The Journal of biological chemistry*, 279(47):49243–49250, 2004.
- [119] Yael Pewzner-Jung, Shifra Ben-Dor, and Anthony H. Futerman. When do Lasses (longevity assurance genes) become CerS (ceramide synthases)? Insights into the regulation of ceramide synthesis. *The Journal of biological chemistry*, 281(35):25001–25005, 2006.
- [120] D. L. Cadena, R. C. Kurten, and G. N. Gill. The product of the MLD gene is a member of the membrane fatty acid desaturase family: overexpression of MLD inhibits EGF receptor biosynthesis. *Biochemistry*, 36(23):6960–6967, 1997.
- [121] L. Obeid, C. Linardic, L. Karolak, and Y. Hannun. Programmed cell death induced by ceramide. *Science*, 259(5102):1769–1771, 1993.
- [122] Nicole A. Bourbon, Lakshman Sandirasegarane, and Mark Kester. Ceramide-induced inhibition of Akt is mediated through protein kinase Czeta: implications for growth arrest. *The Journal of biological chemistry*, 277(5):3286–3292, 2002.
- [123] G. S. Dbaibo, M. Y. Pushkareva, S. Jayadev, J. K. Schwarz, J. M. Horowitz, L. M. Obeid, and Y. A. Hannun. Retinoblastoma gene product as a downstream target for a ceramide-dependent pathway of growth arrest. *Proceedings of the National Academy of Sciences*, 92(5):1347–1351, 1995.
- [124] Shigeru Daido, Takao Kanzawa, Akitsugu Yamamoto, Hayato Takeuchi, Yasuko Kondo, and Seiji Kondo. Pivotal role of the cell death factor BNIP3 in ceramide-induced autophagic cell death in malignant glioma cells. *Cancer research*, 64(12):4286–4293, 2004.
- [125] Francesca Scarlatti, Chantal Bauvy, Annamaria Ventruti, Giusy Sala, Françoise Cluzeaud, Alain Vandewalle, Riccardo Ghidoni, and Patrice Codogno. Ceramide-mediated macroautophagy involves inhibition of protein kinase B and up-regulation of beclin 1. *The Journal of biological chemistry*, 279(18):18384–18391, 2004.
- [126] G. Muller, M. Ayoub, P. Storz, J. Rennecke, D. Fabbro, and K. Pfizenmaier. PKC zeta is a molecular switch in signal transduction of TNF-alpha, bifunctionally regulated by ceramide and arachidonic acid. *The EMBO journal*, 14(9):1961–1969, 1995.
- [127] Charles E. Chalfant, Zdzislaw Szulc, Patrick Roddy, Alicja Bielawska, and Yusuf A. Hannun. The structural requirements for ceramide activation of serine-threonine protein phosphatases. *Journal of lipid research*, 45(3):496–506, 2004.
- [128] Chia-Ling Chen, Chiou-Feng Lin, Wen-Tsan Chang, Wei-Ching Huang, Chiao-Fang Teng, and Yee-Shin Lin. Ceramide induces p38 MAPK and JNK activation through

- a mechanism involving a thioredoxin-interacting protein-mediated pathway. *Blood*, 111(8):4365–4374, 2008.
- [129] Thomas D. Mullen, Yusuf A. Hannun, and Lina M. Obeid. Ceramide synthases at the centre of sphingolipid metabolism and biology. *The Biochemical journal*, 441(3):789–802, 2012.
- [130] K. Funato and H. Riezman. Vesicular and nonvesicular transport of ceramide from ER to the Golgi apparatus in yeast. *The Journal of cell biology*, 155(6):949–959, 2001.
- [131] Kentaro Hanada, Keigo Kumagai, Satoshi Yasuda, Yukiko Miura, Miyuki Kawano, Masayoshi Fukasawa, and Masahiro Nishijima. Molecular machinery for non-vesicular trafficking of ceramide. *Nature*, 426(6968):803–809, 2003.
- [132] Klazien Huitema, Joep van den Dikkenberg, Jos F. H. M. Brouwers, and Joost C. M. Holthuis. Identification of a family of animal sphingomyelin synthases. *The EMBO journal*, 23(1):33–44, 2004.
- [133] Frances M. Platt. Sphingolipid lysosomal storage disorders. *Nature*, 510(7503):68–75, 2014.
- [134] Gerrit van Meer, Dennis R. Voelker, and Gerald W. Feigenson. Membrane lipids: where they are and how they behave. *Nature reviews. Molecular cell biology*, 9(2):112–124, 2008.
- [135] Rui-Dong Duan, Yajun Cheng, Gert Hansen, Erik Hertervig, Jian-Jun Liu, Ingvar Syk, Hans Sjostrom, and Ake Nilsson. Purification, localization, and expression of human intestinal alkaline sphingomyelinase. *Journal of lipid research*, 44(6):1241–1250, 2003.
- [136] Norma Marchesini and Yusuf A. Hannun. Acid and neutral sphingomyelinases: roles and mechanisms of regulation. *Biochemistry and cell biology = Biochimie et biologie cellulaire*, 82(1):27–44, 2004.
- [137] S. L. Schissel, E. H. Schuchman, K. J. Williams, and I. Tabas. Zn<sup>2+</sup>-stimulated sphingomyelinase is secreted by many cell types and is a product of the acid sphingomyelinase gene. *The Journal of biological chemistry*, 271(31):18431–18436, 1996.
- [138] S. L. Schissel, G. A. Keesler, E. H. Schuchman, K. J. Williams, and I. Tabas. The cellular trafficking and zinc dependence of secretory and lysosomal sphingomyelinase, two products of the acid sphingomyelinase gene. *The Journal of biological chemistry*, 273(29):18250–18259, 1998.
- [139] H. Sawai, N. Domae, N. Nagan, and Y. A. Hannun. Function of the cloned putative neutral sphingomyelinase as lyso-platelet activating factor-phospholipase C. *The Journal of biological chemistry*, 274(53):38131–38139, 1999.

- 
- [140] Wilhelm Stoffel, Britta Jenke, Barbara Block, Markus Zumbansen, and Jurgen Koeke. Neutral sphingomyelinase 2 (smpd3) in the control of postnatal growth and development. *Proceedings of the National Academy of Sciences of the United States of America*, 102(12):4554–4559, 2005.
- [141] Oleg Krut, Katja Wiegmann, Hamid Kashkar, Benjamin Yazdanpanah, and Martin Kronke. Novel tumor necrosis factor-responsive mammalian neutral sphingomyelinase-3 is a C-tail-anchored protein. *The Journal of biological chemistry*, 281(19):13784–13793, 2006.
- [142] Cungui Mao and Lina M. Obeid. Ceramidases: regulators of cellular responses mediated by ceramide, sphingosine, and sphingosine-1-phosphate. *Biochimica et biophysica acta*, 1781(9):424–434, 2008.
- [143] Chi-Ming Li, Jae-Ho Park, Calogera M. Simonaro, Xingxuan He, Ronald E. Gordon, Adriana-Haimovitz Friedman, Desiree Ehleiter, Francois Paris, Katia Manova, Stefan Hepbildikler, Zvi Fuks, Konrad Sandhoff, Richard Kolesnick, and Edward H. Schuchman. Insertional mutagenesis of the mouse acid ceramidase gene leads to early embryonic lethality in homozygotes and progressive lipid storage disease in heterozygotes. *Genomics*, 79(2):218–224, 2002.
- [144] Mari Kono, Jennifer L. Dreier, Jessica M. Ellis, Maria L. Allende, Danielle N. Kalkofen, Kathleen M. Sanders, Jacek Bielawski, Alicja Bielawska, Yusuf A. Hannun, and Richard L. Proia. Neutral ceramidase encoded by the *Asah2* gene is essential for the intestinal degradation of sphingolipids. *The Journal of biological chemistry*, 281(11):7324–7331, 2006.
- [145] Motohiro Tani, Yasuyuki Igarashi, and Makoto Ito. Involvement of neutral ceramidase in ceramide metabolism at the plasma membrane and in extracellular milieu. *The Journal of biological chemistry*, 280(44):36592–36600, 2005.
- [146] Michal Levy and Anthony H. Futerman. Mammalian ceramide synthases. *IUBMB life*, 62(5):347–356, 2010.
- [147] Krishnan Venkataraman, Christian Riebeling, Jacques Bodennec, Howard Riezman, Jeremy C. Allegood, M. Cameron Sullards, Alfred H. Merrill, JR, and Anthony H. Futerman. Upstream of growth and differentiation factor 1 (*uog1*), a mammalian homolog of the yeast longevity assurance gene 1 (*LAG1*), regulates N-stearoyl-sphinganine (C18-(dihydro)ceramide) synthesis in a fumonisins B1-independent manner in mammalian cells. *The Journal of biological chemistry*, 277(38):35642–35649, 2002.
- [148] Christian Riebeling, Jeremy C. Allegood, Elaine Wang, Alfred H. Merrill, JR, and Anthony H. Futerman. Two mammalian longevity assurance gene (*LAG1*) family

- members, trh1 and trh4, regulate dihydroceramide synthesis using different fatty acyl-CoA donors. *The Journal of biological chemistry*, 278(44):43452–43459, 2003.
- [149] Yukiko Mizutani, Akio Kihara, and Yasuyuki Igarashi. Mammalian Lass6 and its related family members regulate synthesis of specific ceramides. *The Biochemical journal*, 390(Pt 1):263–271, 2005.
- [150] Junxia Min, Adi Mesika, Mayandi Sivaguru, Paul P. van Veldhoven, Hannah Alexander, Anthony H. Futerman, and Stephen Alexander. (Dihydro)ceramide synthase 1 regulated sensitivity to cisplatin is associated with the activation of p38 mitogen-activated protein kinase and is abrogated by sphingosine kinase 1. *Molecular cancer research : MCR*, 5(8):801–812, 2007.
- [151] Eitan Winter and Chris P. Ponting. TRAM, LAG1 and CLN8: members of a novel family of lipid-sensing domains? *Trends in biochemical sciences*, 27(8):381–383, 2002.
- [152] Krishnan Venkataraman and Anthony H. Futerman. Do longevity assurance genes containing Hox domains regulate cell development via ceramide synthesis? *FEBS letters*, 528(1-3):3–4, 2002.
- [153] Stefka Spassieva, Jae-Gu Seo, James C. Jiang, Jacek Bielawski, Fernando Alvarez-Vasquez, S. Michal Jazwinski, Yusuf A. Hannun, and Lina M. Obeid. Necessary role for the Lag1p motif in (dihydro)ceramide synthase activity. *The Journal of biological chemistry*, 281(45):33931–33938, 2006.
- [154] Adi Mesika, Shifra Ben-Dor, Elad L. Laviad, and Anthony H. Futerman. A new functional motif in Hox domain-containing ceramide synthases: identification of a novel region flanking the Hox and TLC domains essential for activity. *The Journal of biological chemistry*, 282(37):27366–27373, 2007.
- [155] Elad L. Laviad, Lee Albee, Irene Pankova-Kholmyansky, Sharon Epstein, Hyejung Park, Alfred H. Merrill, JR, and Anthony H. Futerman. Characterization of ceramide synthase 2: tissue distribution, substrate specificity, and inhibition by sphingosine 1-phosphate. *The Journal of biological chemistry*, 283(9):5677–5684, 2008.
- [156] Yukiko Mizutani, Akio Kihara, and Yasuyuki Igarashi. LASS3 (longevity assurance homologue 3) is a mainly testis-specific (dihydro)ceramide synthase with relatively broad substrate specificity. *The Biochemical journal*, 398(3):531–538, 2006.
- [157] Ivonne Becker, Lihua Wang-Eckhardt, Afshin Yaghootfam, Volkmar Gieselmann, and Matthias Eckhardt. Differential expression of (dihydro)ceramide synthases in mouse brain: oligodendrocyte-specific expression of CerS2/Lass2. *Histochemistry and cell biology*, 129(2):233–241, 2008.
- [158] Christina Ginkel, Dieter Hartmann, Katharina Vom Dorp, Armin Zlomuzica, Hany Farwanah, Matthias Eckhardt, Roger Sandhoff, Joachim Degen, Mariona Rabionet,

- Ekrem Dere, Peter Dormann, Konrad Sandhoff, and Klaus Willecke. Ablation of neuronal ceramide synthase 1 in mice decreases ganglioside levels and expression of myelin-associated glycoprotein in oligodendrocytes. *The Journal of biological chemistry*, 287(50):41888–41902, 2012.
- [159] Serap Koybasi, Can E. Senkal, Kamala Sundararaj, Stefka Spassieva, Jacek Bielawski, Walid Osta, Terry A. Day, James C. Jiang, S. Michal Jazwinski, Yusuf A. Hannun, Lina M. Obeid, and Besim Ogretmen. Defects in cell growth regulation by C18:0-ceramide and longevity assurance gene 1 in human head and neck squamous cell carcinomas. *The Journal of biological chemistry*, 279(43):44311–44319, 2004.
- [160] Silke Imgrund, Dieter Hartmann, Hany Farwanah, Matthias Eckhardt, Roger Sandhoff, Joachim Degen, Volkmar Gieselmann, Konrad Sandhoff, and Klaus Willecke. Adult ceramide synthase 2 (CERS2)-deficient mice exhibit myelin sheath defects, cerebellar degeneration, and hepatocarcinomas. *The Journal of biological chemistry*, 284(48):33549–33560, 2009.
- [161] Yael Pewzner-Jung, Ori Brenner, Svantje Braun, Elad L. Laviad, Shifra Ben-Dor, Ester Feldmesser, Shirley Horn-Saban, Daniela Amann-Zalcenstein, Calanit Raanan, Tamara Berkutzki, Racheli Erez-Roman, Oshrit Ben-David, Michal Levy, Dorin Holzman, Hyejung Park, Abraham Nyska, Alfred H. Merrill, JR, and Anthony H. Futerman. A critical role for ceramide synthase 2 in liver homeostasis: II. insights into molecular changes leading to hepatopathy. *The Journal of biological chemistry*, 285(14):10911–10923, 2010.
- [162] Suryaprakash Raichur, Siew Tein Wang, Puck Wee Chan, Ying Li, Jianhong Ching, Bhagirath Chaurasia, Shaillay Dogra, Miina K. Ohman, Kosuke Takeda, Shigeki Sugii, Yael Pewzner-Jung, Anthony H. Futerman, and Scott A. Summers. CerS2 haploinsufficiency inhibits beta-oxidation and confers susceptibility to diet-induced steatohepatitis and insulin resistance. *Cell metabolism*, 20(4):687–695, 2014.
- [163] Julia Barthelmes, Anika Manner de Bazo, Yael Pewzner-Jung, Katja Schmitz, Christoph A. Mayer, Christian Foerch, Max Eberle, Nadja Tafferner, Nerea Ferreira, Marina Henke, Gerd Geisslinger, Anthony H. Futerman, Sabine Grosch, and Susanne Schiffmann. Lack of ceramide synthase 2 suppresses the development of experimental autoimmune encephalomyelitis by impairing the migratory capacity of neutrophils. *Brain, behavior, and immunity*, 46:280–292, 2015.
- [164] E. Aflaki, P. Doddapattar, B. Radovic, S. Povoden, D. Kolb, N. Vujic, M. Wegscheider, H. Koefeler, T. Hornemann, W. F. Graier, R. Malli, F. Madeo, and D. Kratky. C16 ceramide is crucial for triacylglycerol-induced apoptosis in macrophages. *Cell death & disease*, 3:e280, 2012.
- [165] Kena Desai, M. Cameron Sullards, Jeremy Allegood, Elaine Wang, Eva M. Schmelz, Michaela Hartl, Hans-Ulrich Humpf, D.C Liotta, Qiong Peng, and Alfred H. Merrill.

- Fumonisin and fumonisin analogs as inhibitors of ceramide synthase and inducers of apoptosis. *Biochimica et Biophysica Acta (BBA) - Molecular and Cell Biology of Lipids*, 1585(2-3):188–192, 2002.
- [166] Yael Pewzner-Jung, Hyejung Park, Elad L. Laviad, Liana C. Silva, Sujoy Lahiri, Johnny Stiban, Racheli Erez-Roman, Britta Brugger, Timo Sachsenheimer, Felix Wieland, Manuel Prieto, Alfred H. Merrill, JR, and Anthony H. Futerman. A critical role for ceramide synthase 2 in liver homeostasis: I. alterations in lipid metabolic pathways. *The Journal of biological chemistry*, 285(14):10902–10910, 2010.
- [167] Sarah M. Turpin, Hayley T. Nicholls, Diana M. Willmes, Arnaud Mourier, Susanne Brodesser, Claudia M. Wunderlich, Jan Mauer, Elaine Xu, Philipp Hammerschmidt, Hella S. Bronneke, Aleksandra Trifunovic, Giuseppe LoSasso, F. Thomas Wunderlich, Jan-Wilhelm Kornfeld, Matthias Bluher, Martin Kronke, and Jens C. Bruning. Obesity-induced CerS6-dependent C16:0 ceramide production promotes weight gain and glucose intolerance. *Cell metabolism*, 20(4):678–686, 2014.
- [168] Woo-Jae Park and Joo-Won Park. The effect of altered sphingolipid acyl chain length on various disease models. *Biological chemistry*, 396(6-7):693–705, 2015.
- [169] Johnny Stiban and Meenu Perera. Very long chain ceramides interfere with C16-ceramide-induced channel formation: A plausible mechanism for regulating the initiation of intrinsic apoptosis. *Biochimica et biophysica acta*, 1848(2):561–567, 2015.
- [170] Takayuki Sassa, Shota Suto, Yuriko Okayasu, and Akio Kihara. A shift in sphingolipid composition from C24 to C16 increases susceptibility to apoptosis in HeLa cells. *Biochimica et biophysica acta*, 1821(7):1031–1037, 2012.
- [171] Daniela Hartmann, Marthe-Susanna Wegner, Ruth Anna Wanger, Nerea Ferreiros, Yannick Schreiber, Jessica Lucks, Susanne Schiffmann, Gerd Geisslinger, and Sabine Grosch. The equilibrium between long and very long chain ceramides is important for the fate of the cell and can be influenced by co-expression of CerS. *The international journal of biochemistry & cell biology*, 45(7):1195–1203, 2013.
- [172] Samy A. F. Morad and Myles C. Cabot. Ceramide-orchestrated signalling in cancer cells. *Nature reviews. Cancer*, 13(1):51–65, 2013.
- [173] Mariona Rabionet, Aarnoud C. van der Spoel, Chia-Chen Chuang, Benita von Tumpling-Radosta, Manja Litjens, Diane Bouwmeester, Christina C. Hellbusch, Christian Korner, Herbert Wiegandt, Karin Gorgas, Frances M. Platt, Hermann-Josef Grone, and Roger Sandhoff. Male germ cells require polyenoic sphingolipids with complex glycosylation for completion of meiosis: a link to ceramide synthase-3. *The Journal of biological chemistry*, 283(19):13357–13369, 2008.

- [174] Mariona Rabionet, Aline Bayerle, Richard Jennemann, Hans Heid, Jens Fuchser, Christian Marsching, Stefan Porubsky, Christian Bolenz, Florian Guillou, Hermann-Josef Grone, Karin Gorgas, and Roger Sandhoff. Male meiotic cytokinesis requires ceramide synthase 3-dependent sphingolipids with unique membrane anchors. *Human molecular genetics*, 24(17):4792–4808, 2015.
- [175] Richard Jennemann, Mariona Rabionet, Karin Gorgas, Sharon Epstein, Alexander Dalpke, Ulrike Rothermel, Aline Bayerle, Franciscus van der Hoeven, Silke Imgrund, Joachim Kirsch, Walter Nickel, Klaus Willecke, Howard Riezman, Hermann-Josef Grone, and Roger Sandhoff. Loss of ceramide synthase 3 causes lethal skin barrier disruption. *Human molecular genetics*, 21(3):586–608, 2012.
- [176] Philipp Ebel, Silke Imgrund, Katharina Vom Dorp, Kristina Hofmann, Helena Maier, Helena Drake, Joachim Degen, Peter Dormann, Matthias Eckhardt, Thomas Franz, and Klaus Willecke. Ceramide synthase 4 deficiency in mice causes lipid alterations in sebum and results in alopecia. *The Biochemical journal*, 461(1):147–158, 2014.
- [177] Franziska Peters, Susanne Vorhagen, Susanne Brodesser, Kristin Jakobshagen, Jens C. Bruning, Carien M. Niessen, and Martin Kronke. Ceramide synthase 4 regulates stem cell homeostasis and hair follicle cycling. *The Journal of investigative dermatology*, 135(6):1501–1509, 2015.
- [178] Dominic Gosejacob, Philipp S. Jager, Katharina Vom Dorp, Martin Frejno, Anne C. Carstensen, Monika Kohnke, Joachim Degen, Peter Dormann, and Michael Hoch. Ceramide Synthase 5 Is Essential to Maintain C16:0-Ceramide Pools and Contributes to the Development of Diet-induced Obesity. *The Journal of biological chemistry*, 291(13):6989–7003, 2016.
- [179] Kazuyuki Kitatani, Jolanta Idkowiak-Baldys, Jacek Bielawski, Tarek A. Taha, Russell W. Jenkins, Can E. Senkal, Besim Ogretmen, Lina M. Obeid, and Yusuf A. Hannun. Protein kinase C-induced activation of a ceramide/protein phosphatase 1 pathway leading to dephosphorylation of p38 MAPK. *The Journal of biological chemistry*, 281(48):36793–36802, 2006.
- [180] Junfei Jin, Qi Hou, Thomas D. Mullen, Youssef H. Zeidan, Jacek Bielawski, Jacqueline M. Kraveka, Alicja Bielawska, Lina M. Obeid, Yusuf A. Hannun, and Yi-Te Hsu. Ceramide generated by sphingomyelin hydrolysis and the salvage pathway is involved in hypoxia/reoxygenation-induced Bax redistribution to mitochondria in NT-2 cells. *The Journal of biological chemistry*, 283(39):26509–26517, 2008.
- [181] Philipp Ebel, Katharina Vom Dorp, Elisabeth Petrasch-Parwez, Armin Zlomuzica, Kiyoka Kinugawa, Jean Mariani, David Minich, Christina Ginkel, Jochen Welcker, Joachim Degen, Matthias Eckhardt, Ekrem Dere, Peter Dormann, and Klaus

- Willecke. Inactivation of ceramide synthase 6 in mice results in an altered sphingolipid metabolism and behavioral abnormalities. *The Journal of biological chemistry*, 288(29):21433–21447, 2013.
- [182] Max Eberle, Philipp Ebel, Christoph A. Mayer, Julia Barthelmes, Nadja Tafferner, Nerea Ferreira, Thomas Ulshofer, Marina Henke, Christian Foerch, Anika Manner de Bazo, Sabine Grosch, Gerd Geisslinger, Klaus Willecke, and Susanne Schiffmann. Exacerbation of experimental autoimmune encephalomyelitis in ceramide synthase 6 knockout mice is associated with enhanced activation/migration of neutrophils. *Immunology and cell biology*, 93(9):825–836, 2015.
- [183] Motoshi Suzuki, Ke Cao, Seiichi Kato, Yuji Komizu, Naoki Mizutani, Kouji Tanaka, Chinatsu Arima, Mei Chee Tai, Kiyoshi Yanagisawa, Norie Togawa, Takahiro Shiraiishi, Noriyasu Usami, Tetsuo Taniguchi, Takayuki Fukui, Kohei Yokoi, Keiko Wakahara, Yoshinori Hasegawa, Yukiko Mizutani, Yasuyuki Igarashi, Jin-ichi Inokuchi, Soichiro Iwaki, Satoshi Fujii, Akira Satou, Yoko Matsumoto, Ryuichi Ueoka, Keiko Tamiya-Koizumi, Takashi Murate, Mitsuhiro Nakamura, Mamoru Kyogashima, and Takashi Takahashi. Targeting ceramide synthase 6-dependent metastasis-prone phenotype in lung cancer cells. *The Journal of clinical investigation*, 126(1):254–265, 2016.
- [184] Annette R. Khaled and Scott K. Durum. Lymphocide: cytokines and the control of lymphoid homeostasis. *Nature reviews. Immunology*, 2(11):817–830, 2002.
- [185] Stuart M. Pitson. Regulation of sphingosine kinase and sphingolipid signaling. *Trends in biochemical sciences*, 36(2):97–107, 2011.
- [186] Thomas H. Beckham, Ping Lu, Joseph C. Cheng, Dan Zhao, Lorianne S. Turner, Xiaoyi Zhang, Stanley Hoffman, Kent E. Armeson, Angen Liu, Tucker Marrison, Yusuf A. Hannun, and Xiang Liu. Acid ceramidase-mediated production of sphingosine 1-phosphate promotes prostate cancer invasion through upregulation of cathepsin B. *International journal of cancer*, 131(9):2034–2043, 2012.
- [187] Ruijuan Xu, Junfei Jin, Wei Hu, Wei Sun, Jacek Bielawski, Zdzislaw Szulc, Tarek Taha, Lina M. Obeid, and Cungui Mao. Golgi alkaline ceramidase regulates cell proliferation and survival by controlling levels of sphingosine and S1P. *FASEB journal : official publication of the Federation of American Societies for Experimental Biology*, 20(11):1813–1825, 2006.
- [188] Hila Zigdon, Aviram Kogot-Levin, Joo-Won Park, Ruth Goldschmidt, Samuel Kelly, Alfred H. Merrill, JR, Avigdor Scherz, Yael Pewzner-Jung, Ann Saada, and Anthony H. Futerman. Ablation of ceramide synthase 2 causes chronic oxidative stress due to disruption of the mitochondrial respiratory chain. *The Journal of biological chemistry*, 288(7):4947–4956, 2013.

- [189] Shinkyu Choi, Ji Ae Kim, Tae Hun Kim, Hai-Yan Li, Kyong-Oh Shin, Yong-Moon Lee, Seikwan Oh, Yael Pewzner-Jung, Anthony H. Futerman, and Suk Hyo Suh. Altering sphingolipid composition with aging induces contractile dysfunction of gastric smooth muscle via K(Ca) 1.1 upregulation. *Aging cell*, 14(6):982–994, 2015.
- [190] Stefka D. Spassieva, Xiaojie Ji, Ye Liu, Kenneth Gable, Jacek Bielawski, Teresa M. Dunn, Erhard Bieberich, and Lihong Zhao. Ectopic expression of ceramide synthase 2 in neurons suppresses neurodegeneration induced by ceramide synthase 1 deficiency. *Proceedings of the National Academy of Sciences of the United States of America*, 113(21):5928–5933, 2016.
- [191] Christiane Kremser, Anna-Lena Klemm, Martina van Uelft, Silke Imgrund, Christina Ginkel, Dieter Hartmann, and Klaus Willecke. Cell-type-specific expression pattern of ceramide synthase 2 protein in mouse tissues. *Histochemistry and cell biology*, 140(5):533–547, 2013.
- [192] H. Charbonneau, N. K. Tonks, K. A. Walsh, and E. H. Fischer. The leukocyte common antigen (CD45): a putative receptor-linked protein tyrosine phosphatase. *Proceedings of the National Academy of Sciences of the United States of America*, 85(19):7182–7186, 1988.
- [193] Werner Held, Hans Clevers, and Rudolf Grosschedl. Redundant functions of TCF-1 and LEF-1 during T and NK cell development, but unique role of TCF-1 for Ly49 NK cell receptor acquisition. *European journal of immunology*, 33(5):1393–1398, 2003.
- [194] A. Janowska-Wieczorek, M. Majka, J. Kijowski, M. Baj-Krzyworzeka, R. Reca, A. R. Turner, J. Ratajczak, S. G. Emerson, M. A. Kowalska, and M. Z. Ratajczak. Platelet-derived microparticles bind to hematopoietic stem/progenitor cells and enhance their engraftment. *Blood*, 98(10):3143–3149, 2001.
- [195] L. Lai, N. Alaverdi, L. Maltais, and H. C. 3rd Morse. Mouse cell surface antigens: nomenclature and immunophenotyping. *Journal of immunology (Baltimore, Md. : 1950)*, 160(8):3861–3868, 1998.
- [196] H. C. 3rd Morse, F. W. Shen, and U. Hammerling. Genetic nomenclature for loci controlling mouse lymphocyte antigens. *Immunogenetics*, 25(2):71–78, 1987.
- [197] Kimberly S. Schluns, Kristina Williams, Averil Ma, Xin X. Zheng, and Leo Lefrancois. Cutting edge: requirement for IL-15 in the generation of primary and memory antigen-specific CD8 T cells. *Journal of immunology (Baltimore, Md. : 1950)*, 168(10):4827–4831, 2002.
- [198] F. W. Shen, Y. Saga, G. Litman, G. Freeman, J. S. Tung, H. Cantor, and E. A. Boyse. Cloning of Ly-5 cDNA. *Proceedings of the National Academy of Sciences of the United States of America*, 82(21):7360–7363, 1985.

- [199] Guoxiang Yang, Hiroko Hisha, Yunze Cui, Tianxue Fan, Tienan Jin, Qing Li, Zhexiong Lian, Naoki Hosaka, Yulin Li, and Susumu Ikehara. A new assay method for late CFU-S formation and long-term reconstituting activity using a small number of pluripotent hemopoietic stem cells. *Stem cells (Dayton, Ohio)*, 20(3):241–248, 2002.
- [200] I. Wiame, S. Remy, R. Swennen, and L. Sagi. Irreversible heat inactivation of DNase I without RNA degradation. *BioTechniques*, 29(2):252–4, 256, 2000.
- [201] Constantin Bode and Markus H. Graler. Quantification of sphingosine-1-phosphate and related sphingolipids by liquid chromatography coupled to tandem mass spectrometry. *Methods in molecular biology (Clifton, N.J.)*, 874:33–44, 2012.
- [202] Ilker Karaca, Irfan Y. Tamboli, Konstantin Glebov, Josefine Richter, Lisa H. Fell, Marcus O. Grimm, Viola J. Hauptenthal, Tobias Hartmann, Markus H. Graler, Gerhild van Echten-Deckert, and Jochen Walter. Deficiency of sphingosine-1-phosphate lyase impairs lysosomal metabolism of the amyloid precursor protein. *The Journal of biological chemistry*, 289(24):16761–16772, 2014.
- [203] Natalie Seach, Kahlia Wong, Maree Hammett, Richard L. Boyd, and Ann P. Chidgey. Purified enzymes improve isolation and characterization of the adult thymic epithelium. *Journal of immunological methods*, 385(1-2):23–34, 2012.
- [204] Zvi Grossman, Booki Min, Martin Meier-Schellersheim, and William E. Paul. Concomitant regulation of T-cell activation and homeostasis. *Nature reviews. Immunology*, 4(5):387–395, 2004.
- [205] Arne N. Akbar, Milica Vukmanovic-Stejic, Leonie S. Taams, and Derek C. Macallan. The dynamic co-evolution of memory and regulatory CD4+ T cells in the periphery. *Nature reviews. Immunology*, 7(3):231–237, 2007.
- [206] Peter H. Krammer, Rudiger Arnold, and Inna N. Lavrik. Life and death in peripheral T cells. *Nature reviews. Immunology*, 7(7):532–542, 2007.
- [207] Charles D. Surh and Jonathan Sprent. Homeostasis of naive and memory T cells. *Immunity*, 29(6):848–862, 2008.
- [208] Erwin F. Wagner and Angel R. Nebreda. Signal integration by JNK and p38 MAPK pathways in cancer development. *Nature reviews. Cancer*, 9(8):537–549, 2009.
- [209] Eulalia de Nadal, Gustav Ammerer, and Francesc Posas. Controlling gene expression in response to stress. *Nature reviews. Genetics*, 12(12):833–845, 2011.
- [210] Mari Kono, Ana E. Tucker, Jennifer Tran, Jennifer B. Bergner, Ewa M. Turner, and Richard L. Proia. Sphingosine-1-phosphate receptor 1 reporter mice reveal receptor activation sites in vivo. *The Journal of clinical investigation*, 124(5):2076–2086, 2014.

- [211] James R. van Brocklyn, Menq-Jer Lee, Ramil Menzeleev, Ana Olivera, Lisa Edsall, Olivier Cuvillier, Dianne M. Thomas, Peter J.P. Coopman, Shobha Thangada, Catherine H. Liu, Timothy Hla, and Sarah Spiegel. Dual Actions of Sphingosine-1-Phosphate: Extracellular through the G<sub>i</sub>-coupled Receptor Edg-1 and Intracellular to Regulate Proliferation and Survival. *The Journal of Cell Biology*, 142(1):229–240, 1998.
- [212] Mingxia Liu, Jeongmin Seo, Jeremy Allegood, Xin Bi, Xuewei Zhu, Elena Boudyguina, Abraham K. Gebre, Dorit Avni, Dharika Shah, Mary G. Sorci-Thomas, Michael J. Thomas, Gregory S. Shelness, Sarah Spiegel, and John S. Parks. Hepatic apolipoprotein M (apoM) overexpression stimulates formation of larger apoM/sphingosine 1-phosphate-enriched plasma high density lipoprotein. *The Journal of biological chemistry*, 289(5):2801–2814, 2014.
- [213] Yalin Emre, Magali Irla, Isabelle Dunand-Sauthier, Romain Ballet, Mehdi Meguevani, Stephane Jemelin, Christian Vesin, Walter Reith, and Beat A. Imhof. Thymic epithelial cell expansion through matricellular protein CYR61 boosts progenitor homing and T-cell output. *Nature communications*, 4:2842, 2013.
- [214] Immanuel Rode and Thomas Boehm. Regenerative capacity of adult cortical thymic epithelial cells. *Proceedings of the National Academy of Sciences of the United States of America*, 109(9):3463–3468, 2012.
- [215] S. M. M. Haeryfar and D. W. Hoskin. Thy-1: More than a Mouse Pan-T Cell Marker. *The Journal of Immunology*, 173(6):3581–3588, 2004.
- [216] Raimon Duran-Struuck and Robert C. Dysko. Principles of bone marrow transplantation (BMT): providing optimal veterinary and husbandry care to irradiated mice in BMT studies. *Journal of the American Association for Laboratory Animal Science : JAALAS*, 48(1):11–22, 2009.
- [217] S. P. Berzins, R. L. Boyd, and J.F.A.P. Miller. The Role of the Thymus and Recent Thymic Migrants in the Maintenance of the Adult Peripheral Lymphocyte Pool. *The Journal of Experimental Medicine*, 187(11):1839–1848, 1998.
- [218] Brent A. Wilkerson and Kelley M. Argraves. The role of sphingosine-1-phosphate in endothelial barrier function. *Biochimica et biophysica acta*, 1841(10):1403–1412, 2014.
- [219] Constantin Bode, Sven-Christian Sensken, Ulrike Peest, Gernot Beutel, Felicitas Thol, Bodo Levkau, Zaiguo Li, Robert Bittman, Tao Huang, Markus Tolle, Markus van der Giet, and Markus H. Graler. Erythrocytes serve as a reservoir for cellular and extracellular sphingosine 1-phosphate. *Journal of cellular biochemistry*, 109(6):1232–1243, 2010.

- [220] Sven-Christian Sensken, Constantin Bode, Manju Nagarajan, Ulrike Peest, Oliver Pabst, and Markus H. Graler. Redistribution of sphingosine 1-phosphate by sphingosine kinase 2 contributes to lymphopenia. *Journal of immunology (Baltimore, Md. : 1950)*, 184(8):4133–4142, 2010.
- [221] Yuquan Xiong and Timothy Hla. S1P Control of Endothelial Integrity. In Michael B. A. Oldstone and Hugh Rosen, editors, *Sphingosine-1-Phosphate signaling in immunology and infectious diseases*, volume 378 of *Current Topics in Microbiology and Immunology*, pages 85–105. Springer, Berlin, 2014.
- [222] Y. Y. Kisanuki, R. E. Hammer, J. Miyazaki, S. C. Williams, J. A. Richardson, and M. Yanagisawa. Tie2-Cre transgenic mice: a new model for endothelial cell-lineage analysis in vivo. *Developmental biology*, 230(2):230–242, 2001.
- [223] Joao Pedro Pereira, Ying Xu, and Jason G. Cyster. A role for S1P and S1P1 in immature-B cell egress from mouse bone marrow. *PloS one*, 5(2):e9277, 2010.
- [224] Joo-Won Park, Woo-Jae Park, and Anthony H. Futerman. Ceramide synthases as potential targets for therapeutic intervention in human diseases. *Biochimica et biophysica acta*, 1841(5):671–681, 2014.
- [225] Sabine Grosch, Susanne Schiffmann, and Gerd Geisslinger. Chain length-specific properties of ceramides. *Progress in lipid research*, 51(1):50–62, 2012.
- [226] Timothy Hla and Richard Kolesnick. C16:0-ceramide signals insulin resistance. *Cell metabolism*, 20(5):703–705, 2014.
- [227] Joseph C. Cheng, Aiping Bai, Thomas H. Beckham, S. Tucker Marrison, Caroline L. Yount, Katherine Young, Ping Lu, Anne M. Bartlett, Bill X. Wu, Barry J. Keane, Kent E. Armeson, David T. Marshall, Thomas E. Keane, Michael T. Smith, E. Ellen Jones, Richard R. Drake, JR, Alicja Bielawska, James S. Norris, and Xiang Liu. Radiation-induced acid ceramidase confers prostate cancer resistance and tumor relapse. *The Journal of clinical investigation*, 123(10):4344–4358, 2013.
- [228] Kai Wang, Ruijuan Xu, Jennifer Schrandt, Prithvi Shah, Yong Z. Gong, Chet Preston, Louis Wang, Jae Kyo Yi, Chih-Li Lin, Wei Sun, Demetri D. Spyropoulos, Soyoung Rhee, Mingsong Li, Jie Zhou, Shaoyu Ge, Guofeng Zhang, Ashley J. Snider, Yusuf A. Hannun, Lina M. Obeid, and Cungui Mao. Alkaline Ceramidase 3 Deficiency Results in Purkinje Cell Degeneration and Cerebellar Ataxia Due to Dyshomeostasis of Sphingolipids in the Brain. *PLoS genetics*, 11(10):e1005591, 2015.
- [229] Wei Sun, Ruijuan Xu, Wei Hu, Junfei Jin, Heather A. Crellin, Jacek Bielawski, Zdzislaw M. Szulc, Bruce H. Thiers, Lina M. Obeid, and Cungui Mao. Upregulation of the human alkaline ceramidase 1 and acid ceramidase mediates calcium-induced differentiation of epidermal keratinocytes. *The Journal of investigative dermatology*, 128(2):389–397, 2008.

- [230] Kiyoharu Ito, Yoshihiro Anada, Motohiro Tani, Mika Ikeda, Takamitsu Sano, Akio Kihara, and Yasuyuki Igarashi. Lack of sphingosine 1-phosphate-degrading enzymes in erythrocytes. *Biochemical and biophysical research communications*, 357(1):212–217, 2007.
- [231] Susanne Schiffmann, Daniela Hartmann, Sina Fuchs, Kerstin Birod, Nerea Ferreira, Yannick Schreiber, Aleksandra Zivkovic, Gerd Geisslinger, Sabine Grosch, and Holger Stark. Inhibitors of specific ceramide synthases. *Biochimie*, 94(2):558–565, 2012.
- [232] Madduri Srinivasarao, Chris V. Galliford, and Philip S. Low. Principles in the design of ligand-targeted cancer therapeutics and imaging agents. *Nature reviews. Drug discovery*, 14(3):203–219, 2015.
- [233] Avinash Bhandoola and Arivazhagan Sambandam. From stem cell to T cell: one route or many? *Nature reviews. Immunology*, 6(2):117–126, 2006.
- [234] Abbe N. Vallejo. Immune remodeling: lessons from repertoire alterations during chronological aging and in immune-mediated disease. *Trends in molecular medicine*, 13(3):94–102, 2007.
- [235] Donald B. Palmer. The effect of age on thymic function. *Frontiers in immunology*, 4:316, 2013.
- [236] F. T. Fitzpatrick, M. D. Kendall, M. J. Wheeler, I. M. Adcock, and B. D. Greenstein. Reappearance of thymus of ageing rats after orchidectomy. *The Journal of endocrinology*, 106(3):R17–9, 1985.
- [237] J. S. Sutherland, G. L. Goldberg, M. V. Hammett, A. P. Uldrich, S. P. Berzins, T. S. Heng, B. R. Blazar, J. L. Millar, M. A. Malin, A. P. Chidgey, and R. L. Boyd. Activation of Thymic Regeneration in Mice and Humans following Androgen Blockade. *The Journal of Immunology*, 175(4):2741–2753, 2005.
- [238] Jarrod A. Dudakov, Gabrielle L. Goldberg, Jessica J. Reiseger, Katerina Vlahos, Ann P. Chidgey, and Richard L. Boyd. Sex steroid ablation enhances hematopoietic recovery following cytotoxic antineoplastic therapy in aged mice. *Journal of immunology (Baltimore, Md. : 1950)*, 183(11):7084–7094, 2009.
- [239] A. L. Zoller and G. J. Kersh. Estrogen Induces Thymic Atrophy by Eliminating Early Thymic Progenitors and Inhibiting Proliferation of -Selected Thymocytes. *The Journal of Immunology*, 176(12):7371–7378, 2006.
- [240] Tracy S. P. Heng, Gabrielle L. Goldberg, Daniel H. D. Gray, Jayne S. Sutherland, Ann P. Chidgey, and Richard L. Boyd. Effects of castration on thymocyte development in two different models of thymic involution. *Journal of immunology (Baltimore, Md. : 1950)*, 175(5):2982–2993, 2005.

- [241] Lisa A. Pieper, Michaela Strotbek, Till Wenger, Martin Gamer, Monilola A. Olayioye, and Angelika Hausser. Secretory pathway optimization of CHO producer cells by co-engineering of the mitoRNA-1978 target genes CerS2 and Tbc1D20. *Metabolic engineering*, 40:69–79, 2017.

## Acknowledgements

I am grateful to Prof. Dr. Waldemar Kolanus for his outstanding scientific guidance in the last years and for giving me the opportunity to develop my "exotic" PhD project independently.

I also want to thank Prof. Dr. Irmgard Förster as second reviewer, as well as Prof. Dr. Christian Kurts and Prof. Dr. Ulf Meißner as additional members of the examination board.

I would like to express my deep gratitude to all present and former members of the Laboratory of Molecular Immunology and Cell Biology for the nice and productive atmosphere, for the constant support in all scientific and non-scientific aspects, as well as for the numerous enjoyable activities inside and outside the lab.

I am deeply grateful to Prof. Dr. Christian Kurts, Dr. Elisabeth Mettke and Katarzyna Jobin for helping me with the bone marrow reconstitution and the thymus transplantation experiments.

My project also immensely benefited from the help of Prof. Dr. Markus Gräler, who performed the mass spectrometric measurements of S1P and other sphingolipids.

Additionally, I would like to express my gratitude to Prof. Dr. Klaus Willecke, Dr. Christiane Kremser, Dr. Andreas Bickert, Dr. Phillip Ebel and Martina van Uelft from the Laboratory of Molecular Genetic and Cell Biology for providing the CERS-deficient mice and supporting my work with their expertise on sphingolipid metabolism.

Finally, I would like to thank Jacqueline and my family for the unreserved support and encouragement over the last years.